

DOKUZ EYLÜL UNIVERSITY
GRADUATE SCHOOL OF NATURAL AND APPLIED SCIENCES

SYNTHESIS OF PROBING WAVEFORMS
SATISFYING SPECTRO-TEMPORAL
CONSTRAINTS

by

Osman Tayfun BİŞKİN

August, 2018

İZMİR

**SYNTHESIS OF PROBING WAVEFORMS
SATISFYING SPECTRO-TEMPORAL
CONSTRAINTS**

**A Thesis Submitted to the
Graduate School of Natural and Applied Sciences of Dokuz Eylül University
In Partial Fulfillment of the Requirements for the Degree of Doctor of
Philosophy in Electrical and Electronics Engineering Program**

by

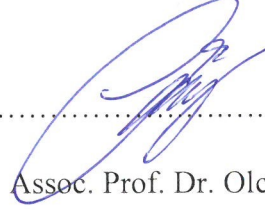
Osman Tayfun BİŞKİN

August, 2018

İZMİR

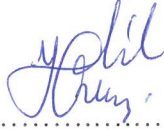
Ph.D. THESIS EXAMINATION RESULT FORM

We have read the thesis entitled “SYNTHESIS OF PROBING WAVEFORMS SATISFYING SPECTRO-TEMPORAL CONSTRAINTS” completed by **OSMAN TAYFUN BİŞKİN** under supervision of **ASSOC. PROF. DR. OLCAY AKAY** and we certify that in our opinion it is fully adequate, in scope and in quality, as a thesis for the degree of Doctor of Philosophy.



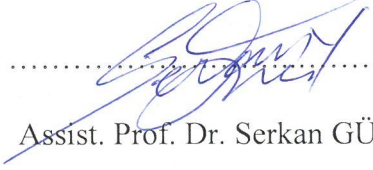
Assoc. Prof. Dr. Olcay AKAY

Supervisor



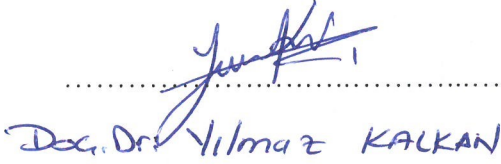
Prof. Dr. Halil ORUÇ

Thesis Committee Member



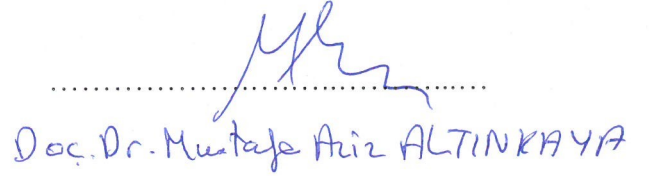
Assist. Prof. Dr. Serkan GÜNEL

Thesis Committee Member



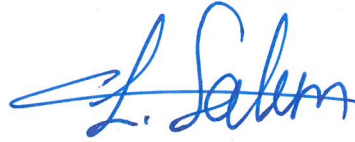
Doc. Dr. Yılmaz KALKAN

Examining Committee Member



Doc. Dr. Mustafa Ariz ALTINKAYA

Examining Committee Member



Prof. Dr. Latif SALUM

Director

Graduate School of Natural and Applied Sciences

ACKNOWLEDGMENTS

First of all, I would like to thank my advisor Assoc. Prof. Dr. Olcay AKAY for his patient support and valuable guidance during this thesis study. I must express that his encouragement and polite attitude made this work possible. I also would like to thank thesis committee members, Prof. Dr. Halil ORUÇ and Assist. Prof. Dr. Serkan GÜNEL, for their encouragement and new ideas throughout the progress of this thesis.

I also would like to thank TUBİTAK BİDEB for supporting my education through 2211-A Doctoral Fellowship Program.

Finally, I want to extend my greatest thanks to my family, the meaning of my life, for their never-ending support throughout my life.

Osman Tayfun BİŞKİN

SYNTHESIS OF PROBING WAVEFORMS SATISFYING SPECTRO-TEMPORAL CONSTRAINTS

ABSTRACT

In this thesis, several algorithms are proposed for designing radar transmit sequences satisfying temporal correlation and spectral stopband constraints. Unimodular constant modulus sequences are specifically focused on.

Studies in the literature have been mostly interested in minimizing certain performance metrics such as integrated sidelobe level (ISL) and weighted integrated sidelobe level (WISL). Additionally, shaping the spectrum of the transmit waveform to avoid certain frequencies is one of the desired tasks in cognitive radars. Therefore, various algorithms have been proposed in the literature for designing sequences having low ISL or WISL values and, at the same time, satisfying some spectral constraints.

In this thesis, we first utilize the genetic algorithm (GA) for designing a sequence by minimizing ISL in the frequency domain.

Secondly, a new algorithm called FWISL (frequency domain WISL) is proposed to design unimodular sequences utilizing the majorization minimization (MM) method for directly minimizing the WISL metric in the frequency domain. FWISL is the first frequency domain employment of the MM method for minimizing WISL.

Thirdly, we develop four more algorithms, named SMISLN (stopband MISL-new), SWPISL (stopband WPISL), SMWISL (stopband MWISL), and SFWISL (stopband FWISL), by directly minimizing ISL or WISL using the MM method in order to design unimodular sequences with suppressed power in arbitrary spectral bands and, at the same time, possessing reduced autocorrelation sidelobes. Numerical examples show that our newly proposed methods outperform some already existing methods in the literature with regard to computation time, converge in less number of iterations, and achieve better suppression in stopbands.

Keywords: Unimodular sequences, integrated sidelobe level, majorization-minimization, spectral stopband constraints

SPEKTRAL VE ZAMANSAL KISITLARI SAĞLAYAN GÖNDERİM DALGALARININ SENTEZLENMESİ

ÖZ

Bu tez çalışmasında zamansal ilinti ve spektral sönümlenme bandı kısıtlarını sağlayan radar gönderim sinyallerinin optimal olarak sentezlenmesi için çeşitli algoritmalar önerilmiştir. Özel olarak bu tezin ilgilendiği diziler ise bir birimsel sabit genlikli dizilerdir.

Literatürdeki çalışmalar, dizilerin öz ilinti fonksiyonunun tümleşik yankulak seviyesi (TYS) ve ağırlıklandırılmış tümleşik yankulak seviyesi (ATYS) gibi performans metriklerini eniyilemek üzerine yoğunlaşmıştır. Bununla birlikte, belirli frekanslardan kaçınmak için gönderilen dalga biçiminin spektrumunun uyarlanabilmesi bilişsel radarların istenilen özelliklerinden birisidir. Bu nedenle, düşük TYS veya ATYS değerlerine sahipken aynı zamanda bir takım spektral kısıtları da sağlayan diziler tasarlamak için bazı algoritmalar literatürde önerilmiştir.

Bu tez çalışmasında, ilk olarak, TYS değerini frekans boyutunda eniyileyerek bir dizi tasarlamak için genetik algoritma (GA) kullanılmıştır.

İkinci olarak, büyüklük enküçültmesi (BE) metodunu kullanarak frekans boyutunda ATYS'yi doğrudan eniyilemek için FWISL isimli yeni bir algoritma önerilmiştir. Bu algoritma ATYS'yi eniyileyen BE metodunun frekans boyutundaki ilk uygulamasıdır.

Üçüncü olarak, belirli spektral bantlardaki gücü sönümlenmiş ve aynı zamanda düşük özilinti yankulak seviyesine sahip bir birimsel sabit genlikli diziler üretmek için, TYS veya ATYS'yi büyüklük enküçültmesi metodunu kullanarak doğrudan eniyileyen SMISLN (stopband MISL-New), SWPISL (stopband WPISL), SMWISL (stopband MWISL), ve SFWISL (stopband FWISL) isiminde dört yeni algoritma önerilmiştir. Sayısal örnekler önerilen metodların hesaplama süresi bakımından literatürde halihazırda var olan algoritmalarından üstün olduklarını, daha az özyineleme sayısı ile yakınsadıklarını ve sönümlenme bantlarında daha iyi bastırma sağladıklarını göstermiştir.

Anahtar Kelimeler: Bir birimsel diziler, tümleşik yankulak seviyesi, büyüklük enküültmesi, spektral sönümlene bandı kısıtları



CONTENTS

	Page
Ph.D. THESIS EXAMINATION RESULT FORM	ii
ACKNOWLEDGMENTS	iii
ABSTRACT	iv
ÖZ	v
LIST OF FIGURES	x
LIST OF TABLES	xii
CHAPTER ONE – INTRODUCTION	1
1.1 History of Designing Radar Transmit Sequences	6
CHAPTER TWO – BACKGROUND AND EXISTING METHODS	11
2.1 Cyclic Algorithms for Minimizing Approximately Equivalent Metrics	13
2.1.1 CAN - Minimization of Approximate ISL	13
2.1.2 SCAN.....	17
2.1.3 WeCAN - Minimization of Approximate WISL	20
2.1.4 WeSCAN (Weighted SCAN)	24
2.2 MM-Based Methods.....	27
2.2.1 MISL.....	28
2.2.2 MWISL	32
2.2.3 WPISL	37

CHAPTER THREE – DESIGN OF SEQUENCES WITH LOW AUTOCORRELATION SIDELOBES USING GENETIC ALGORITHMS 42

3.1 Genetic Algorithms 42
3.2 Numerical Examples for Minimizing ISL..... 44

CHAPTER FOUR – A NEW FREQUENCY DOMAIN SEQUENCE DESIGN ALGORITHM MINIMIZING WISL 48

4.1 FWISL 48
4.2 Simplifying Majorization for Efficient Computation..... 53
4.3 Numerical Examples for FWISL..... 53

CHAPTER FIVE – DESIGNING SEQUENCES SATISFYING SIMULTANEOUS TEMPORAL ISL AND SPECTRAL STOPBAND CONSTRAINTS..... 64

5.1 Sequence Design with ISL and Stopband Constraints 64
5.2 Stopband MISL-New (SMISLN) 64
5.3 Stopband WPISL (SWPISL)..... 70
5.4 Numerical Examples for Designing Sequences with ISL and Stopband Constraints..... 74

CHAPTER SIX – DESIGNING SEQUENCES SATISFYING SIMULTANEOUS TEMPORAL WISL AND SPECTRAL STOPBAND CONSTRAINTS 80

6.1 Sequence Design with WISL and Stopband Constraints 80
6.2 Stopband MWISL (SMWISL) 80

6.3 Stopband WPISL (SWPISL).....	83
6.4 Stopband FWISL (SFWISL).....	83
6.5 Numerical Examples for Designing with WISL and Stopband Constraints ...	86
CHAPTER SEVEN – CONCLUSIONS	92
REFERENCES.....	95
APPENDICES	100
APPENDIX 1: CAZAC Sequences.....	100
APPENDIX 2: Acceleration Scheme	101
APPENDIX 3: Proof of Hermitian Toeplitz Matrix	103
APPENDIX 4: Computation of the Matrix R	105

LIST OF FIGURES

	Page
Figure 2.1 Correlation level of the Golomb sequence (in dB).....	16
Figure 2.2 Correlation level of the transmit sequence designed by the CAN algorithm (in dB)	16
Figure 2.3 (a) Normalized power spectrum, (b) correlation level (dB) of the sequence designed by SCAN	19
Figure 2.4 Correlation level of a transmit signal with length $N=100$ designed by WeCAN.....	24
Figure 2.5 (a) Normalized power spectrum, (b) correlation level of the sequence designed by WeSCAN	26
Figure 2.6 The updating procedure of the MM method.....	28
Figure 2.7 Correlation level of the transmit sequence designed by the MISL algorithm (in dB)	32
Figure 2.8 Correlation level of a transmit sequence designed by the MWISL algorithm (in dB).....	37
Figure 2.9 Correlation level of the transmit sequence designed by the WPISL algorithm (in dB).....	41
Figure 3.1 An example of crossover	43
Figure 3.2 An example of mutation	43
Figure 3.3 Correlation level (in dB) of the transmit sequence designed by GA.....	44
Figure 3.4 Average MF versus sequence length (initialization by random sequence)	46
Figure 3.5 MF versus sequence length (initialization by Golomb sequence).....	47
Figure 4.1 WISL versus the number of iterations	56
Figure 4.2 WISL versus CPU time	57
Figure 4.3 Correlation levels of the sequences designed by WeCAN, MWISL-acc, and FWISL-acc	57
Figure 4.4 Number of iterations versus sequence length N	58
Figure 4.5 CPU time versus sequence length N	58
Figure 4.6 MMF versus sequence length N	59

Figure 4.7 Average correlation level in suppressed lags (dB) versus sequence length N.....	59
Figure 4.8 Number of iterations versus sequence length N	60
Figure 4.9 CPU time versus sequence length N.....	60
Figure 4.10 MMF versus sequence length N	61
Figure 4.11 Average correlation level in suppressed lags (dB) versus sequence length N.....	61
Figure 5.1 (a) Normalized power spectrum, (b) correlation level of the sequence designed by SCAN	75
Figure 5.2 (a) Normalized power spectrum, (b) correlation level of the sequence designed by SMISLN-acc	76
Figure 5.3 (a) Normalized power spectrum, (b) correlation level of the sequence designed by SWPISL-acc.....	76
Figure 5.4 Normalized power spectra of sequences designed by SCAN, SMISLN-acc, and SWPISL-acc.....	77
Figure 5.5 Objective function (dB) versus (a) iteration number and (b) CPU time (sec).....	78
Figure 6.1 (a) Normalized power spectrum, (b) correlation level of the sequence designed by WeSCAN	87
Figure 6.2 (a) Normalized power spectrum, (b) correlation level of the sequence designed by SMWISL-acc	88
Figure 6.3 (a) Normalized power spectrum, (b) correlation level of the sequence designed by SWPISL-acc.....	88
Figure 6.4 (a) Normalized power spectrum, (b) correlation level of the sequence designed by SFWISL-acc.....	88
Figure 6.5 Normalized power spectra of sequences designed by WeSCAN, SMWISL-acc, SWPISL-acc, and SFWISL-acc	89
Figure 6.6 Objective function (dB) versus (a) iteration number and (b) CPU time (sec.)	90

LIST OF TABLES

	Page
Table 1.1 Algorithms for designing unimodular sequences.....	5
Table 3.1 Average MF values (initialization by random sequence)	45
Table 3.2 MF values (initialization by Golomb sequence)	46
Table 4.1 Required number of iterations, CPU time, MMF, and average correlation levels in suppressed lags ($N=100$, $Tol=10^{-13}$, initialization by Golomb sequence)	62
Table 4.2 Required number of iterations, CPU time, MMF, and average correlation levels in suppressed lags ($N=100$, $Tol=10^{-13}$, initialization by the sequence designed by CAP).....	63
Table 5.1 Numerical results	79
Table 6.1 Numerical results	91

CHAPTER ONE

INTRODUCTION

The aim of active sensing applications (including radar, sonar, communications, and medical imaging) is the transmission of a probing signal, reception of its reflected waveform, and to obtain information of interest by processing this received signal (Roberts, He, Li, & Stoica, 2010).

One of the active sensing systems is called RADAR which is derived from RAdio Detection And Ranging. Main tasks of a radar system can be inferred from its name. These are detection of a target and determining its range. The range is determined by measuring the round-trip delay of the transmitted waveform. Direction and velocity of the target can also be found out as by-products of this process (Levanon & Mozeson, 2004).

Christian Hülsmeyer accomplished the first radar experiment using his telemobiloscope to detect ships in fog by utilizing the radio waves in 1904 (He, Li, & Stoica, 2012). During the two world wars there were several developments on radar and sonar. Later on, this research field spread into different fields such as weather monitoring, flight control, and underwater sensing (He et al., 2012).

There are two critical elements which greatly affect the performance of a radar system; transmit waveform and receive filter. Receive filter is employed to extract the information of interest using the return of the transmit waveform which has to be designed properly to obtain accurate estimates of parameters of interest (Skolnik, 2008). In order to increase the efficiency and performance of active sensing applications, transmit waveforms are synthesized according to some performance criteria. In that respect, better range and Doppler resolution are two fundamental requirements that should be met as much as possible by transmit waveforms.

The aim of this thesis is developing algorithms for designing transmit sequences satisfying some temporal correlation and spectral stopband constraints. For the same purpose, several algorithms have already been proposed in the literature to design unimodular sequences for radar and communication systems (He, Stoica, & Li, 2010;

Petrolati, Angeletti, & Toso, 2012; Song, Babu, & Palomar, 2015b, 2015a, 2016b, 2016a; Stoica, He, & Li, 2009; Zhao, Song, Babu, & Palomar, 2016). After a sequence is designed, some metrics can be used in order to measure its goodness in terms of its autocorrelation sequence. Some of those metrics are integrated sidelobe level (ISL), peak sidelobe level (PSL), weighted-integrated sidelobe level (WISL), merit factor (MF), etc (Levanon & Mozeson, 2004; Roberts et al., 2010). Selection of a metric depends on the application.

In designing a sequence, above metrics can be employed as constraints towards minimizing autocorrelation sidelobes with the aim of reducing clutter from interfering targets. Autocorrelation mainlobe, on the other hand, could be considered as an important parameter for separating closely spaced targets. As stated in (Levanon & Mozeson, 2004), designing radar signals amounts to finding signals that yield a matched-filter response conforming to a given application. Thus, determining the metric to be employed depends mostly on the application. For example, the level of interference expected from a point target is characterized by the peak sidelobe level ratio (PSLR) of the matched filter output. However, the matched filter integrated sidelobe level ratio (ISLR) characterizes interference from volume or surface clutter. Additionally, radar signals having matched filter responses that exhibit a narrow mainlobe (the peak) and low sidelobes are required when one wants to detect and distinguish closely separated targets (Levanon & Mozeson, 2004).

In this thesis, we first utilize genetic algorithm (GA) (Capraro, Bradaric, Capraro, & Lue, 2008; Lellouch, Mishra, & Inggs, 2015, 2016; Martone, Ranney, & Sherbondy, 2016; Smith-Martinez, Agah, & Stiles, 2013; G. Sun, Wang, Zhang, Tao, & Zhou, 2016; Weile & Michielssen, 1997) to design a unimodular constant modulus sequence by minimizing the metric of ISL in the frequency domain. Unimodular sequences having large MF values are desired in applications where a transmit sequence with large MF ensures that the received waveform is not obscured by correlated multipath and clutter interference (Stoica et al., 2009). Unimodular constant modulus sequences with desirable autocorrelation function properties are widely used in radar and communication systems. Studies in the literature have focused on minimizing the metric of ISL (Song et al., 2015b, 2015a; Stoica et al., 2009). Our proposed method

utilizing GA is initialized by either a random sequence or the Golomb sequence (Zhang & Golomb, 1993) (See Appendix 1) whose autocorrelation is known to have good properties. By this way, radar transmit signals with minimum ISL are designed using GA. Finally, performance of GA based design is compared against the already existing cyclic algorithm-new (CAN) and monotonic minimizer for integrated sidelobe level (MISL) algorithms. Our simulations indicate that minimization of ISL using GA produces better results than the CAN algorithm. Hence, GA could alternatively be used to design radar transmit sequences by minimizing ISL in the frequency domain.

Secondly, we propose a new algorithm to design unimodular sequences utilizing the majorization minimization (MM) method for directly minimizing the WISL in the frequency domain. Some control over the autocorrelation lags of the designed sequence is provided by WISL. Hence, minimizing WISL becomes crucial in applications where we want to reduce the interference arising from some known multipath or clutter (Stoica et al., 2009). Therefore, in this thesis we propose a new algorithm named frequency domain WISL (FWISL) to design unimodular constant modulus sequences by minimizing the metric of WISL. As the first frequency domain application of the MM method for minimizing WISL, FWISL utilizes the fast Fourier transform (FFT), and thus, decreases the computation time. In our method, after proposing a function majorizing the frequency domain representation of the WISL metric, a closed-form solution of the minimization problem is derived as an iterative algorithm. Additionally, we provide an acceleration scheme to allow fast convergence of the newly designed algorithm.

Numerical examples show that FWISL not only outperforms existing cyclic algorithms such as CA-pruned (CAP) (Stoica et al., 2009) and weighted-CAN (WeCAN) (Stoica et al., 2009) in terms of computation time, but also converges in less number of iterations than the time domain implementation of MM-based algorithms. Furthermore, the new algorithm allows design of long sequences in a computationally efficient manner and achieves high merit factors (MFs).

Thirdly, we propose new algorithms to design unimodular sequences with suppressed power in some spectral bands and, at the same time, having low ISL and WISL values. Shaping the spectrum of the transmit waveform in order to avoid certain

frequencies is one of the desired tasks in cognitive radars. Additionally, one may want to design unimodular sequences with low autocorrelation sidelobes. In the literature, various algorithms have been proposed for designing sequences having low ISL values and, at the same time, satisfying some spectral constraints. SCAN and WeSCAN algorithms were proposed (He et al., 2010) for that purpose as extensions of the CAN (Stoica et al., 2009) and weighted CAN (WeCAN) (Stoica et al., 2009) algorithms, respectively. SCAN was proposed to design unimodular sequences with suppressed power in arbitrary spectral bands and having low ISL values as well. WeSCAN was proposed to design sequences having low WISL values. However, CAN and WeCAN algorithms minimize some approximations of ISL and WISL metrics, respectively, instead of minimizing the exact ISL and WISL metrics themselves. In the literature, MM-based methods were also proposed to minimize the exact ISL, directly (Song et al., 2015a, 2015b). Spectral-MISL algorithm, which is based on the MM method, was proposed to design unimodular sequences by minimizing ISL and restricting of power in certain pre-specified frequency bands (Song et al., 2015a).

In this thesis, we propose to use the MM-based algorithms to design unimodular sequences with their power suppressed in arbitrary spectral bands and having low ISL or WISL values. Numerical examples show that our proposed methods outperform SCAN and WeSCAN algorithms in terms of computation time, converge in less number of iterations, and achieve lower ISL, WISL, and stopband power values.

A summary of the algorithms designed by cyclic methods and the MM method are given in Table 1.1. The new algorithms proposed in this thesis are also indicated in the same table by boldfaced italic fonts. In the ensuing chapters, after developing those algorithms we perform their numerical simulation examples employing different parameter values and compare their performances.

Table 1.1 Algorithms for designing unimodular sequences (New algorithms developed in this thesis are indicated by boldfaced italic fonts)

Methodology		Employed Metric			
		ISL	WISL	Stopband-ISL	Stopband-WISL
Cyclic Algorithms (Approximately Equivalent Metrics)	Time	-	-	-	-
	Frequency	CAN	WeCAN	SCAN	WeSCAN
MM-Based Methods	Time	WPISL	WPISL MWISL	<i>SWPISL</i>	<i>SWPISL</i> <i>SMWISL</i>
	Frequency	MISL	<i>FWISL</i>	spectral-MISL <i>SMISLN</i>	<i>SFWISL</i>

The rest of the thesis is organized as follows. In Chapter One, some brief information and basic concepts of radar signal processing are given.

In Chapter Two, background information on already existing algorithms for designing radar waveforms is provided. Review of cyclic algorithms and MM-based methods are given in Sections 2.1 and 2.2, respectively.

In Chapter Three, first GA is explained briefly. Then, GA is utilized to design sequences by minimizing ISL in the frequency domain. At the end of the chapter, numerical examples are presented.

In Chapter Four, we propose a new frequency domain sequence design algorithm, FWISL (see Table 1.1), which minimizes the WISL metric using the MM method in the frequency domain. Then, an accelerated version of the proposed algorithm is developed. We also present some numerical examples.

In Chapter Five, we focus on designing waveforms satisfying simultaneous temporal correlation and spectral stopband constraints. We develop two algorithms named SMISLN and SWPISL (see Table 1.1) for designing waveforms with minimum ISL and spectral stopband constraints. Numerical examples for the proposed algorithms are also presented.

In Chapter Six, we develop three other algorithms, SMWISL, SWPISL, and SFWISL (see Table 1.1), for designing waveforms satisfying simultaneous temporal WISL and spectral stopband constraints. Numerical examples are also presented at the end of the chapter.

Finally, the thesis is concluded in Chapter Seven by a general discussion of the results obtained for the newly proposed algorithms.

1.1 History of Designing Radar Transmit Sequences

Many transmit signal waveforms with nice properties have been proposed in the radar literature. Unmodulated pulse, linear frequency-modulated pulse, and coherent train of identical unmodulated pulses can be mentioned as the most fundamental ones (Levanon & Mozeson, 2004). Since the unmodulated pulse has high sidelobes in the frequency domain, its use of frequency band is inefficient. In addition, it has poor range and Doppler resolution. By means of pulse compression better range resolution can be obtained. Similarly, by employing a coherent pulse train better Doppler resolution is achieved.

In radars, improving the range resolution can be accomplished by decreasing the width of the probing pulse and increasing the transmitted energy (Stoica, Li, & Xue, 2008). However, this necessitates use of large peak power levels which cannot be handled by most systems. Therefore, a technique termed as pulse compression is employed to overcome the large peak power requirement. In this method, a modulated subpulse train which has smaller peak power than a single pulse is transmitted. However, it has the same transmitted energy as the single pulse.

Linear frequency modulation is one of the pulse compression techniques providing better range resolution than the unmodulated pulse (Levanon & Mozeson, 2004). A

chirp waveform is a linear frequency modulated (LFM) pulse which is widely used in radar applications (He et al., 2012). A chirp signal can be defined as (He et al., 2012; Levanon & Mozeson, 2004)

$$s(t) = \frac{1}{\sqrt{T}} e^{j\pi kt^2}, \quad 0 \leq t \leq T, \quad (1.1)$$

where $k = \pm \frac{B}{T}$ is called the chirp rate with T representing the pulse duration and B denoting the bandwidth of the pulse.

Phase coding is another technique of pulse compression. Several phase codes can be derived using chirp signals (He et al., 2012; Levanon & Mozeson, 2004). (Barker, 1953) proposed a set of binary codes where phases of the sequence elements, ϕ_n , are in the range $\phi_n \in \{-\pi, \pi\}$, $n = 1, \dots, N$ and N represents sequence length. Barker sequences have optimal peak to side-peak ratio (PSPR). However, there is a limitation on the length of Barker code. The known longest Barker code is of length $N = 13$ and it is believed that no Barker code exist for $N > 13$ (Levanon & Mozeson, 2004). In order to overcome this problem, scientists have proposed several different methods for synthesizing longer sequences.

Various analytical and computational methods for synthesizing longer sequences have been proposed (He et al., 2012; Levanon & Mozeson, 2004). Some of those sequences have closed-form expressions such as Frank code (Frank, 1963), polyphase P codes (P1, P2, P3, P4) (B. L. Lewis & Kretschmer, 1981; Bernard L. Lewis & Kretschmer, 1982), Px code (Rapajic & Kennedy, 1998), Chu code (Chu, 1972), and Golomb code (Zhang & Golomb, 1993). Golomb, Frank, P1, Chu, and P4 codes are named “constant amplitude with zero autocorrelation” (CAZAC) sequences (Roberts et al., 2010). Phase codes with zero periodic autocorrelation sidelobes are called perfect sequences (Levanon & Mozeson, 2004). In (Roberts et al., 2010), perfect waveforms are referred to as CAZAC sequences (see Appendix 1 for the closed-form expressions of Golomb, Frank, and P4 sequences).

(Levanon & Mozeson, 2004) states that, although sidelobes of periodic autocorrelation of a phase coded sequence can be zero, it is not possible to synthesize a phase coded sequence with zero aperiodic correlation sidelobes. Therefore, in contrast to CAZAC sequences, it is more challenging to design a sequence with low ISL of aperiodic autocorrelation (Roberts et al., 2010).

In addition to those fixed sequences, some computational methods such as evolutionary algorithms (Kocabaş & Atalar, 2003), heuristic search (Wang, 2008), and stochastic optimization (Borwein & Ferguson, 2005) have also been exploited to generate sequences with desirable properties. Since computational complexity of those techniques increases with the length of the designed sequence, some alternative minimization methods such as cyclic algorithms (He et al., 2012; Roberts et al., 2010; Stoica et al., 2009; Stoica & Selen, 2004) and MM techniques (Song et al., 2015a, 2016b; Stoica & Selen, 2004; Zhao et al., 2016) have also been proposed.

While cyclic algorithms such as CAN and WeCAN are based on expressing the ISL and WISL metrics, respectively, in the frequency domain, CA-pruned (CAP) is based on expressing the WISL metric in the time domain. WeCAN+CAP was also proposed as a concatenation of WeCAN and CAP algorithms. CAN minimizes a quadratic (with respect to the designed sequence) approximation of ISL as opposed to exact ISL which is a quartic (fourth degree) function of the designed sequence. Similarly, WeCAN and CAP minimize quadratic approximations of WISL as opposed to exact WISL which is quartic with respect to the designed sequence (He et al., 2012; Jian, Stoica, & Xiayu, 2008; Roberts et al., 2010; Stoica et al., 2009; Stoica, Li, Zhu, & Guo, 2007; Stoica, Li, & Zhu, 2008). MM-based techniques have been proposed (Song et al., 2015a, 2016b) for direct minimization of ISL and WISL metrics and for minimization of a unified metric named “weighted peak or integrated sidelobe level” (WPISL) (Zhao et al., 2016). Those MM-based methods perform minimization of the aforementioned metrics directly in the time domain.

On the other hand, adaptation of the spectrum of transmit waveform in order to avoid certain frequencies is one of the main tasks in cognitive radars (Haykin, 2006; He et al., 2010). Transmitted waveforms should avoid utilizing some of the frequency bands that are allocated for specific applications. Therefore, transmit waveforms

should be designed so that they have low spectral power in the reserved frequency bands (He et al., 2010; Lindenfeld, 2004).

Since sequences with low autocorrelation sidelobes are widely used in communication and radar systems, in addition to having nulls in specific frequency bands of the power spectrum, it may also be desired to have low ISL or WISL values for the transmitted waveforms. Besides, transmitted sequences are usually designed as unimodular (constant modulus) waveforms. There are a few studies in the literature for designing unimodular transmit waveforms satisfying simultaneous temporal correlation and spectral stopband constraint (He et al., 2010; Song et al., 2015a). In this thesis, we also address the same problem using different methods.

In (He et al., 2010), the SCAN algorithm was proposed to design unimodular sequences with their spectral power suppressed in arbitrary frequency bands and having low ISL values, respectively. SCAN is an extension of the CAN algorithm which aims designing sequences with low ISL. Similarly, WeSCAN was proposed as an extension of the WeCAN algorithm which aims designing sequences with low WISL (Stoica et al., 2009). On the other hand, the MM method is employed in (Song et al., 2015a) to design unimodular constant modulus sequences with low ISL and constrained spectral power in certain frequency bands. The developed algorithm was named spectral-MISL (spectral-monotonic minimizer for integrated sidelobe level) (He et al., 2010). However, no algorithms have been proposed for designing transmit waveforms with low WISL and constrained spectra using the MM method. Although, both (He et al., 2010) and (Song et al., 2015a) are interested in designing sequences with low ISL and having some spectral constraints, there are differences between them. These differences arise not only from the employed methods for solving the problem but also from the problem statements as explained in the following sections. In the problem statement of spectral-MISL algorithm, the spectral constraint is given so that it should be lower than a pre-specified threshold value.

In this thesis, we develop alternative algorithms to design unimodular sequences with their spectral power suppressed in arbitrary frequency bands and having low ISL (or low WISL) using the MM method. We employ the MM method both in time and

frequency domains for solving the transmit waveform design problem introduced in (He et al., 2010).

Notation: In this thesis, boldface lowercase and uppercase letters represent vectors and matrices, respectively. $\|\cdot\|$ denotes Euclidean norm for vectors and Frobenius norm for matrices. $[\cdot]^H$ and $[\cdot]^T$ represent Hermitian and transpose operations, respectively, and $(\cdot)^*$ denotes conjugate of complex numbers. \odot indicates Hadamard product.

Simulations: All the simulations in this thesis are performed via MATLAB 2017a software on a PC with i7-4500U CPU having 12-GB memory and 1.8-GHz processor speed. We run the simulated recursive algorithms until the employed stopping criterion is reached.

CHAPTER TWO

BACKGROUND AND EXISTING METHODS

In order to synthesize transmit sequences, some performance measures that are based on the autocorrelation function of the sequence should be taken into consideration.

Engineers and scientists have long been working on the design of sequences with low autocorrelation sidelobes. Those sequences are widely employed in radar and communication systems. In communication systems, they are used for synchronization purposes and in radar systems they are mostly utilized as transmit waveforms because of their improved detection performance especially for weak targets (He et al., 2012; Kocabaş & Atalar, 2003; Song et al., 2015a, 2015b; Zhao et al., 2016). Those transmit sequences are usually designed as unimodular (i.e. having a constant modulus of unity) waveforms due to such practical considerations as limitations of sequence generating hardware components including analog-to-digital converters (ADCs) (He et al., 2012, 2010; Rowe, Stoica, & Li, 2014; Zhao et al., 2016).

Let $\{x_n\}_{n=1}^N$ denote a complex unimodular constant modulus sequence satisfying

$$|x_n| = 1, \quad n = 1, \dots, N \quad (2.1)$$

and vector \mathbf{x} be represented as $\mathbf{x} = [x_1 \ \dots \ x_N]^T$. Let $C_o \subseteq \mathbb{C}^N$ be the domain of \mathbf{x} such that $C_o = \{\mathbf{x} \in \mathbb{C}^N \mid |x_n| = 1 \text{ for } n = 1, \dots, N\}$. The autocorrelation function of $\{x_n\}_{n=1}^N$ is defined as (Song et al., 2015a, 2016b; Stoica et al., 2009; Zhao et al., 2016)

$$r_k = \sum_{n=k+1}^N x_n x_{n-k}^* = r_{-k}^*, \quad k = 0, \dots, N-1, \quad (2.2)$$

where $(\cdot)^*$ denotes complex conjugation. Goodness of synthesized sequences can be measured using the metric of integrated sidelobe level (ISL) which can be defined as (Song et al., 2015a, 2016b; Stoica et al., 2009; Zhao et al., 2016)

$$\text{ISL} = \sum_{k=1}^{N-1} |r_k|^2. \quad (2.3)$$

Some researchers also utilize merit factor (MF) as an alternative metric to measure goodness of any designed sequence. It is inversely proportional to ISL and can be defined as (Song et al., 2015a; Stoica et al., 2009)

$$\text{MF} = \frac{|r_0|^2}{\sum_{\substack{k=-(N-1) \\ k \neq 0}}^{N-1} |r_k|^2} = \frac{N^2}{2(\text{ISL})}. \quad (2.4)$$

Unimodular sequences having large MF values are desired in applications of radar where a transmit sequence with large MF ensures that the received waveform is not obscured by correlated multipath and clutter interference (Stoica et al., 2009).

In addition to above mentioned metrics, weighted ISL (WISL) is employed in (Stoica et al., 2009) to suppress not all but some of the autocorrelation lags of a designed sequence. It is defined as

$$\text{WISL} = \sum_{k=1}^{N-1} w_k |r_k|^2 \quad (2.5)$$

where w_k represents the real-valued, nonnegative ($w_k \geq 0$) weight of the k^{th} lag of the autocorrelation function. Thus, some control over the autocorrelation lags of the designed sequence is provided by WISL. Minimizing WISL becomes crucial in applications where we want to reduce the interference arising from some known multipath or clutter (Stoica et al., 2009). Similar to MF in (2.4), modified merit factor (MMF) can be defined (Stoica et al., 2009) in terms of WISL as

$$\text{MMF} = \frac{|r_0|^2}{2 \sum_{k=1}^{N-1} w_k |r_k|^2} = \frac{N^2}{2(\text{WISL})}. \quad (2.6)$$

2.1 Cyclic Algorithms for Minimizing Approximately Equivalent Metrics

2.1.1 CAN - Minimization of Approximate ISL

Unimodular constant modulus sequence design with minimum ISL can be formulated as follows

$$\begin{aligned} & \underset{\mathbf{x}}{\text{minimize}} && \text{ISL} \\ & \text{subject to} && |x_n| = 1, n = 1, \dots, N. \end{aligned} \quad (2.7)$$

CAN algorithm is based on the minimization of ISL in the frequency domain. Using the well-known Wiener-Khinchine property (Proakis & Manolakis, 2006), the Fourier transform (FT) of the autocorrelation function can be expressed as

$$\left| \sum_{n=1}^N x_n e^{-j\omega n} \right|^2 = \sum_{k=-(N-1)}^{N-1} r_k e^{-j\omega k} \triangleq \Phi(\omega) \quad (2.8)$$

where $\Phi(\omega)$ is the energy density spectrum (Proakis & Manolakis, 2006; Stoica & R. L. Moses, 2005) of $\{x_n\}_{n=1}^N$ and, due to periodicity of the FT, $\omega \in [0, 2\pi]$. Using $\Phi(\omega)$, ISL in (2.3) is alternatively expressed in (Roberts et al., 2010; Stoica et al., 2009; Zhao et al., 2016) as

$$\text{ISL} = \frac{1}{4N} \sum_{p=1}^{2N} [\Phi(\omega_p) - N]^2 \quad (2.9)$$

where $\{\omega_p\}_{p=1}^{2N}$ is defined as

$$\omega_p = \frac{2\pi}{2N} p, \quad p = 0, \dots, 2N-1. \quad (2.10)$$

Then, the ISL metric in (2.9) can also be written as follows

$$\text{ISL} = \frac{1}{4N} \sum_{p=1}^{2N} \left[\left| \sum_{n=1}^N x_n e^{-j\omega_p n} \right|^2 - N \right]^2. \quad (2.11)$$

Thus, in order to minimize ISL, one can minimize the following quantity

$$\sum_{p=1}^{2N} \left[\left| \sum_{n=1}^N x_n e^{-j\omega_p n} \right|^2 - N \right]^2. \quad (2.12)$$

Minimization of the above quantity is challenging because it is a quartic (fourth degree) function of $\{x_n\}_{n=1}^N$. Therefore, an almost equivalent formulation instead of (2.12) is proposed to be used (Stoica et al., 2009). In that respect, minimization of an approximate ISL metric is expressed as (Stoica et al., 2009)

$$\underset{\mathbf{x}, \psi_p}{\text{minimize}} \sum_{p=1}^{2N} \left| \sum_{n=1}^N x_n e^{-j\omega_p n} - \sqrt{N} e^{j\psi_p} \right|^2. \quad (2.13)$$

Minimizing the ISL metric in (2.12) is not exactly equal to the minimization of the ISL-related metric in (2.13). However, they are “almost equivalent” in the sense that if the metric in (2.12) takes on a small value for a certain x_n , than the metric in (2.13) also takes a small value at the same x_n (Stoica et al., 2009). Additionally, if the global minimum of the exact ISL metric in (2.12) is sufficiently small, then the sequences obtained by minimizing (2.12) and (2.13) are close to each other. It is also stated in (Stoica et al., 2009) that minimization of the exact metric in (2.12) is often much slower than that of the ISL-related metric in (2.13).

The expression in (2.13) to be minimized can be more compactly written as

$$\left\| \mathbf{F}_{2N}^H \bar{\mathbf{x}} - \mathbf{v} \right\|^2 \quad (2.14)$$

where \mathbf{F}_{2N}^H is the $2N \times 2N$ DFT matrix

$$\mathbf{F}_{2N}^H = \frac{1}{\sqrt{2N}} \begin{bmatrix} \mathbf{a}_1^H \\ \vdots \\ \mathbf{a}_{2N}^H \end{bmatrix}, \quad \mathbf{a}_p^H = \left[e^{-j\omega_p} \quad \dots \quad e^{-j2N\omega_p} \right] \quad (2.15)$$

and $2N \times 1$ vectors $\bar{\mathbf{x}}$ and \mathbf{v} are defined as

$$\bar{\mathbf{x}} = [x_1 \quad \dots \quad x_N \quad 0 \quad \dots \quad 0]^T, \quad (2.16)$$

$$\mathbf{v} = \frac{1}{\sqrt{2}} \begin{bmatrix} e^{j\psi_1} & \dots & e^{j\psi_{2N}} \end{bmatrix}. \quad (2.17)$$

FFT of the vector $\bar{\mathbf{x}}$ is calculated as

$$\mathbf{f} = \mathbf{F}_{2N}^H \bar{\mathbf{x}}. \quad (2.18)$$

Denoting the elements of the vector \mathbf{f} via $\mathbf{f} = [f_1 \ \dots \ f_{2N}]^T$, then, one has

$$\psi_p = \arg(f_p), \quad p = 1, \dots, 2N. \quad (2.19)$$

Similarly, the inverse Fourier transform of \mathbf{v} is given as

$$\mathbf{g} = \mathbf{F}_{2N} \mathbf{v}. \quad (2.20)$$

Again, denoting the elements of the vector \mathbf{g} as $\mathbf{g} = [g_1 \ \dots \ g_{2N}]^T$, then finally, the designed sequence x_n is obtained as

$$x_n = e^{j\arg(g_n)}, \quad n = 1, \dots, N. \quad (2.21)$$

As an example, a transmit sequence of length $N = 1000$ is designed by the CAN algorithm. The algorithm is initialized by Golomb sequence. Correlation level (dB) of the Golomb sequence and the sequence designed by CAN are illustrated in Figure 2.1 and Figure 2.2, respectively. Correlation level of a sequence is defined (Song et al., 2015a, 2015b; Stoica et al., 2009; Zhao et al., 2016) as

$$\text{Correlation Level} = 20 \log_{10} \frac{|r_k|}{|r_0|}, \quad k = -(N-1), \dots, N-1. \quad (2.22)$$

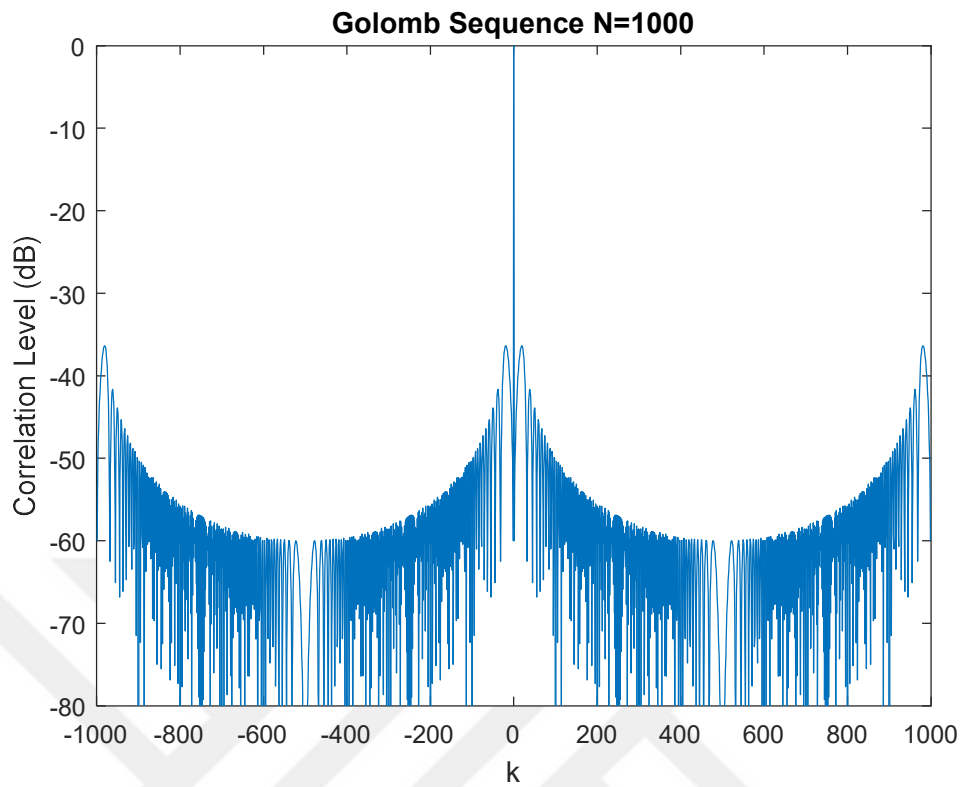


Figure 2.1 Correlation level of the Golomb sequence (in dB)

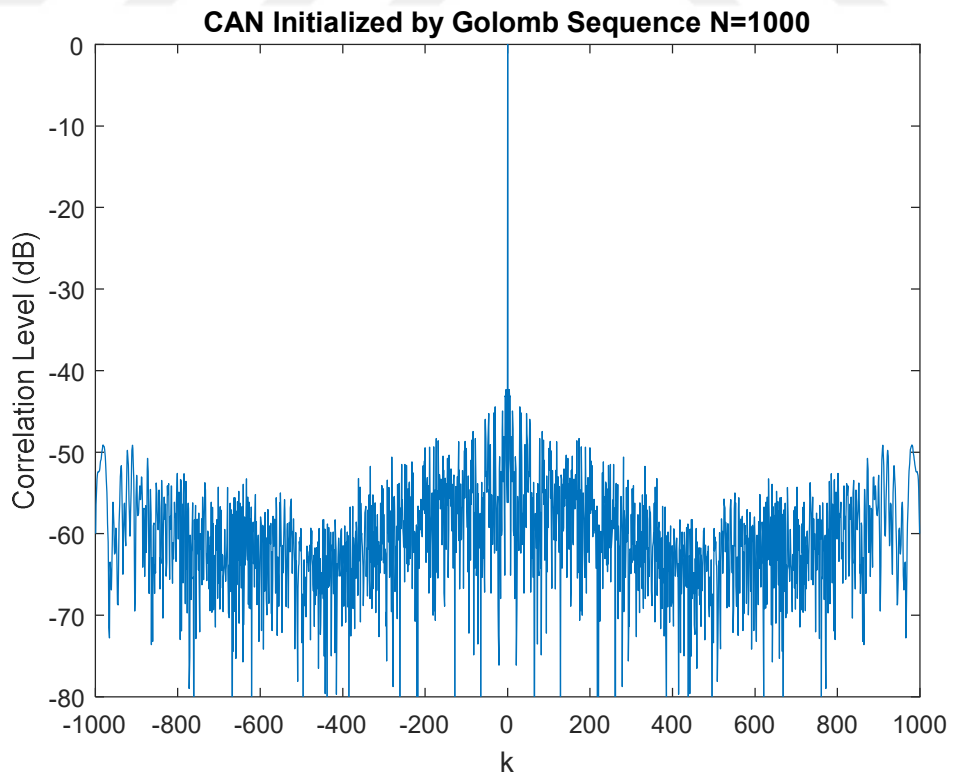


Figure 2.2 Correlation level of the transmit sequence designed by the CAN algorithm (in dB)

2.1.2 SCAN

The SCAN algorithm was proposed in (He et al., 2010) as an extension of CAN algorithm for accommodating additional spectral constraints. The frequency stopbands of a unimodular sequence, $\{x_n\}_{n=1}^N$, can be expressed as

$$\Omega = \bigcup_{k=1}^{N_s} (f_{k1}, f_{k2}) \quad (2.23)$$

where (f_{k1}, f_{k2}) and N_s represent the stopband edge frequencies and the number of stopbands, respectively. If we denote the number of DFT bins by \tilde{N} , which is taken to be large enough in order to densely cover the corresponding frequency band Ω , the $(k, l)^{\text{th}}$ element of the $\tilde{N} \times \tilde{N}$ DFT matrix, $\mathbf{F}_{\tilde{N}}^H$, is given as

$$[\mathbf{F}_{\tilde{N}}^H]_{kl} = \frac{1}{\sqrt{\tilde{N}}} \exp\left(-j \frac{2\pi kl}{\tilde{N}}\right), \quad k, l = 0, \dots, \tilde{N} - 1, \quad (2.24)$$

where $\frac{1}{\sqrt{\tilde{N}}}$ ensures that $\mathbf{F}_{\tilde{N}}$ is unitary. We construct a matrix, \mathbf{S} , using columns of $\mathbf{F}_{\tilde{N}}$ corresponding to the stopband frequency bands, Ω . Then, the following quantity is minimized to suppress the frequency stopbands

$$\left\| \mathbf{S}^H \begin{bmatrix} \mathbf{x} \\ \mathbf{0}_{(\tilde{N}-N) \times 1} \end{bmatrix} \right\|^2 \quad (2.25)$$

where $\|\cdot\|^2$ denotes the norm square of a vector and $\mathbf{0}_{(\tilde{N}-N) \times 1} = \begin{bmatrix} 0 & \dots & 0 \end{bmatrix}^T$.

Denoting the null space of \mathbf{S}^H by \mathbf{G} , the equivalent minimization problem was proposed in (He et al., 2010) as

$$\begin{aligned} & \underset{\mathbf{x}, \mathbf{a}}{\text{minimize}} \quad J_1(\mathbf{x}, \mathbf{a}) = \|\hat{\mathbf{x}} - \mathbf{G}\mathbf{a}\|^2 \\ & \text{subject to} \quad |x_n| = 1, \quad n = 1, \dots, N \end{aligned} \quad (2.26)$$

where $\boldsymbol{\alpha}$ is an auxiliary vector of variables and $\hat{\mathbf{x}} = \begin{bmatrix} \mathbf{x} \\ \mathbf{0}_{(\tilde{N}-N) \times 1} \end{bmatrix}$ is of length $\tilde{N} \times 1$. In

(He et al., 2010), the CAN algorithm is used to suppress the sidelobes of the autocorrelation function of the designed waveform. The frequency domain representation of ISL in (2.11) can be written as (He et al., 2010)

$$\frac{1}{4N} \sum_{p=1}^{2N} \left[\left| \sqrt{2N} \mathbf{a}_p \bar{\mathbf{x}} \right|^2 - N \right]^2 = N \sum_{p=1}^{2N} \left[\left| \mathbf{a}_p \bar{\mathbf{x}} \right|^2 - \frac{1}{2} \right]^2. \quad (2.27)$$

The ISL metric above can be further simplified as $N \left\| \mathbf{F}_{2N}^H \bar{\mathbf{x}} - \frac{1}{2} \mathbf{1} \right\|^2$ which is a quartic function of x_n . Therefore, (Stoica et al., 2009) proposes to use a quadratic approximation of the exact ISL metric. The ‘‘almost equivalent’’ approximation of the ISL metric is given (Stoica et al., 2009) as

$$N \left\| \mathbf{F}_{2N}^H \bar{\mathbf{x}} - \mathbf{v} \right\|^2 \quad (2.28)$$

where \mathbf{v} is the auxiliary vector of variables defined in (2.17). Thus, using the quadratic approximation of ISL, the CAN algorithm suppresses the correlation sidelobes by solving the following problem

$$\begin{aligned} & \underset{\mathbf{x}, \mathbf{v}}{\text{minimize}} \quad J_2(\mathbf{x}, \mathbf{v}) = N \left\| \mathbf{F}_{2N}^H \bar{\mathbf{x}} - \mathbf{v} \right\|^2 \\ & \text{subject to} \quad |x_n| = 1, \quad n = 1, \dots, N \\ & \quad \quad \quad |v_n| = \frac{1}{\sqrt{2}}, \quad n = 1, \dots, 2N. \end{aligned} \quad (2.29)$$

In (He et al., 2010), stopband and correlation constraints are combined and the following optimization problem is posed

$$\begin{aligned} & \underset{\mathbf{x}, \boldsymbol{\alpha}, \mathbf{v}}{\text{minimize}} \quad J(\mathbf{x}, \boldsymbol{\alpha}, \mathbf{v}) = \lambda J_1(\mathbf{x}, \boldsymbol{\alpha}) + (1 - \lambda) J_2(\mathbf{x}, \mathbf{v}) \\ & \text{subject to} \quad |x_n| = 1, \quad n = 1, \dots, N \\ & \quad \quad \quad |v_n| = \frac{1}{\sqrt{2}}, \quad n = 1, \dots, 2N \end{aligned} \quad (2.30)$$

where λ represents a relative weight parameter that is used to control the two penalty functions J_1 and J_2 . The above problem can also be rewritten as

$$\begin{aligned} & \underset{\mathbf{x}, \boldsymbol{\alpha}, \mathbf{v}}{\text{minimize}} && J(\mathbf{x}, \boldsymbol{\alpha}, \mathbf{v}) = \lambda \|\hat{\mathbf{x}} - \mathbf{G}\boldsymbol{\alpha}\|^2 + (1 - \lambda)N \|\mathbf{F}_{2N}^H \bar{\mathbf{x}} - \mathbf{v}\|^2 \\ & \text{subject to} && |x_n| = 1, \quad n = 1, \dots, N \\ & && |v_n| = \frac{1}{\sqrt{2}}, \quad n = 1, \dots, 2N. \end{aligned} \quad (2.31)$$

In order to solve the above optimization problem, only one variable of $J(\mathbf{x}, \boldsymbol{\alpha}, \mathbf{v})$ in (2.31) is minimized at a time (He et al., 2010).

As an example, one can design a unimodular sequence of length $N = 100$ having two stopbands given as $\Omega = [0.2, 0.3) \cup [0.7, 0.8)$ Hz in terms of normalized frequency. The relative weight parameter, λ , is taken as $\lambda = 0.8$. Normalized power spectrum and correlation level of the sequence designed by the SCAN algorithm can be seen in Figure 2.3.

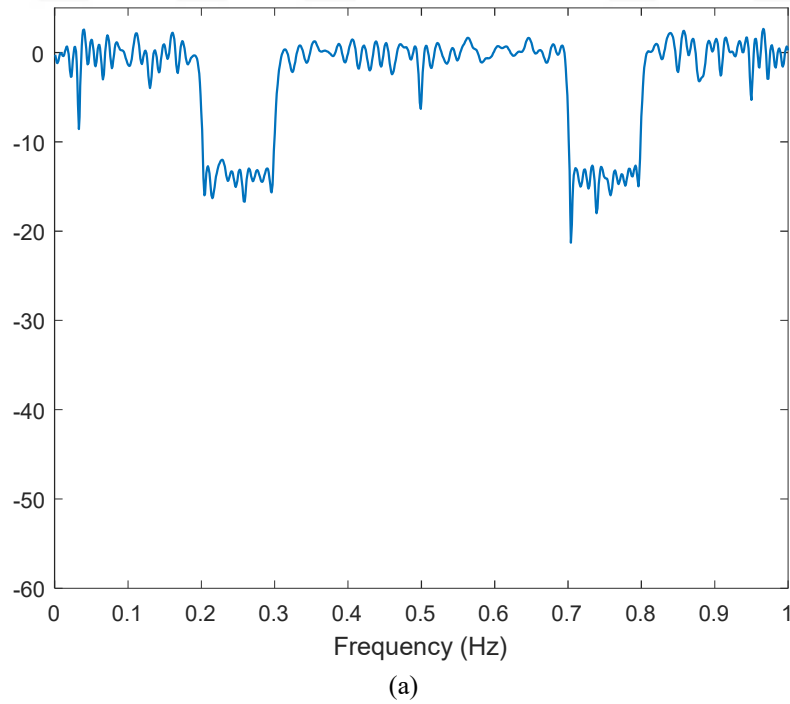


Figure 2.3 (a) Normalized power spectrum, (b) correlation level (dB) of the sequence designed by SCAN

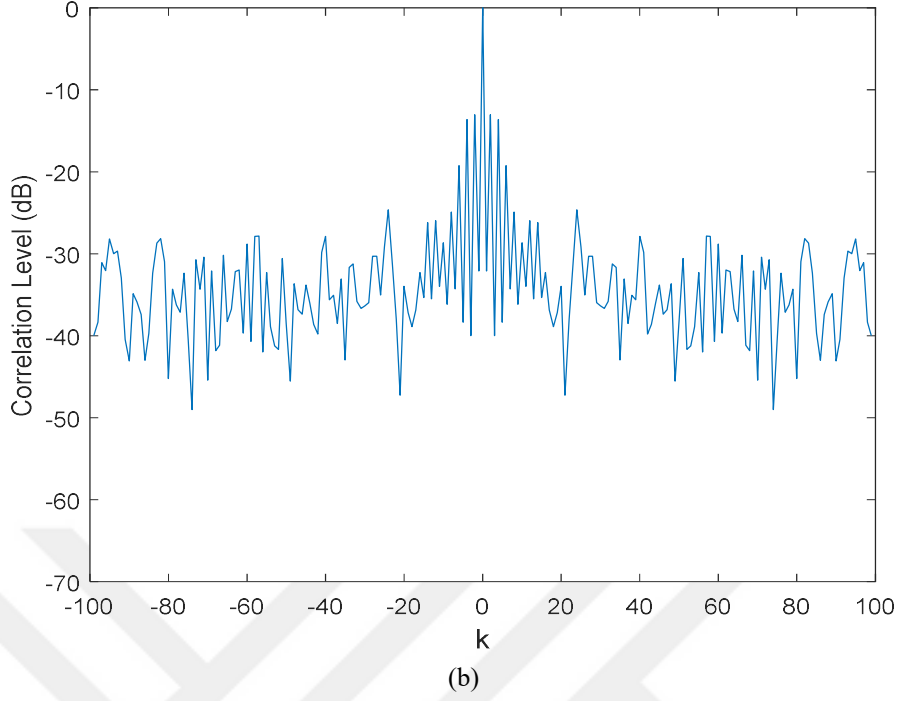


Figure 2.3 continues

2.1.3 WeCAN - Minimization of Approximate WISL

The WISL metric in (2.5) is alternatively expressed in (Stoica et al., 2009) as

$$\text{WISL} = \sum_{k=1}^{N-1} \gamma_k^2 |r_k|^2 = \frac{1}{4N} \sum_{p=1}^{2N} [\tilde{\Phi}(\omega_p) - \gamma_0 N]^2 \quad (2.32)$$

where $\{\gamma_k\}_{k=1}^{N-1}$ are real valued coefficients with $\gamma_k = \gamma_{-k}$. Autocorrelation lags can be weighted by choosing $\{\gamma_k\}_{k=1}^{N-1}$ appropriately. The relation between γ_k in (2.32) and w_k in (2.5) is given as $\gamma_k^2 = w_k$. $\tilde{\Phi}(\omega_p)$ in (2.32) is defined as

$$\tilde{\Phi}(\omega_p) \triangleq \sum_{k=-(N-1)}^{N-1} \gamma_k r_k e^{-j\omega_p k} \quad (2.33)$$

and $\{\omega_p\}_{p=1}^{2N}$ is given as $\omega_p = \frac{2\pi}{2N} p$, $p = 0, \dots, 2N-1$. The coefficients $\{\gamma_k\}_{k=1}^{N-1}$ are chosen so that the matrix

$$\mathbf{\Pi} = \frac{1}{\gamma_0} \begin{bmatrix} \gamma_0 & \gamma_1 & \cdots & \gamma_{N-1} \\ \gamma_1 & \gamma_0 & \ddots & \vdots \\ \vdots & \ddots & \ddots & \gamma_1 \\ \gamma_{N-1} & \cdots & \gamma_1 & \gamma_0 \end{bmatrix} \quad (2.34)$$

is positive semidefinite; that is $\mathbf{\Pi} \succeq 0$. This condition can be satisfied by selecting γ_0 as $\gamma_0 + \lambda_{\min} \geq 0$ where λ_{\min} is the minimum eigenvalue of the matrix $\tilde{\mathbf{\Pi}} = \gamma_0 \mathbf{\Pi}$ with all its diagonal elements being zero (Stoica et al., 2009). Using the properties of the discrete Fourier transform (DFT) and the definitions given in (2.8) and (2.33), we can write the following equalities (Stoica et al., 2009)

$$\begin{aligned} \{r_k\} &\stackrel{\text{DFT}\{\cdot\}}{\underset{\text{IDFT}\{\cdot\}}{\rightleftharpoons}} \Phi(\omega) = |X(\omega)|^2 \\ \{\gamma_k r_k\} &\stackrel{\text{DFT}\{\cdot\}}{\underset{\text{IDFT}\{\cdot\}}{\rightleftharpoons}} \tilde{\Phi}(\omega) = \Pi(\omega) * |X(\omega)|^2 \end{aligned} \quad (2.35)$$

where $*$ represents the convolution operation. $X(\omega)$ and $\Pi(\omega)$ are defined as follows

$$\begin{aligned} X(\omega) &= \sum_{n=1}^N x_n e^{-j\omega n}, \\ \Pi(\omega) &= \sum_{k=-(N-1)}^{N-1} \gamma_k e^{-j\omega k}. \end{aligned} \quad (2.36)$$

Then, $\tilde{\Phi}(\omega_p)$ and the WISL metric can be written (Stoica et al., 2009) as

$$\begin{aligned} \tilde{\Phi}(\omega_p) &= \sum_{n=1}^N \sum_{\tilde{n}=1}^N \gamma_{n-\tilde{n}} x_n x_{\tilde{n}}^* e^{-j\omega_p(n-\tilde{n})} = \tilde{\mathbf{x}}_p^H (\gamma_0 \mathbf{\Pi}) \tilde{\mathbf{x}}_p \\ \text{WISL} &= \frac{\gamma_0^2}{4N} \sum_{p=1}^{2N} [\tilde{\mathbf{x}}_p^H \mathbf{\Pi} \tilde{\mathbf{x}}_p - N]^2 \end{aligned} \quad (2.37)$$

where $\tilde{\mathbf{x}}_p = [x_1 e^{-j\omega_p} \quad x_2 e^{-j2\omega_p} \quad \cdots \quad x_N e^{-jN\omega_p}]^T$. Thus, the frequency domain minimization problem to be solved can be expressed as

$$\begin{aligned}
& \underset{\mathbf{x}}{\text{minimize}} && \frac{\gamma_0^2}{4N} \sum_{p=1}^{2N} [\tilde{\mathbf{x}}_p^H \mathbf{\Pi} \tilde{\mathbf{x}}_p - N]^2 \\
& \text{subject to} && |x_n| = 1, \quad n = 1, \dots, N.
\end{aligned} \tag{2.38}$$

The WISL metric as given in (2.38) is a quartic function of unknowns, $\{x_n\}_{n=1}^N$. Instead, (Stoica et al., 2009) suggests an ‘‘almost equivalent’’ minimization problem in which the following quadratic approximate function of $\{x_n\}_{n=1}^N$ is minimized,

$$\begin{aligned}
& \underset{\mathbf{x}, \boldsymbol{\eta}_p}{\text{minimize}} && \sum_{p=1}^{2N} \|\mathbf{C} \tilde{\mathbf{x}}_p - \boldsymbol{\eta}_p\|^2 \\
& \text{subject to} && \|\boldsymbol{\eta}_p\|^2 = N, \quad p = 1, \dots, 2N \\
& && |x_n| = 1, \quad n = 1, \dots, N.
\end{aligned} \tag{2.39}$$

Here, \mathbf{C} is an $N \times N$ matrix defined as the square root of the matrix $\mathbf{\Pi}$, i.e., $\mathbf{\Pi} = \mathbf{C}^T \mathbf{C}$. In order to express the matrix $\mathbf{\Pi}$ as $\mathbf{\Pi} = \mathbf{C}^T \mathbf{C}$, it must be a positive semidefinite matrix.

We can also express (2.39) as follows,

$$\begin{aligned}
& \underset{\boldsymbol{\eta}_p}{\text{minimize}} && \|\mathbf{f}_p - \boldsymbol{\eta}_p\|^2 \\
& \text{subject to} && \|\boldsymbol{\eta}_p\|^2 = N
\end{aligned} \tag{2.40}$$

where $\mathbf{f}_p = \mathbf{C} \tilde{\mathbf{x}}_p$. In (Stoica et al., 2009), $\boldsymbol{\eta}_p$ is found as

$$\boldsymbol{\eta}_p = \sqrt{N} \frac{\mathbf{f}_p}{\|\mathbf{f}_p\|}. \tag{2.41}$$

Let \mathbf{A} be a matrix whose p^{th} row corresponds to the transpose of the vector \mathbf{f}_p . One can evaluate \mathbf{A} as

$$\mathbf{A} = \sqrt{2N} \mathbf{F}_{2N}^H \cdot [\mathbf{z}_1 \quad \mathbf{z}_2 \quad \dots \quad \mathbf{z}_N]_{2N \times N} \tag{2.42}$$

where

$$\mathbf{z}_k = [c_{k1}x_1 \quad \dots \quad c_{kN}x_N \quad 0 \quad \dots \quad 0]_{(2N \times 1)}^T. \quad (2.43)$$

In (2.43), c_{kn} corresponds to the (k, n) th element of \mathbf{C} . One can express

$\sum_{p=1}^{2N} \|\mathbf{C}\tilde{\mathbf{x}}_p - \boldsymbol{\eta}_p\|^2$ alternatively as

$$\sum_{p=1}^{2N} \|\mathbf{C}\tilde{\mathbf{x}}_p - \boldsymbol{\eta}_p\|^2 = \sum_{k=1}^N \|\mathbf{z}_k - \mathbf{F}_{2N}\boldsymbol{\beta}_k\|^2 \quad (2.44)$$

where $\boldsymbol{\beta}_k = \frac{1}{\sqrt{2N}} [\eta_{1k} \quad \dots \quad \eta_{2Nk}]^T$, $k = 1, \dots, N$. For a specific element, x_m , of

$\{x_n\}_{n=1}^N$, (2.44) becomes

$$\begin{aligned} \sum_{k=1}^N |\mu_k x_m - v_k|^2 &= \sum_{k=1}^N \left(|\mu_k x_m|^2 - \mu_k^* x_m^* v_k - \mu_k x_m v_k^* + |v_k|^2 \right) \\ &= \text{constant} - 2 \operatorname{Re} \left\{ \left(\sum_{k=1}^N \mu_k^* v_k \right) x_m^* \right\} \end{aligned} \quad (2.45)$$

where μ_k and v_k are the corresponding elements of \mathbf{z}_k and $\mathbf{F}_{2N}\boldsymbol{\beta}_k$, respectively.

Finally, x_m can be found as follows

$$\begin{aligned} x_m &= e^{j\phi_m}, \\ \phi_m &= \arg \left(\sum_{k=1}^N \mu_k^* v_k \right). \end{aligned} \quad (2.46)$$

Correlation level of a transmit signal with length $N = 100$ designed by the WeCAN algorithm can be seen in Figure 2.4. The algorithm is initialized by Golomb sequence.

The weighting factors γ_k are taken as

$$\gamma_k = \begin{cases} 1, & k \in \{1, \dots, 20\} \cup \{51, \dots, 70\} \\ 0, & \text{otherwise.} \end{cases} \quad (2.47)$$

γ_0 is selected as $\gamma_0 = 13.1950$ so that the matrix $\boldsymbol{\Pi}$ in (2.34) is positive semidefinite.

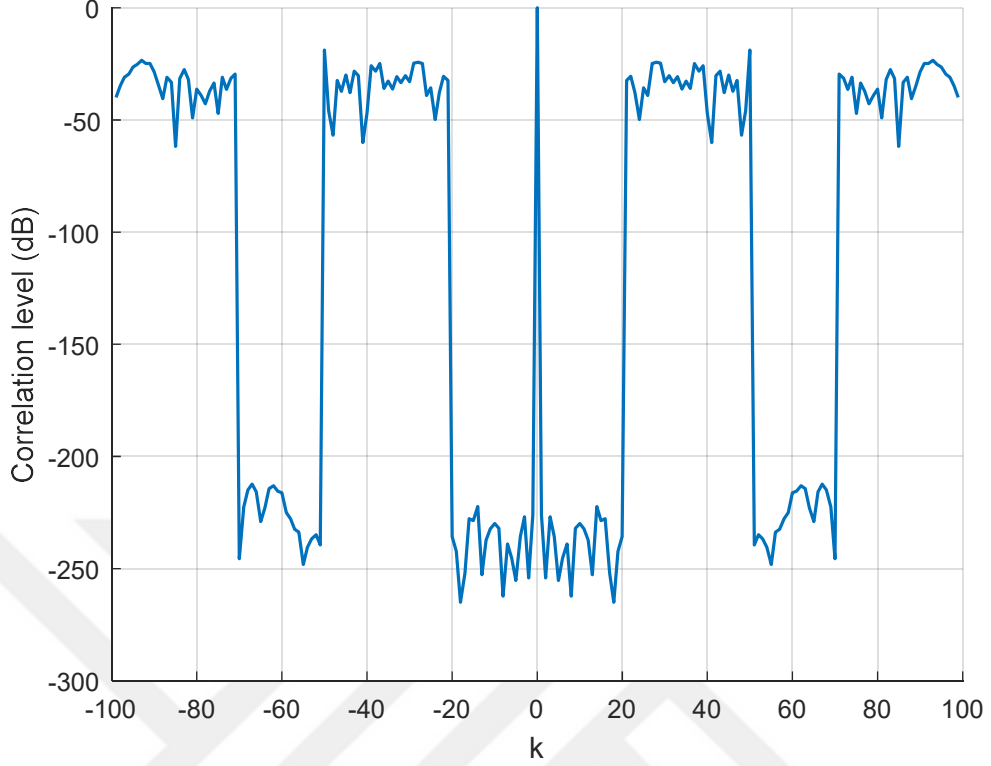


Figure 2.4 Correlation level of a transmit signal with length $N = 100$ designed by WeCAN

2.1.4 WeSCAN (Weighted SCAN)

WeSCAN was proposed in (He et al., 2010) to control both the stopband and correlation constraints. It is an extension of the WeCAN algorithm (Stoica et al., 2009) and a modified version of SCAN. WISL metric in (2.37) can be written as

$$\text{WISL} = \frac{\gamma_0}{4N} \sum_{p=1}^{2N} \left[\tilde{\mathbf{x}}_p^H \mathbf{C}^T \mathbf{C} \tilde{\mathbf{x}}_p - N \right]^2. \quad (2.48)$$

Then one can also write the above WISL metric as

$$\begin{aligned} \text{WISL} &= \frac{\gamma_0}{4N} \sum_{p=1}^{2N} \left[\sum_{k=1}^N \left| \sqrt{2N} \mathbf{a}_p^H \mathbf{z}_k \right|^2 - N \right]^2 \\ &= \gamma_0 N \sum_{p=1}^{2N} \left[\sum_{k=1}^N \left| \mathbf{a}_p^H \mathbf{z}_k \right|^2 - \frac{1}{2} \right]^2 \end{aligned} \quad (2.49)$$

where \mathbf{z}_k is given in (2.43).

The exact WISL metric in (2.49) is a quartic function with respect to x_n . Therefore, (Stoica et al., 2009) proposed to use a quadratic approximation of the exact WISL metric. The ‘‘almost equivalent’’ approximation of the WISL metric can be written (He et al., 2010; Stoica et al., 2009) as $\gamma_0 N \|\mathbf{F}_{2N}^H \mathbf{Z} - \mathbf{\Delta}\|^2$ which is minimized by solving the following optimization problem proposed in (He et al., 2010; Stoica et al., 2009)

$$\begin{aligned} & \underset{\mathbf{x}, \boldsymbol{\delta}_p}{\text{minimize}} && J_3(\mathbf{x}, \mathbf{V}) = \gamma_0 N \|\mathbf{F}_{2N}^H \mathbf{Z} - \mathbf{\Delta}\|^2 \\ & \text{subject to} && |x_n| = 1, \quad n = 1, \dots, N \\ & && \|\boldsymbol{\delta}_p\|^2 = 1, \quad p = 1, \dots, 2N. \end{aligned} \quad (2.50)$$

In the expressions above, the following matrices are utilized

$$\begin{aligned} \mathbf{Z} &= [\mathbf{z}_1 \quad \mathbf{z}_2 \quad \dots \quad \mathbf{z}_N]_{2N \times N}, \\ \mathbf{\Delta} &= \frac{1}{\sqrt{2N}} [\boldsymbol{\delta}_1 \quad \boldsymbol{\delta}_2 \quad \dots \quad \boldsymbol{\delta}_{2N}]_{2N \times N}^T. \end{aligned} \quad (2.51)$$

The optimization problem in (2.50) can also be written by using the cost functions J_1 and J_3 in (2.26) and (2.50), respectively, as follows

$$\begin{aligned} & \underset{\mathbf{x}, \boldsymbol{\alpha}, \boldsymbol{\delta}}{\text{minimize}} && J(\mathbf{x}, \boldsymbol{\alpha}, \boldsymbol{\delta}) = \lambda \|\hat{\mathbf{x}} - \mathbf{G}\boldsymbol{\alpha}\|^2 + (1 - \lambda) \gamma_0 N \|\mathbf{F}_{2N}^H \mathbf{Z} - \mathbf{\Delta}\|^2 \\ & \text{subject to} && |x_n| = 1, \quad n = 1, \dots, N \\ & && \|\boldsymbol{\delta}_p\|^2 = 1, \quad p = 1, \dots, 2N. \end{aligned} \quad (2.52)$$

In order to solve the above optimization problem, only one variable of $J(\mathbf{x}, \boldsymbol{\alpha}, \boldsymbol{\delta})$ in (2.52) is minimized at a time (He et al., 2010).

As an example, one can design a unimodular sequence of length $N = 100$ having a stopband given as $\Omega = [0.2, 0.3)$ Hz in terms of normalized frequency. The weighting factors γ_k are taken as given in (2.47). The relative weight parameter, λ , is taken as $\lambda = 0.8$. The number of DFT points is selected as $\tilde{N} = 1000$. Normalized power

spectrum and correlation level of the sequence designed by the WeSCAN algorithm is shown in Figure 2.5.

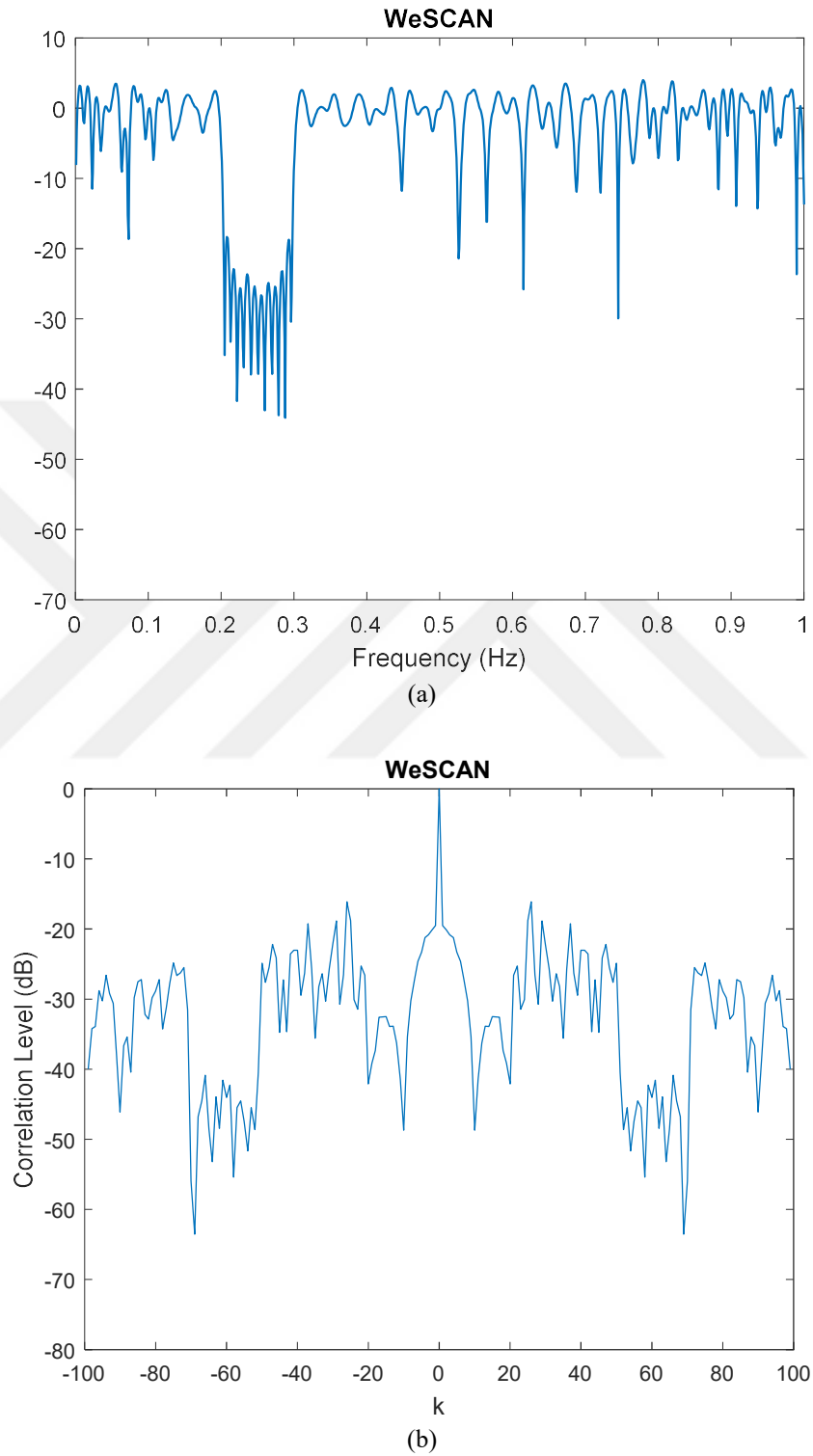


Figure 2.5 (a) Normalized power spectrum, (b) correlation level of the sequence designed by WeSCAN

2.2 MM-Based Methods

The MM method is used to solve rather difficult optimization problems by transforming them into simpler ones (Song et al., 2015a, 2016b; Zhao et al., 2016). In this section, we briefly summarize the MM method.

Let $f(\mathbf{x})$ denote a function to be minimized over $\mathcal{X} \subseteq \mathbb{C}^n$. Now, we can formulate an optimization problem as (Song et al., 2015a, 2016b; Zhao et al., 2016)

$$\begin{aligned} & \text{minimize} && f(\mathbf{x}) \\ & \text{subject to} && \mathbf{x} \in \mathcal{X}. \end{aligned} \tag{2.53}$$

We minimize a simpler function that majorizes $f(\mathbf{x})$ instead of minimizing $f(\mathbf{x})$ by employing the MM method. In order to understand the principle of the MM method, first of all, consider that the MM method starts from an initial point represented as $\mathbf{x}^{(0)}$ and produces a sequence at the k^{th} iteration which is represented as $\mathbf{x}^{(k)}$. The sequence update rule is given as follows (Song et al., 2015a, 2016b; Zhao et al., 2016)

$$\mathbf{x}^{(k+1)} \in \arg \min_{\mathbf{x} \in \mathcal{X}} u(\mathbf{x}, \mathbf{x}^{(k)}) \tag{2.54}$$

where $u(\mathbf{x}, \mathbf{x}^{(k)})$ is the majorization function of $f(\mathbf{x})$ at $\mathbf{x}^{(k)}$ satisfying the following expressions

$$\begin{aligned} u(\mathbf{x}, \mathbf{x}^{(k)}) & \geq f(\mathbf{x}) \quad \forall \mathbf{x} \in \mathcal{X} \\ u(\mathbf{x}^{(k)}, \mathbf{x}^{(k)}) & = f(\mathbf{x}^{(k)}). \end{aligned} \tag{2.55}$$

The updating procedure of the MM method is illustrated in Figure 2.6. The critical point here is determining the majorization function. More details about the MM method can be found in (Song et al., 2015a, 2016b; Stoica & Selen, 2004; Zhao et al., 2016). In the following sections, existing algorithms from the literature derived by using the MM method for direct minimization of ISL and WISL metrics are reviewed.

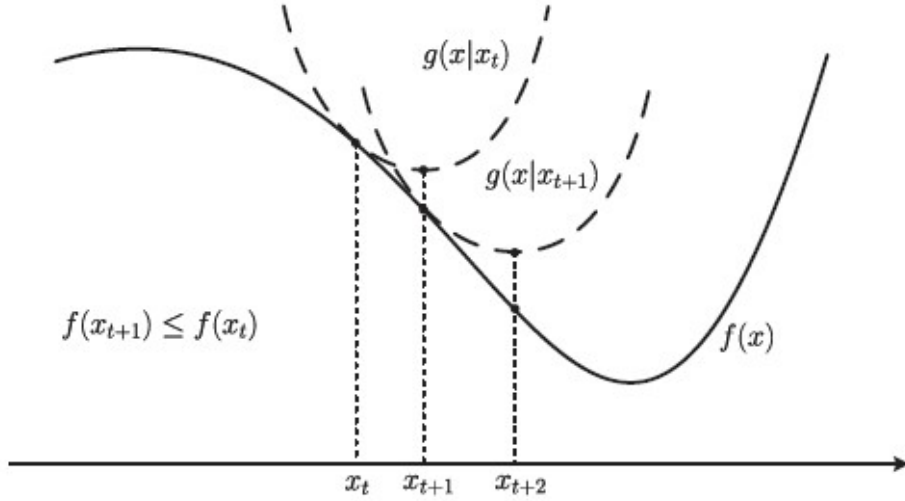


Figure 2.6 The updating procedure of the MM method (Y. Sun, Babu, & Palomar, 2017)

2.2.1 MISL

In order to employ the MM method for direct minimization of ISL, the minimization problem in (2.7) is first rewritten using the alternative expression of ISL in (2.12) as (Song et al., 2015a)

$$\begin{aligned} & \underset{\mathbf{x}}{\text{minimize}} && \sum_{p=1}^{2N} \left[\mathbf{a}_p^H \mathbf{x} \mathbf{x}^H \mathbf{a}_p - N \right]^2 \\ & \text{subject to} && |x_n| = 1, \quad n = 1, \dots, N \end{aligned} \quad (2.56)$$

where $\mathbf{a}_p = \left[1 e^{j\omega_p} \dots e^{j\omega_p(N-1)} \right]^T$, $p = 1, \dots, 2N$. Expanding the square in the objective function, one obtains

$$\begin{aligned} & \underset{\mathbf{x}}{\text{minimize}} && \sum_{p=1}^{2N} \left[\left(\mathbf{a}_p^H \mathbf{x} \mathbf{x}^H \mathbf{a}_p \right)^2 - 2N \mathbf{a}_p^H \mathbf{x} \mathbf{x}^H \mathbf{a}_p + N^2 \right] \\ & \text{subject to} && |x_n| = 1, \quad n = 1, \dots, N. \end{aligned} \quad (2.57)$$

Due to Parseval's relation, $\sum_{p=1}^{2N} \left| \mathbf{a}_p^H \mathbf{x} \right|^2 = \|\mathbf{x}\|^2 = N$, the second term is a constant. After ignoring the constant term in (2.57), the minimization problem can be expressed (Song et al., 2015a) as

$$\begin{aligned}
& \underset{\mathbf{x}}{\text{minimize}} && \sum_{p=1}^{2N} (\mathbf{a}_p^H \mathbf{x} \mathbf{x}^H \mathbf{a}_p)^2 \\
& \text{subject to} && |x_n| = 1, \quad n = 1, \dots, N.
\end{aligned} \tag{2.58}$$

Construction of majorization function for the ISL metric is started by using the following lemma.

Lemma 1 (Song et al., 2015a): Let \mathbf{K} and \mathbf{L} be $n \times n$ Hermitian matrices such that $\mathbf{K} \succeq \mathbf{L}$. Then, for any point $\mathbf{x}_0 \in \mathbb{C}^n$, the quadratic function $\mathbf{x}^H \mathbf{L} \mathbf{x}$ is majorized by the following function $\mathbf{x}^H \mathbf{K} \mathbf{x} + 2 \operatorname{Re}[\mathbf{x}^H (\mathbf{L} - \mathbf{K}) \mathbf{x}_0] + \mathbf{x}_0^H (\mathbf{K} - \mathbf{L}) \mathbf{x}_0$ at \mathbf{x}_0 .

The proof of Lemma 1 can be found in (Song et al., 2015a). Utilizing Lemma 1, a function that majorizes the objective function can be found.

Defining $\mathbf{A}_p = \mathbf{a}_p \mathbf{a}_p^H$ and $\mathbf{X} = \mathbf{x} \mathbf{x}^H$, the objective function in (2.58) can be written as $\sum_{p=1}^{2N} (\mathbf{a}_p^H \mathbf{x} \mathbf{x}^H \mathbf{a}_p)^2 = \sum_{p=1}^{2N} \operatorname{Tr}(\mathbf{X} \mathbf{A}_p)^2$. Since $\operatorname{Tr}(\mathbf{X} \mathbf{A}_p) = [\operatorname{vec}(\mathbf{X})]^H \operatorname{vec}(\mathbf{A}_p)$ (Song et al., 2015a), the problem in (2.58) can be expressed as follows

$$\begin{aligned}
& \underset{\mathbf{x}, \mathbf{X}}{\text{minimize}} && [\operatorname{vec}(\mathbf{X})]^H \boldsymbol{\Sigma}_1 \operatorname{vec}(\mathbf{X}) \\
& \text{subject to} && \mathbf{X} = \mathbf{x} \mathbf{x}^H \\
& && |x_n| = 1, \quad n = 1, \dots, N
\end{aligned} \tag{2.59}$$

where $\boldsymbol{\Sigma}_1 = \sum_{p=1}^{2N} \operatorname{vec}(\mathbf{A}_p) [\operatorname{vec}(\mathbf{A}_p)]^H$ and $\operatorname{vec}(\mathbf{X})$ forms a column vector by stacking all the columns of the matrix \mathbf{X} . Now, one can apply Lemma 1 on the objective function in (2.59). Lemma 1 can be applied with $\mathbf{K} = \lambda_{\max}(\boldsymbol{\Sigma}_1) \mathbf{I}$ where $\lambda_{\max}(\boldsymbol{\Sigma}_1)$ is the maximum eigenvalue of $\boldsymbol{\Sigma}_1$. Then, $[\operatorname{vec}(\mathbf{X})]^H \boldsymbol{\Sigma}_1 \operatorname{vec}(\mathbf{X})$ is majorized at $\mathbf{X}^{(k)}$ by $u_1(\mathbf{X}, \mathbf{X}^{(k)})$ given as follows (Song et al., 2015a)

$$\begin{aligned}
u_1(\mathbf{X}, \mathbf{X}^{(k)}) &= \lambda_{\max}(\boldsymbol{\Sigma}_1) [\text{vec}(\mathbf{X})]^H \text{vec}(\mathbf{X}) \\
&\quad + 2 \text{Re} \left([\text{vec}(\mathbf{X})]^H (\boldsymbol{\Sigma}_1 - \lambda_{\max}(\boldsymbol{\Sigma}_1) \mathbf{I}) \text{vec}(\mathbf{X}^{(k)}) \right) \\
&\quad + [\text{vec}(\mathbf{X}^{(k)})]^H (\lambda_{\max}(\boldsymbol{\Sigma}_1) \mathbf{I} - \boldsymbol{\Sigma}_1) \text{vec}(\mathbf{X}^{(k)}).
\end{aligned} \tag{2.60}$$

It can be clearly seen that $[\text{vec}(\mathbf{X})]^H \text{vec}(\mathbf{X}) = N^2$ and $\lambda_{\max}(\boldsymbol{\Sigma}_1) = 2N^2$ as stated in (Song et al., 2015a). Therefore, the first and third terms are constant in (2.60). After ignoring the constant terms, one can rewrite (2.59) as follows

$$\begin{aligned}
&\underset{\mathbf{x}, \mathbf{X}}{\text{minimize}} && \text{Re} \left([\text{vec}(\mathbf{X})]^H (\boldsymbol{\Sigma}_1 - 2N^2 \mathbf{I}) \text{vec}(\mathbf{X}^{(k)}) \right) \\
&\text{subject to} && \mathbf{X} = \mathbf{x} \mathbf{x}^H \\
&&& |x_n| = 1, \quad n = 1, \dots, N.
\end{aligned} \tag{2.61}$$

The objective function in (2.61) can also be written as

$$\sum_{p=1}^{2N} \text{Tr}(\mathbf{X}^{(k)} \mathbf{A}_p) \text{Tr}(\mathbf{A}_p \mathbf{X}) - 2\lambda_{\max}(\boldsymbol{\Sigma}) \text{Tr}(\mathbf{X}^{(k)} \mathbf{X}). \tag{2.62}$$

Then, the minimization problem in (2.61) can be expressed as follows (Song et al., 2015a)

$$\begin{aligned}
&\underset{\mathbf{x}}{\text{minimize}} && \sum_{p=1}^{2N} |\mathbf{a}_p^H \mathbf{x}^{(k)}|^2 |\mathbf{a}_p^H \mathbf{x}|^2 - 2N^2 |\mathbf{x}^H \mathbf{x}^{(k)}|^2 \\
&\text{subject to} && |x_n| = 1, \quad n = 1, \dots, N.
\end{aligned} \tag{2.63}$$

Minimization problem in (2.63) can alternatively be written as

$$\begin{aligned}
&\underset{\mathbf{x}}{\text{minimize}} && \mathbf{x}^H \left(\mathbf{A} \text{Diag}(\mathbf{p}^{(k)}) \mathbf{A}^H - 2N^2 \mathbf{x}^{(k)} (\mathbf{x}^{(k)})^H \right) \mathbf{x} \\
&\text{subject to} && |x_n| = 1, \quad n = 1, \dots, N
\end{aligned} \tag{2.64}$$

where $\mathbf{A} = [\mathbf{a}_1 \ \mathbf{a}_2 \ \dots \ \mathbf{a}_{2N}]$ and $\mathbf{p}^{(k)} = |\mathbf{A}^H \mathbf{x}^{(k)}|^2$.

In order to further simplify the optimization problem in (2.64), the second majorization is applied with $\mathbf{K} = p_{\max}^{(k)} \mathbf{A} \mathbf{A}^H \succeq \mathbf{A} \text{Diag}(\mathbf{p}^{(k)}) \mathbf{A}^H - 2N^2 \mathbf{x}^{(k)} (\mathbf{x}^{(k)})^H$. Then, the majorizing function can be expressed as follows

$$\begin{aligned} u_2(\mathbf{x}, \mathbf{x}^{(k)}) &= p_{\max}^{(k)} \mathbf{x}^H \mathbf{A} \mathbf{A}^H \mathbf{x} \\ &+ 2 \text{Re} \left(\mathbf{x}^H \left(\tilde{\mathbf{A}} - 2N^2 \mathbf{x}^{(k)} (\mathbf{x}^{(k)})^H \right) \mathbf{x}^{(k)} \right) \\ &+ (\mathbf{x}^{(k)})^H \left(2N^2 \mathbf{x}^{(k)} (\mathbf{x}^{(k)})^H - \tilde{\mathbf{A}} \right) \mathbf{x}^{(k)}. \end{aligned} \quad (2.65)$$

After ignoring the constant terms in the majorizing function in (2.65), one has the following optimization problem

$$\begin{aligned} &\underset{\mathbf{x}}{\text{minimize}} \quad \text{Re} \left(\mathbf{x}^H \left(\tilde{\mathbf{A}} - 2N^2 \mathbf{x}^{(k)} (\mathbf{x}^{(k)})^H \right) \mathbf{x} \right) \\ &\text{subject to} \quad |x_n| = 1, \quad n = 1, \dots, N \end{aligned} \quad (2.66)$$

where $\tilde{\mathbf{A}} = \mathbf{A} \left(\text{Diag}(\mathbf{p}^{(k)}) - p_{\max}^{(k)} \mathbf{I} \right) \mathbf{A}^H$.

Defining $\mathbf{y} = - \left(\tilde{\mathbf{A}} - 2N^2 \mathbf{x}^{(k)} (\mathbf{x}^{(k)})^H \right) \mathbf{x}^{(k)}$, (2.66) can be rewritten as follows (Song et al., 2015a)

$$\begin{aligned} &\underset{\mathbf{x}}{\text{minimize}} \quad \|\mathbf{x} - \mathbf{y}\| \\ &\text{subject to} \quad |x_n| = 1, \quad n = 1, \dots, N. \end{aligned} \quad (2.67)$$

In (Song et al., 2015a, 2015b) the solution of (2.67) is given as follows

$$x_n = e^{j \arg(y_n)}, \quad n = 1, \dots, N. \quad (2.68)$$

As an example, the MISL algorithm is initialized by Golomb sequence of length $N = 1000$. Correlation level (dB) of the sequence designed by MISL is plotted in Figure 2.7.

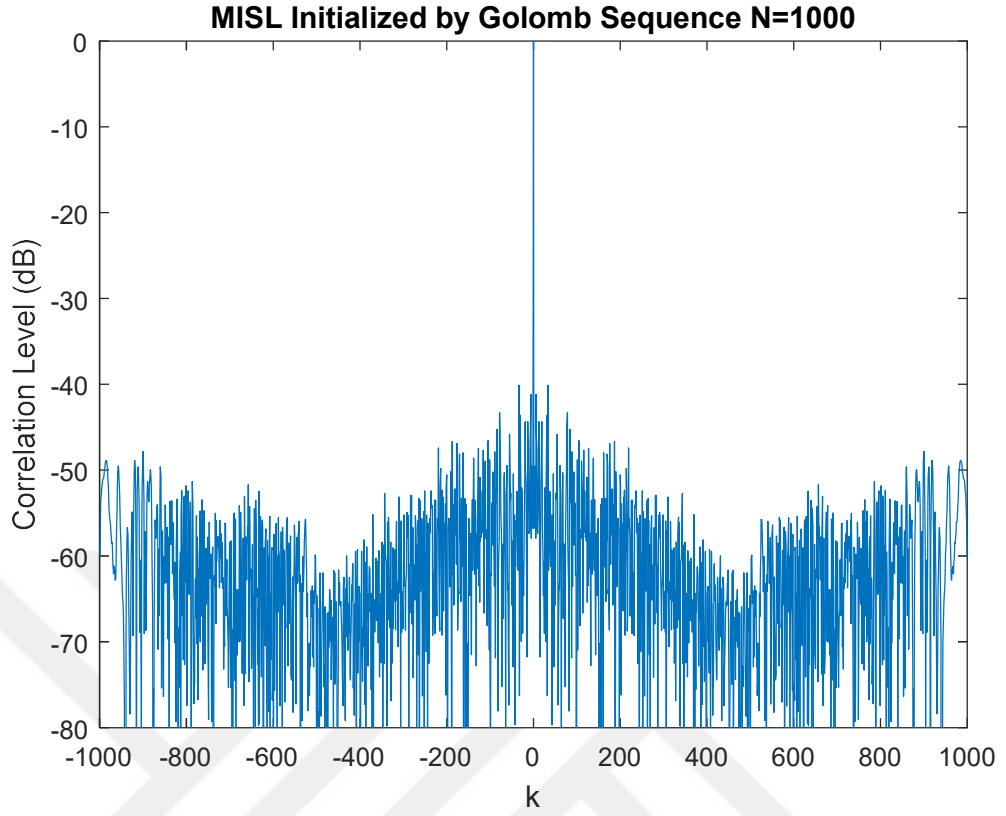


Figure 2.7 Correlation level of the transmit sequence designed by the MISL algorithm (in dB)

2.2.2 MWISL

Autocorrelation function of the sequence $\{x_n\}_{n=1}^N$ can be expressed alternatively as (Song et al., 2016b)

$$r_k = \text{Tr}(\mathbf{U}_k \mathbf{x} \mathbf{x}^H), \quad k = 0, \dots, N-1 \quad (2.69)$$

where \mathbf{U}_k is a Toeplitz matrix with its k^{th} diagonal elements being 1 and other elements being 0. Then, the optimization problem for minimizing WISL in (2.5) can be rewritten (Song et al., 2016b) as

$$\begin{aligned} & \underset{\mathbf{x}, \mathbf{X}}{\text{minimize}} && \frac{1}{2} \sum_{k=-(N-1)}^{N-1} w_k |\text{Tr}(\mathbf{U}_k \mathbf{X})|^2 \\ & \text{subject to} && \mathbf{X} = \mathbf{x} \mathbf{x}^H \\ & && |x_n| = 1, \quad n = 1, \dots, N \end{aligned} \quad (2.70)$$

where $w_{-k} = w_k$ and $w_0 = 0$. Since $\text{Tr}(\mathbf{U}_k \mathbf{X}) = \text{vec}(\mathbf{X})^H \text{vec}(\mathbf{U}_k)$, (2.70) can be written as (Song et al., 2016b)

$$\begin{aligned} & \underset{\mathbf{X}}{\text{minimize}} && \frac{1}{2} \sum_{k=-(N-1)}^{N-1} w_k [\text{vec}(\mathbf{X})]^H \text{vec}(\mathbf{U}_k) [\text{vec}(\mathbf{U}_k)]^H \text{vec}(\mathbf{X}) \\ & \text{subject to} && \mathbf{X} = \mathbf{x}\mathbf{x}^H \\ & && |x_n| = 1, \quad n = 1, \dots, N. \end{aligned} \quad (2.71)$$

The above problem can alternatively be expressed as (Song et al., 2016b)

$$\begin{aligned} & \underset{\mathbf{X}}{\text{minimize}} && \frac{1}{2} [\text{vec}(\mathbf{X})]^H \mathbf{E}_1 \text{vec}(\mathbf{X}) \\ & \text{subject to} && \mathbf{X} = \mathbf{x}\mathbf{x}^H \\ & && |x_n| = 1, \quad n = 1, \dots, N \end{aligned} \quad (2.72)$$

where

$$\mathbf{E}_1 = \sum_{k=-(N-1)}^{N-1} w_k \text{vec}(\mathbf{U}_k) [\text{vec}(\mathbf{U}_k)]^H. \quad (2.73)$$

Construction of the majorizing function for the WISL metric is started using Lemma 1. The objective function in (2.72) is a quadratic function of \mathbf{X} . Then, one can apply Lemma 1 to $[\text{vec}(\mathbf{X})]^H \mathbf{E}_1 \text{vec}(\mathbf{X})$ with $\mathbf{K} = \lambda_{\max}(\mathbf{E}_1) \mathbf{I}$ where $\lambda_{\max}(\mathbf{E}_1)$ is the maximum eigenvalue of \mathbf{E}_1 . It is given as $\lambda_{\max}(\mathbf{E}_1) = \max_k \{w_k (N-k) \mid k = 1, \dots, N-1\}$ (Song et al., 2016b). Then, the majorizing function for the objective function is (Song et al., 2016b) found as

$$\begin{aligned} u_1(\mathbf{X}, \mathbf{X}^{(l)}) &= \frac{1}{2} \lambda_{\max}(\mathbf{E}_1) [\text{vec}(\mathbf{X})]^H \text{vec}(\mathbf{X}) \\ &+ \text{Re} \left([\text{vec}(\mathbf{X})]^H (\mathbf{E}_1 - \lambda_{\max}(\mathbf{E}_1) \mathbf{I}) \text{vec}(\mathbf{X}^{(l)}) \right) \\ &+ \frac{1}{2} [\text{vec}(\mathbf{X}^{(l)})]^H (\lambda_{\max}(\mathbf{E}_1) \mathbf{I} - \mathbf{E}_1) \text{vec}(\mathbf{X}^{(l)}). \end{aligned} \quad (2.74)$$

Since $[\text{vec}(\mathbf{X})]^H \text{vec}(\mathbf{X}) = (\mathbf{x}^H \mathbf{x})^2 = N^2$, the first term is a constant. Therefore, the majorized version of (2.72) can be written as follows (Song et al., 2016b)

$$\begin{aligned} & \underset{\mathbf{x}, \mathbf{X}}{\text{minimize}} \quad \text{Re} \left([\text{vec}(\mathbf{X})]^H (\mathbf{E}_1 - \lambda_{\max}(\mathbf{E}_1) \mathbf{I}) \text{vec}(\mathbf{X}^{(l)}) \right) \\ & \text{subject to} \quad \mathbf{X} = \mathbf{x}\mathbf{x}^H \\ & \quad |x_n| = 1, \quad n = 1, \dots, N. \end{aligned} \quad (2.75)$$

(2.75) can be expressed by using (2.73) as (Song et al., 2016b)

$$\begin{aligned} & \underset{\mathbf{x}, \mathbf{X}}{\text{minimize}} \quad \sum_{k=-(N-1)}^{N-1} w_k \text{Re} \left[\text{Tr}(\mathbf{U}_{-k} \mathbf{X}^{(l)}) \text{Tr}(\mathbf{U}_k \mathbf{X}) \right] \\ & \quad - \lambda_{\max}(\mathbf{E}_1) \text{Tr}(\mathbf{X}^{(l)} \mathbf{X}) \\ & \text{subject to} \quad \mathbf{X} = \mathbf{x}\mathbf{x}^H \\ & \quad |x_n| = 1, \quad n = 1, \dots, N. \end{aligned} \quad (2.76)$$

It can be seen from (2.69) that $\text{Tr}(\mathbf{U}_{-k} \mathbf{X}^{(l)}) = r_{-k}^{(l)}$. Then, (2.76) can be rewritten as

$$\begin{aligned} & \underset{\mathbf{x}, \mathbf{X}}{\text{minimize}} \quad \text{Re} \left(\text{Tr} \left(\sum_{k=-(N-1)}^{N-1} w_k r_{-k}^{(l)} \mathbf{U}_{-k} \mathbf{X} \right) \right) - \lambda_{\max}(\mathbf{E}_1) \text{Tr}(\mathbf{X}^{(l)} \mathbf{X}) \\ & \text{subject to} \quad \mathbf{X} = \mathbf{x}\mathbf{x}^H \\ & \quad |x_n| = 1, \quad n = 1, \dots, N. \end{aligned} \quad (2.77)$$

Defining a Hermitian Toeplitz matrix as

$$\mathbf{R}_1 = \sum_{k=-(N-1)}^{N-1} w_k r_{-k}^{(l)} \mathbf{U}_k = \begin{bmatrix} 0 & w_1 r_{-1}^{(l)} & \dots & w_{N-1} r_{1-N}^{(l)} \\ w_1 r_1^{(l)} & 0 & \ddots & \vdots \\ \vdots & \ddots & \ddots & w_1 r_{-1}^{(l)} \\ w_{N-1} r_{N-1}^{(l)} & \dots & w_1 r_1^{(l)} & 0 \end{bmatrix}, \quad (2.78)$$

the objective function in (2.77) is written as $\text{Re}[\text{Tr}(\mathbf{R}_1 \mathbf{X})] - \lambda_{\max}(\mathbf{E}_1) \text{Tr}(\mathbf{X}^{(l)} \mathbf{X})$. The

first term can be expressed as $\text{Re}(\mathbf{x}^H \mathbf{R}_1 \mathbf{x})$. Using the fact that $\text{Re}(\mathbf{b}) = \frac{\mathbf{b} + \mathbf{b}^H}{2}$ for any

complex vector \mathbf{b} , the first term of the objective function in (2.77) is equal to $\mathbf{x}^H \mathbf{R}_1 \mathbf{x}$. Therefore, the optimization problem in (2.77) can be rewritten as

$$\begin{aligned} & \underset{\mathbf{x}}{\text{minimize}} \quad \mathbf{x}^H \left(\mathbf{R}_1 - \lambda_{\max}(\mathbf{E}_1) \mathbf{x}^{(l)} (\mathbf{x}^{(l)})^H \right) \mathbf{x} \\ & \text{subject to} \quad |x_n| = 1, \quad n = 1, \dots, N. \end{aligned} \quad (2.79)$$

The objective function in (2.79) is a quadratic function of \mathbf{x} . Then, the majorization function of the objective function can be obtained by applying Lemma 1 with $\lambda_{\max} \left(\mathbf{R}_1 - \lambda_{\max}(\mathbf{E}_1) \mathbf{x}^{(l)} (\mathbf{x}^{(l)})^H \right)$. However, in (Song et al., 2016b) it is proposed to use some upper bound of $\lambda_{\max} \left(\mathbf{R}_1 - \lambda_{\max}(\mathbf{E}_1) \mathbf{x}^{(l)} (\mathbf{x}^{(l)})^H \right)$ for the purpose of computational efficiency and simplicity.

Lemma 2 (Song et al., 2016b): Let \mathbf{T} be an $N \times N$ Hermitian Toeplitz matrix given as

$$\mathbf{T} = \begin{bmatrix} t_0 & t_1^* & \dots & t_{N-1}^* \\ t_1 & t_0 & \ddots & \vdots \\ \vdots & \ddots & \ddots & t_1^* \\ t_{N-1} & \dots & t_1 & t_0 \end{bmatrix} \quad (2.80)$$

and \mathbf{F}_{2N}^H be the $2N \times 2N$ DFT matrix defined as

$$\left[\mathbf{F}_{2N}^H \right]_{k,l} = e^{-j \frac{2\pi}{2N} kl}, \quad 0 \leq k, l \leq 2N-1. \quad (2.81)$$

Then, the following boundaries can be written,

$$\begin{aligned} \lambda_{\max}(\mathbf{T}) &\leq \frac{1}{2} \left(\max_{1 \leq i \leq N} \mu_{2i} + \max_{1 \leq i \leq N} \mu_{2i-1} \right) = \lambda_u \\ \lambda_{\min}(\mathbf{T}) &\geq \frac{1}{2} \left(\min_{1 \leq i \leq N} \mu_{2i} + \min_{1 \leq i \leq N} \mu_{2i-1} \right) = \lambda_l \end{aligned} \quad (2.82)$$

with $\boldsymbol{\mu} = \mathbf{F}_{2N}^H \mathbf{c}$ and $\mathbf{c} = [t_0 \quad t_1 \quad \dots \quad t_{N-1} \quad 0 \quad t_{N-1}^* \quad \dots \quad t_1^*]^T$.

Since $\lambda_{\max}(\mathbf{E}_1) \geq 0$ (Song et al., 2016b), the following inequality can be written (Song et al., 2016b)

$$\lambda_u \geq \lambda_{\max}(\mathbf{R}_1) \geq \lambda_{\max}\left(\mathbf{R}_1 - \lambda_{\max}(\mathbf{E}_1)\mathbf{x}^{(l)}\left(\mathbf{x}^{(l)}\right)^H\right). \quad (2.83)$$

Then, one can apply Lemma 1 to the objective function in (2.79) with $\mathbf{K} = \lambda_u \mathbf{I}$. Thus, the majorizing function of the objective function in (2.79) can be written as follows

$$\begin{aligned} u_2(\mathbf{x}, \mathbf{x}^{(l)}) &= \lambda_u (\mathbf{E}_1) \mathbf{x}^H \mathbf{x} \\ &+ 2 \operatorname{Re}\left(\mathbf{x}^H \left(\mathbf{R}_1 - \lambda_{\max}(\mathbf{E}_1)\mathbf{x}^{(l)}\left(\mathbf{x}^{(l)}\right)^H - \lambda_u \mathbf{I}\right)\mathbf{x}^{(l)}\right) \\ &+ \left(\mathbf{x}^{(l)}\right)^H \left(\lambda_{\max}(\mathbf{E}_1)\mathbf{I} - \mathbf{E}_1\right)\mathbf{x}^{(l)}. \end{aligned} \quad (2.84)$$

Since $\mathbf{x}^H \mathbf{x} = N$, the first term on the right hand side is constant. After ignoring constant terms, optimization problem can be reformulated using the majorizing function as follows

$$\begin{aligned} &\underset{\mathbf{x}}{\text{minimize}} \quad 2 \operatorname{Re}\left(\mathbf{x}^H \left(\mathbf{R}_1 - \lambda_{\max}(\mathbf{E}_1)\mathbf{x}^{(l)}\left(\mathbf{x}^{(l)}\right)^H - \lambda_u \mathbf{I}\right)\mathbf{x}^{(l)}\right) \\ &\text{subject to} \quad |x_n| = 1, \quad n = 1, \dots, N. \end{aligned} \quad (2.85)$$

Finally, after expressing the optimization problem in (2.85) as

$$\begin{aligned} &\underset{\mathbf{x}}{\text{minimize}} \quad \|\mathbf{x} - \mathbf{y}\| \\ &\text{subject to} \quad |x_n| = 1, \quad n = 1, \dots, N \end{aligned} \quad (2.86)$$

where $\mathbf{y} = -\left(\mathbf{R}_1 - \lambda_{\max}(\mathbf{E}_1)\mathbf{x}^{(l)}\left(\mathbf{x}^{(l)}\right)^H - \lambda_u \mathbf{I}\right)\mathbf{x}^{(l)}$, the closed form solution of the minimization problem in (2.86) is given as follows (Song et al., 2016b)

$$x_n = e^{j \arg(y_n)}, \quad n = 1, \dots, N. \quad (2.87)$$

As a numerical example, correlation level of a transmit sequence with length $N = 100$ designed by the MWISL algorithm can be seen in Figure 2.8. The algorithm is initialized by Golomb sequence and the weighting factors are taken as in (2.47).

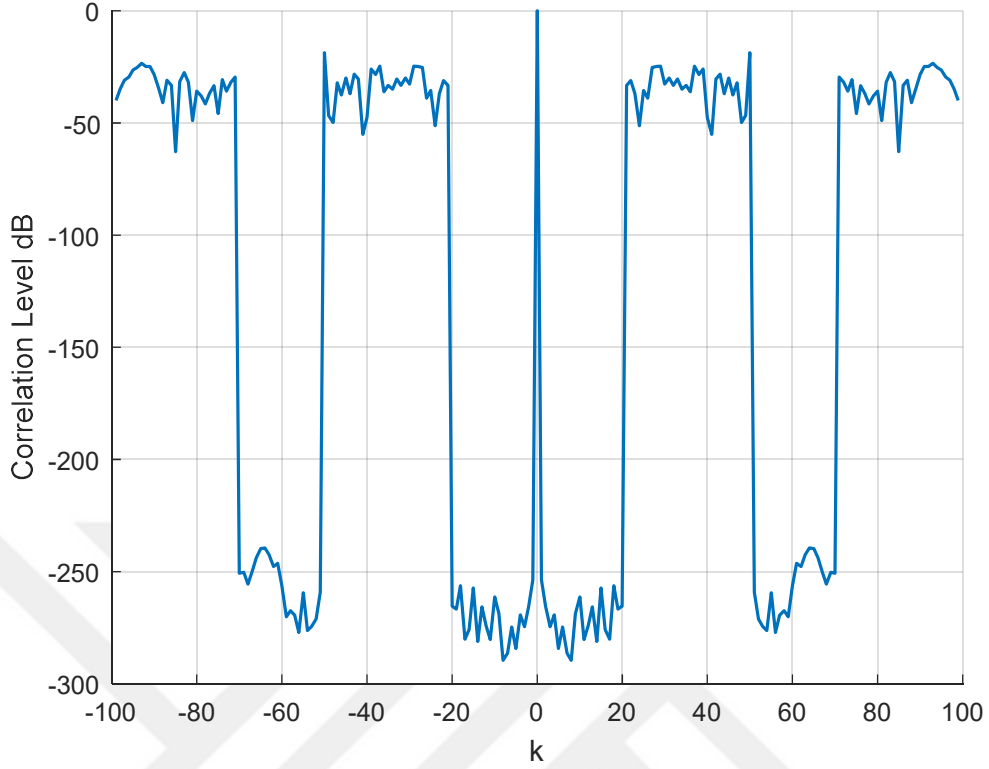


Figure 2.8 Correlation level of a transmit sequence designed by the MWISL algorithm (in dB)

2.2.3 WPISL

In (Zhao et al., 2016), a unified metric named “weighted peak or the integrated sidelobe level” (WPISL) was proposed as follows

$$\text{WPISL} = \sum_{k=1}^{N-1} w_k |r_k|^p \quad (2.88)$$

where $2 \leq p < +\infty$ and $\{w_k\}_{k=1}^{N-1}$ are nonnegative weights. This metric encompasses the metrics of ISL, WISL, and PSL by assigning the values of p and $\{w_k\}_{k=1}^{N-1}$ appropriately. Hence, it was termed as the unified metric. For example, if one lets $p = 2$, then (2.88) becomes the WISL metric. If $p = 2$ and $\{w_k\}_{k=1}^{N-1} = 1$ are substituted, then (2.88) reduces to the ISL metric. Finally, if $p \rightarrow +\infty$ and $\{w_k\}_{k=1}^{N-1} = 1$, then the PSL metric is recovered.

The optimization problem for finding a unimodular sequence which minimizes the metric of WPISL is given as follows

$$\begin{aligned} & \underset{\mathbf{x}}{\text{minimize}} && \text{WPISL} \\ & \text{subject to} && |x_n| = 1, n = 1, \dots, N. \end{aligned} \quad (2.89)$$

Then, the problem can be rewritten by using (2.88) as

$$\begin{aligned} & \underset{\mathbf{x}}{\text{minimize}} && \sum_{k=1}^{N-1} w_k |r_k|^p \\ & \text{subject to} && |x_n| = 1, n = 1, \dots, N. \end{aligned} \quad (2.90)$$

In (Zhao et al., 2016), the MM method was proposed to solve the problem in (2.90). For this purpose, construction of majorizing function for WPISL metric is started by using the following lemma.

Lemma 3 (*Lemma 2* in (Song et al., 2015a), *Lemma 10* in (Song et al., 2016b), *Lemma 1* in (Song et al., 2016a)): Let $h(x)$ be a scalar function of x^p , i.e. $h(x) = x^p$, where $p \geq 2$. The local majorizing function of $h(x)$ at $x_0 \in [0, \bar{x}]$ on the interval $[0, \bar{x}]$ is $\bar{h}(x; x_0) = ax^2 + bx + ax_0^2 - (p-1)x_0^p$. a and b in the local majorizing function are given as $a = [\bar{x}^p - x_0^p - px_0^{p-1}(\bar{x} - x_0)] / (\bar{x} - x_0)^2 \geq 0$ and $b = px_0^{p-1} - 2ax_0 \leq 0$, respectively. In (Zhao et al., 2016), it is stated that monotonicity is maintained and infeasibility will not occur by using such a local majorizing function.

Let the function $f(\mathbf{x})$ denote the WPISL metric. Thus, one can define $f(\mathbf{x}) \triangleq \sum_{k=1}^{N-1} w_k |r_k|^p$ where $r_k = \mathbf{x}^H \mathbf{U}_k \mathbf{x}$ and $\mathbf{U}_k \in \mathbb{R}^{N \times N}$. In Lemma 3, x corresponds to $|r_k|$ and x_0 corresponds to $|r_k(\mathbf{x}^{(l)})|$ where $\mathbf{x}^{(l)}$ represents the sequence at the l^{th} iteration of the MM algorithm. Then, by using Lemma 1, we can write

$$f(\mathbf{x}) \leq \sum_{k=1}^{N-1} w_k \left(a_k |r_k|^2 + b_k |r_k| + \text{constant} \right) \quad (2.91)$$

where a_k and b_k are calculated using the definition in Lemma 3. These parameters are different for each k value like the upper limit, \bar{x} . The upper limit for each k value is calculated as follows (Zhao et al., 2016)

$$\bar{x}_k = \begin{cases} \left(\frac{1}{w_k} \sum_{m=1}^{N-1} w_m |r_m^{(l)}|^p \right)^{1/p}, & w_k \neq 0 \\ 0, & w_k = 0. \end{cases} \quad (2.92)$$

After employing Lemma 3 by considering $w_{-k} = w_k$, $w_0 = 0$, $b_{-k} = b_k$, and $b_0 = 0$, the result of the first majorization is expressed in (Zhao et al., 2016) as follows

$$f(\mathbf{x}) \leq \sum_{k=1}^{N-1} w_k a_k |r_k|^2 + \frac{1}{2} \mathbf{x}^H \mathbf{B} \mathbf{x} + \text{constant} \quad (2.93)$$

where

$$\mathbf{B} = \sum_{k=-(N-1)}^{N-1} w_k b_k \frac{r_{-k}^{(l)}}{|r_{-k}^{(l)}|} \mathbf{U}_k \quad (2.94)$$

and $\mathbf{U}_{-k} = \mathbf{U}_k^H$. As can be seen from (2.93), the second term of the majorizing function is quadratic but the first term is still quartic. Therefore, the second majorization is used applying Lemma 1.

The first term of the majorizing function in (2.93), $\sum_{k=1}^{N-1} w_k a_k |r_k|^2 = \sum_{k=1}^{N-1} w_k a_k \left| \mathbf{x}^H \mathbf{U}_k \mathbf{x} \right|^2$, can be written as (Zhao et al., 2016)

$$\frac{1}{2} [\text{vec}(\mathbf{X})]^H \mathbf{E}_2 \text{vec}(\mathbf{X}) \quad (2.95)$$

where $\mathbf{X} = \mathbf{x}\mathbf{x}^H$ and

$$\mathbf{E}_2 = \sum_{k=-(N-1)}^{N-1} w_k a_k \text{vec}(\mathbf{U}_{-k}) [\text{vec}(\mathbf{U}_{-k})]^H, \quad (2.96)$$

with $a_k = a_{-k}$ and $a_0 = 0$. After employing majorization using Lemma 1 with $\mathbf{K} = \lambda_{\max}(\mathbf{E}_2)\mathbf{I}$, the result is given in (Zhao et al., 2016) as

$$\frac{1}{2}\lambda_{\max}(\mathbf{E}_2)\|\mathbf{x}\|^4 + \mathbf{x}^H \left(\mathbf{R}_2 - \lambda_{\max}(\mathbf{E}_2)\mathbf{x}^{(l)}(\mathbf{x}^{(l)})^H \right) \mathbf{x} + \text{constant} \quad (2.97)$$

where

$$\mathbf{R}_2 = \sum_{k=-(N-1)}^{N-1} \frac{p}{2} w_k |r_k^{(l)}|^{p-2} r_{-k}^{(l)} \mathbf{U}_k. \quad (2.98)$$

The expression in (2.97) majorizes the objective function in (2.93). Then, one can apply Lemma 1 on the second term in (2.97) with $\mathbf{K} = \lambda_R \mathbf{I}$ where λ_R is chosen such that $\lambda_R \geq \lambda_{\max}(\mathbf{R}_2)$ and the majorizing function of the second term is obtained as (Zhao et al., 2016)

$$\begin{aligned} u_3(\mathbf{x}, \mathbf{x}^{(l)}) &\leq \lambda_R \mathbf{x}^H \mathbf{x} + 2 \operatorname{Re} \left[\mathbf{x}^H \left(\mathbf{R}_2 - \lambda_{\max}(\mathbf{E}_2)\mathbf{x}^{(l)}(\mathbf{x}^{(l)})^H - \lambda_R \mathbf{I} \right) \mathbf{x}^{(l)} \right] + \text{constant} \\ &= \lambda_R \|\mathbf{x}\|^2 - 2\lambda_R \operatorname{Re}[\mathbf{y}^H \mathbf{x}] + \text{constant}. \end{aligned} \quad (2.99)$$

Finally, the optimization problem to find the constant modulus unimodular sequence minimizing the WPISL metric can be written as follows

$$\begin{aligned} &\underset{\mathbf{x}}{\text{minimize}} && -\operatorname{Re}[\mathbf{y}^H \mathbf{x}] \\ &\text{subject to} && |x_n| = 1, n = 1, \dots, N \end{aligned} \quad (2.100)$$

where $\mathbf{y} = \left(1 + \frac{\lambda_{\max}(\mathbf{E}_2)}{\lambda_R} \|\mathbf{x}^{(l)}\|^2 \right) \mathbf{x}^{(l)} - \frac{1}{\lambda_R} \mathbf{R}_2 \mathbf{x}^{(l)}$. Then, the closed form solution of the problem in (2.100) is given as follows

$$x_n = e^{j \arg(y_n)}, n = 1, \dots, N. \quad (2.101)$$

To provide a numerical example, correlation level of a transmit sequence with length $N = 100$ obtained by the WPISL algorithm can be seen in Figure 2.9. The

algorithm is initialized by Golomb sequence and the weighting coefficients are taken as in (2.47).

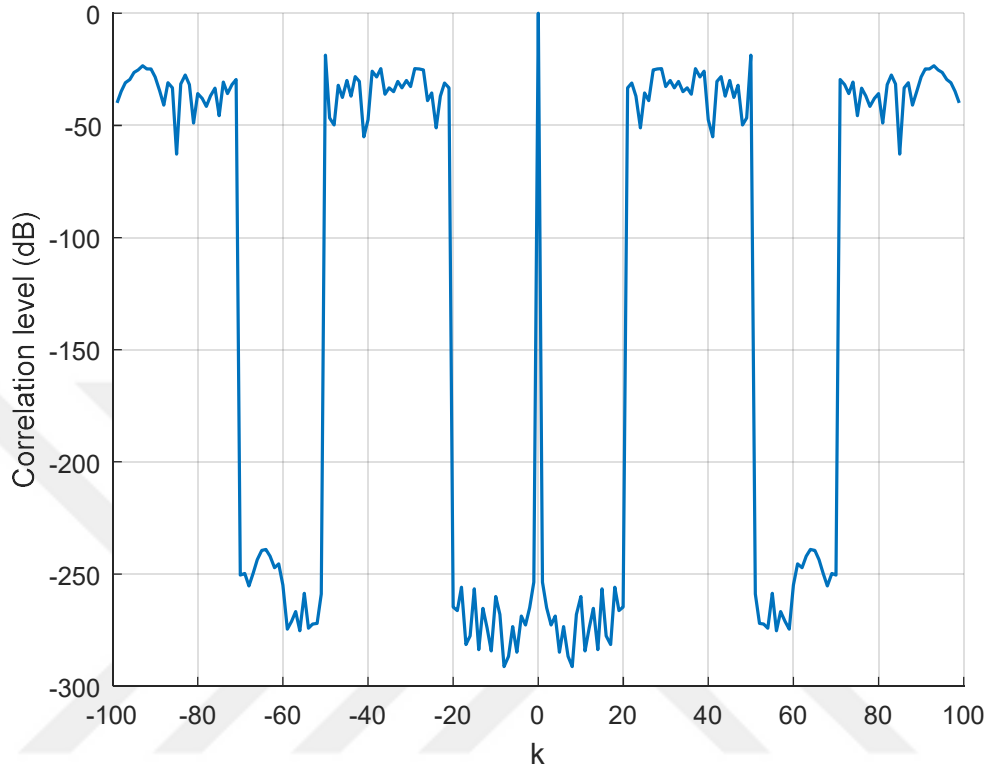


Figure 2.9 Correlation level of the transmit sequence designed by the WPISL algorithm (in dB)

CHAPTER THREE

DESIGN OF SEQUENCES WITH LOW AUTOCORRELATION SIDELOBES USING GENETIC ALGORITHMS

In this chapter, we employ genetic algorithm (GA) to synthesize unimodular sequences with low ISL and compare the results against the CAN algorithm. Although the CAN algorithm minimizes an “almost equivalent” ISL metric which is quadratic in the sequence designed, GA is employed to minimize the exact metric of ISL which is quartic. Our simulation results demonstrate that minimization of ISL utilizing GA produces slightly better results than CAN (Bişkin & Akay, 2017).

As mentioned in Section 1.1, computational methods such as GA are not efficient in terms of computation time for designing sequences. On the other hand, the methods given in Chapter 2 may converge to a local minimum and the corresponding algorithms might obtain a suboptimal solution instead of the optimal one. Thus, in this thesis, we employ GA not for designing sequences, but as a benchmark solution for the minimization problem in order to decipher how close the proposed algorithms in Chapter 2 are able to converge to the optimal global solution. Because of this, performance evaluation of GA in designing sequences is out of scope of this thesis.

3.1 Genetic Algorithms

In this section, the following exact quartic cost function is minimized using GA to obtain a sequence with minimum ISL

$$\sum_{p=1}^{2N} \left[\left| \sum_{n=1}^N x_n e^{-j\omega_p n} \right|^2 - N \right]^2. \quad (3.1)$$

GA is one of the global optimization algorithms developed by taking inspiration from biological mechanisms of natural selection. In biology, the most adaptable generations manage to stay alive after natural selection mechanisms ongoing through the years. In the same way, the most probable solution of an optimization problem eliminates the alternative solutions after execution of the GA for that problem.

Generally, GA is used when the analytic solution of the optimization problem cannot be found easily. Another advantage of GA is that it is less likely to converge to a local minimum. Therefore, GA is able to both provide performance improvement and solve complex optimization problems (Capraro et al., 2008; Lellouch et al., 2015, 2016; Martone et al., 2016; Smith-Martinez et al., 2013; G. Sun et al., 2016; Weile & Michielssen, 1997). The basic concepts relevant to GA are explained as follows:

Population: The set which may include the possible solutions of the problem.

Individual: Each element in the population set is named as an individual.

Generation: The process of reproduction of the individuals which are included in the population.

Parents: Individuals which are used in the reproduction process.

Child: An individual arising from two parents after reproduction process.

Initialization: The process to create the initial population of the algorithm.

Selection: The process of determining the appropriate parents in order to give a child.

Crossover: Changing the chromosome of individuals from generations to generations (see Figure 3.1).

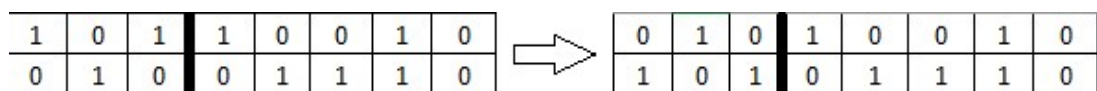


Figure 3.1 An example of crossover

Mutation: A random change which occurs in the chromosome of individuals (see Figure 3.2)

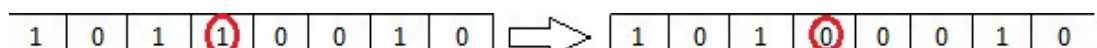


Figure 3.2 An example of mutation

As the first numerical example, GA is initialized with Golomb sequence of length $N = 100$ in order to minimize the exact cost function in (3.1). Correlation level (dB) of the sequence designed by GA can be seen in Figure 3.3.

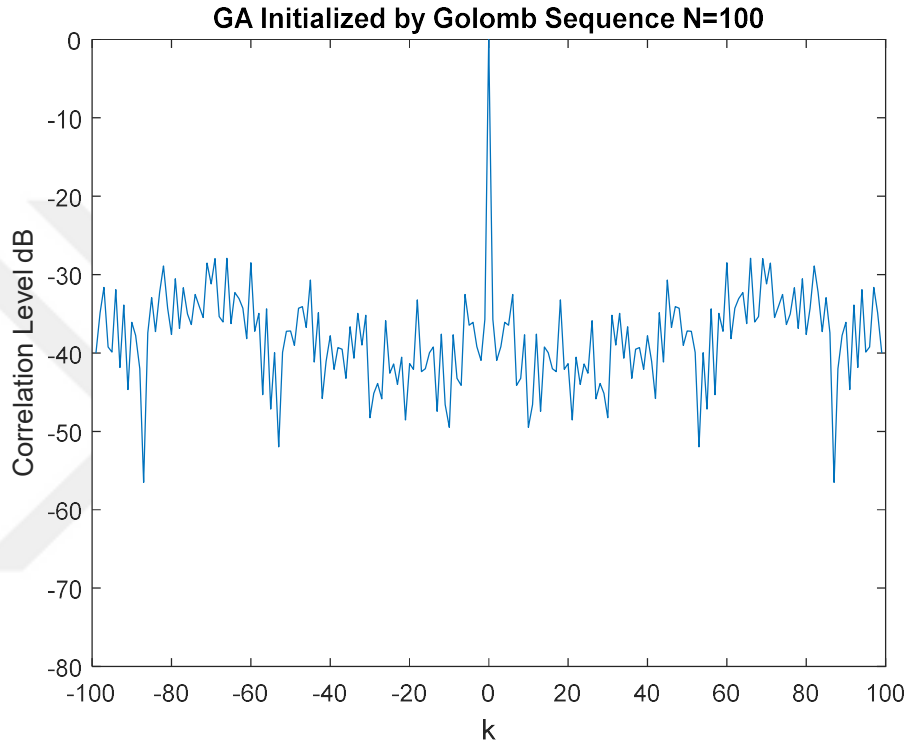


Figure 3.3 Correlation level (in dB) of the transmit sequence designed by GA

3.2 Numerical Examples for Minimizing ISL

For CAN and MISL algorithms, the stopping criterion is determined as $\|\mathbf{x}^{(k+1)} - \mathbf{x}^{(k)}\| \leq 10^{-3}$ in parallel to (Stoica et al., 2009). For GA, the stopping criterion is selected as the maximum number of generations. The population size, maximum number of generations, crossover, and mutation operations explained in the previous section are also presented as other inputs for GA. We decided the population size to be 150 and the maximum number of generations is assigned as 20000. We use both crossover and mutation operations in order to increase the diversity in the population.

5 % of the population is selected as elite individuals in each generation. They maintain their chromosomes without any mutation or crossover (Bişkin & Akay, 2017).

Simulations were performed by employing two different initialization scenarios. In the first experiment, the initialization sequence $\mathbf{x} = [e^{j\varphi_1} \dots e^{j\varphi_N}]^T$ is formed by selecting phases $\{\varphi_p\}_{p=1}^N$ as independent random variables uniformly distributed in the interval $[-\pi, \pi]$. Sequence lengths of $N=9, 25, 32, 64,$ and 100 were tried out. Experiments were repeated several times and performance of the algorithms was calculated by taking the average value of the output metrics for each simulation. Due to its long computation time, GA was repeated only 10 times as opposed to CAN and MISL which were repeated 100 times. Average MF values of the designed sequences using the three algorithms are presented in Table 3.1. MFs of designed sequences versus signal length can be seen in Figure 3.4. It can be understood from Figure 3.4 that GA performs better than CAN in terms of MF for all the simulated sequence lengths. However, it performs slightly worse than MISL for larger sequence lengths. The reason for this is that GA parameters such as population size, maximum generation number, etc. are selected in order to speed up the algorithm. We have to note that computational complexity of GA increases with larger sequence lengths.

Table 3.1 Average MF values (initialization by random sequence)

Algorithm	N				
	9	25	32	64	100
GA	35.1422	14.6810	13.5195	16.9899	16.8717
CAN	17.7849	11.3143	11.6779	13.8035	14.8095
MISL	20.9399	13.5751	14.4039	16.2363	17.7229

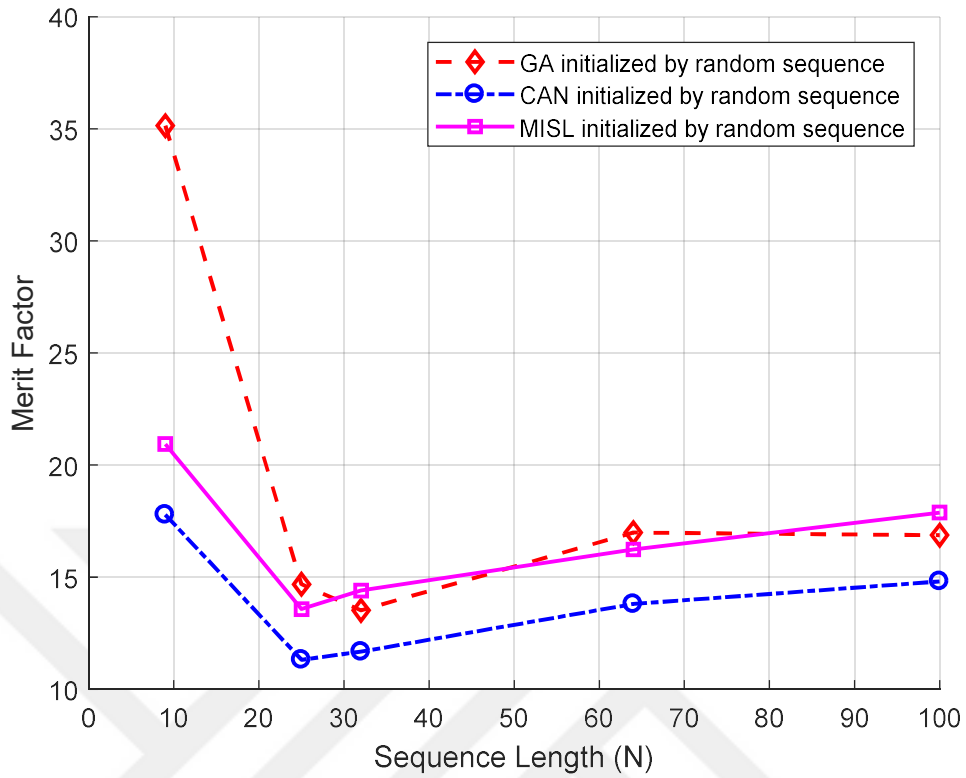


Figure 3.4 Average MF versus sequence length (initialization by random sequence)

As a second experiment, the algorithms were initialized with Golomb sequence. Resulting MFs can be seen in Table 3.2. In Figure 3.5, MFs of the resulting designed sequences with respect to sequence length are plotted.

Table 3.2 MF values (initialization by Golomb sequence)

Algorithm	N				
	9	25	32	64	100
Golomb	5.3666	8.2047	9.1800	12.7733	15.8731
GA	38.2296	20.3287	14.9499	47.9392	57.1046
CAN	38.0151	25.0084	16.9131	46.6691	56.4701
MISL	38.2296	25.6093	14.1476	47.9391	42.4780

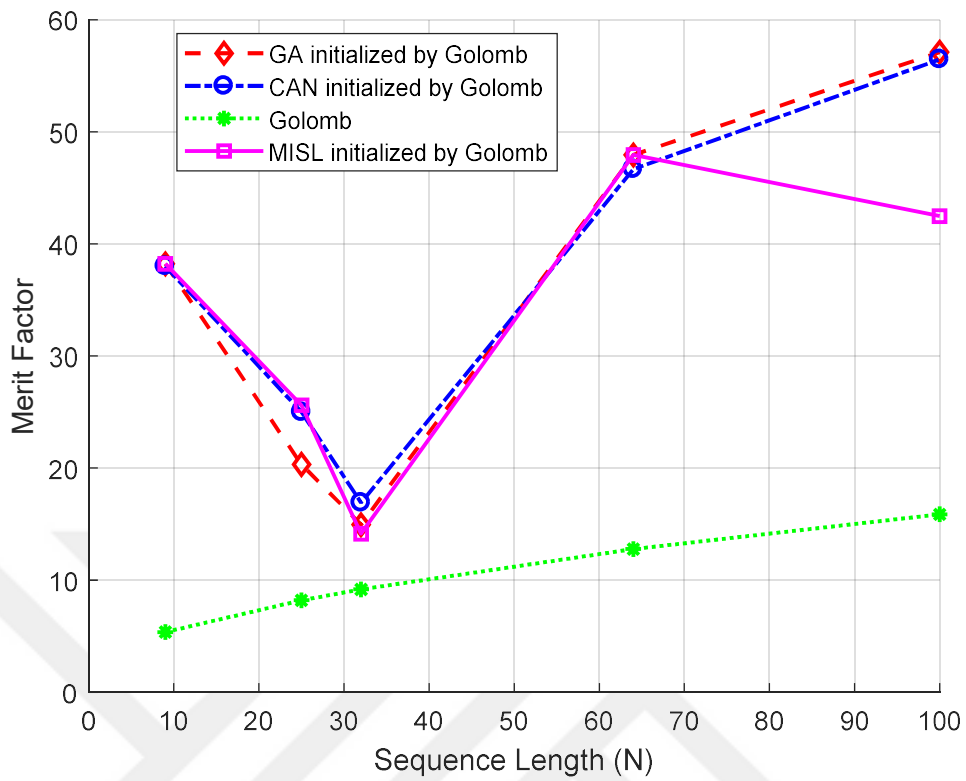


Figure 3.5 MF versus sequence length (initialization by Golomb sequence)

We can see that when algorithms are initialized by a sequence having good correlation properties (e.g. Golomb), their performance in terms of MF increases. As opposed to Figure 3.4, in Figure 3.5 MFs obtained by CAN, MISL, and GA are fairly close to each other.

CHAPTER FOUR
A NEW FREQUENCY DOMAIN SEQUENCE DESIGN ALGORITHM
MINIMIZING WISL

In this chapter, we are interested in designing unimodular sequences via minimizing WISL in (2.5) by way of formulating and implementing the MM method in the frequency domain. Although the already existing WeCAN algorithm is also formulated in the frequency domain, it does not minimize the exact WISL metric but an “almost equivalent” approximation of it. Therefore, we develop an algorithm for directly minimizing the quartic WISL metric in the frequency domain (Bişkin & Akay 2018a). Our simulation results demonstrate that minimization in the frequency domain via the MM method converges to a stationary point in less number of iterations and CPU time (sec.) and can achieve lower WISL levels.

4.1 FWISL

To minimize the exact quartic frequency domain WISL metric in (2.38), we can start by constructing the majorizing function using Lemma 1 (Song et al., 2015a, 2016b; Zhao et al., 2016). By this way, we find a function that majorizes the objective function in (2.38). First of all, we alternatively express the objective function in (2.38) as

$$\text{WISL} = \frac{\gamma_0^2}{4N} \sum_{p=1}^{2N} [\tilde{\mathbf{x}}_p^H \mathbf{\Pi} \tilde{\mathbf{x}}_p - N]^2 = \frac{\gamma_0^2}{4N} \sum_{p=1}^{2N} [\mathbf{x}^H (\mathbf{A}_p \odot \mathbf{\Pi}) \mathbf{x} - N]^2 \quad (4.1)$$

where $\mathbf{a}_p = [e^{j\omega_p} \quad \dots \quad e^{jN\omega_p}]^T$ and $\mathbf{A}_p = \mathbf{a}_p \mathbf{a}_p^H$. In (4.1), \odot represents the Hadamard product. Thus, we can express the minimization problem in (2.38) as

$$\begin{aligned} & \underset{\mathbf{x}}{\text{minimize}} \quad \sum_{p=1}^{2N} \left[(\mathbf{x}^H (\mathbf{A}_p \odot \mathbf{\Pi}) \mathbf{x})^2 + 2N (\mathbf{x}^H (\mathbf{A}_p \odot \mathbf{\Pi}) \mathbf{x}) + N^2 \right] \\ & \text{subject to} \quad |x_n| = 1, n = 1, \dots, N. \end{aligned} \quad (4.2)$$

Let us define $\mathbf{M}_p \triangleq \mathbf{A}_p \odot \mathbf{\Pi}$ and $\mathbf{X} = \mathbf{x} \mathbf{x}^H$. Then, we can rewrite the minimization problem in (4.2) as follows

$$\begin{aligned}
& \underset{\mathbf{x}, \mathbf{X}}{\text{minimize}} && \sum_{p=1}^{2N} \left[\text{Tr}(\mathbf{M}_p \mathbf{X}) \right]^2 - 2N \sum_{p=1}^{2N} \text{Tr}(\mathbf{M}_p \mathbf{X}) \\
& \text{subject to} && \mathbf{X} = \mathbf{x}\mathbf{x}^H \\
& && |x_n| = 1, \quad n = 1, \dots, N
\end{aligned} \tag{4.3}$$

where $\text{Tr}(\cdot)$ denotes trace of a matrix. Since $\mathbf{x}^H (\mathbf{A}_p \odot \mathbf{\Pi}) \mathbf{x} = \text{Tr}(\mathbf{M}_p \mathbf{X})$ is identical to $\frac{1}{\gamma_0} \tilde{\Phi}(\omega_p)$ in (2.37), it is a real-valued scalar. Considering the following equality

$$\text{Tr}(\mathbf{M}_p \mathbf{X}) = \left[\text{vec}(\mathbf{M}_p) \right]^H \text{vec}(\mathbf{X}) = \left[\text{vec}(\mathbf{X}) \right]^H \text{vec}(\mathbf{M}_p), \tag{4.4}$$

where $\text{vec}(\mathbf{X})$ forms a column vector by stacking all the columns of the matrix \mathbf{X} , we can express (4.3) as

$$\begin{aligned}
& \underset{\mathbf{x}, \mathbf{X}}{\text{minimize}} && \left[\text{vec}(\mathbf{X}) \right]^H \boldsymbol{\Sigma}_2 \text{vec}(\mathbf{X}) - 2N \sum_{p=1}^{2N} \text{Tr}(\mathbf{M}_p \mathbf{X}) \\
& \text{subject to} && \mathbf{X} = \mathbf{x}\mathbf{x}^H \\
& && |x_n| = 1, \quad n = 1, \dots, N.
\end{aligned} \tag{4.5}$$

In (4.5), we utilize the definition $\boldsymbol{\Sigma}_2 = \sum_{p=1}^{2N} \text{vec}(\mathbf{M}_p) \left[\text{vec}(\mathbf{M}_p) \right]^H$. Now, we can apply Lemma 1 to $\left[\text{vec}(\mathbf{X}) \right]^H \boldsymbol{\Sigma}_2 \text{vec}(\mathbf{X})$ with $\mathbf{K} = \lambda_{\max}(\boldsymbol{\Sigma}_2) \mathbf{I}$ where $\lambda_{\max}(\boldsymbol{\Sigma}_2)$ denotes the maximum eigenvalue of the matrix $\boldsymbol{\Sigma}_2$. If we denote the matrix at the k^{th} iteration by $\mathbf{X}^{(k)}$, $\left[\text{vec}(\mathbf{X}) \right]^H \boldsymbol{\Sigma}_2 \text{vec}(\mathbf{X})$ is majorized at $\text{vec}(\mathbf{X}^{(k)})$ by the following function,

$$\begin{aligned}
u\left(\text{vec}(\mathbf{X}), \text{vec}(\mathbf{X}^{(k)})\right) &= \lambda_{\max}(\boldsymbol{\Sigma}_2) \left[\text{vec}(\mathbf{X}) \right]^H \text{vec}(\mathbf{X}) \\
&+ 2 \text{Re} \left\{ \left[\text{vec}(\mathbf{X}) \right]^H (\boldsymbol{\Sigma}_2 - \lambda_{\max}(\boldsymbol{\Sigma}_2) \mathbf{I}) \text{vec}(\mathbf{X}^{(k)}) \right\} \\
&+ \left[\text{vec}(\mathbf{X}^{(k)}) \right]^H (\lambda_{\max}(\boldsymbol{\Sigma}_2) \mathbf{I} - \boldsymbol{\Sigma}_2) \text{vec}(\mathbf{X}^{(k)}).
\end{aligned} \tag{4.6}$$

Since $\left[\text{vec}(\mathbf{X}) \right]^H \text{vec}(\mathbf{X}) = N^2$, the first term in (4.6) is constant. The last term, on the other hand, does not depend on the independent variable, \mathbf{x} , and therefore, it is

constant as well. Ignoring those constant terms, we can perform the following minimization problem instead,

$$\begin{aligned}
& \underset{\mathbf{x}, \mathbf{X}}{\text{minimize}} && 2 \operatorname{Re} \left\{ \left[\operatorname{vec}(\mathbf{X}) \right]^H \left(\boldsymbol{\Sigma}_2 - \lambda_{\max}(\boldsymbol{\Sigma}_2) \mathbf{I} \right) \operatorname{vec}(\mathbf{X}^{(k)}) \right\} \\
& && - 2N \sum_{p=1}^{2N} \operatorname{Tr}(\mathbf{M}_p \mathbf{X}) \\
& \text{subject to} && \mathbf{X} = \mathbf{x} \mathbf{x}^H \\
& && |x_n| = 1, n = 1, \dots, N.
\end{aligned} \tag{4.7}$$

Using the equality in (4.4), the above problem can be further simplified as

$$\begin{aligned}
& \underset{\mathbf{x}, \mathbf{X}}{\text{minimize}} && 2 \sum_{p=1}^{2N} \operatorname{Tr}(\mathbf{X}^{(k)} \mathbf{M}_p) \operatorname{Tr}(\mathbf{M}_p \mathbf{X}) - 2 \lambda_{\max}(\boldsymbol{\Sigma}_2) \operatorname{Tr}(\mathbf{X}^{(k)} \mathbf{X}) - 2N \sum_{p=1}^{2N} \operatorname{Tr}(\mathbf{M}_p \mathbf{X}) \\
& \text{subject to} && \mathbf{X} = \mathbf{x} \mathbf{x}^H \\
& && |x_n| = 1, n = 1, \dots, N.
\end{aligned} \tag{4.8}$$

We can alternatively express the minimization problem in (4.8) as

$$\begin{aligned}
& \underset{\mathbf{x}, \mathbf{X}}{\text{minimize}} && 2 \sum_{p=1}^{2N} \operatorname{Tr}(\mathbf{X}^{(k)} \mathbf{M}_p) \mathbf{x}^H \mathbf{M}_p \mathbf{x} - 2 \lambda_{\max}(\boldsymbol{\Sigma}_2) \left| \mathbf{x}^H \mathbf{x}^{(k)} \right|^2 \\
& && - 2N \sum_{p=1}^{2N} \mathbf{x}^H \mathbf{M}_p \mathbf{x} \\
& \text{subject to} && \mathbf{X} = \mathbf{x} \mathbf{x}^H \\
& && |x_n| = 1, n = 1, \dots, N.
\end{aligned} \tag{4.9}$$

The summation expression in the last term above can be written as

$\sum_{p=1}^{2N} \mathbf{x}^H \mathbf{M}_p \mathbf{x} = \mathbf{x}^H \left(\sum_{p=1}^{2N} \mathbf{A}_p \odot \boldsymbol{\Pi} \right) \mathbf{x} = \mathbf{x}^H \left(\boldsymbol{\Pi} \odot \sum_{p=1}^{2N} \mathbf{A}_p \right) \mathbf{x}$. Since $\sum_{p=1}^{2N} \mathbf{A}_p = 2N \mathbf{I}$, this term is constant and does not affect the minimization. Ignoring this term, we can rewrite (4.9) as

$$\begin{aligned}
& \underset{\mathbf{x}}{\text{minimize}} && \mathbf{x}^H \left[\sum_{p=1}^{2N} \mathbf{M}_p \left([\mathbf{x}^{(k)}]^H \mathbf{M}_p \mathbf{x}^{(k)} \right) - \lambda_{\max}(\boldsymbol{\Sigma}_2) \mathbf{x}^{(k)} [\mathbf{x}^{(k)}]^H \right] \mathbf{x} \\
& \text{subject to} && |x_n| = 1, n = 1, \dots, N.
\end{aligned} \tag{4.10}$$

The above minimization problem can be expressed more compactly as

$$\begin{aligned}
& \underset{\mathbf{x}}{\text{minimize}} && \mathbf{x}^H \left(\mathbf{\Pi} \odot \left(\mathbf{A} \text{Diag} \{ \mathbf{m}^{(k)} \} \mathbf{A}^H \right) \right. \\
& && \left. - \lambda_{\max} (\mathbf{\Sigma}_2) \mathbf{x}^{(k)} [\mathbf{x}^{(k)}]^H \right) \mathbf{x} \\
& \text{subject to} && |x_n| = 1, n = 1, \dots, N.
\end{aligned} \tag{4.11}$$

Here, $\text{Diag} \{ \mathbf{m}^{(k)} \}$ denotes the $2N \times 2N$ diagonal matrix whose diagonal is formed by the elements of the $2N \times 1$ vector $\mathbf{m}^{(k)} = [m_1^{(k)} \ m_2^{(k)} \ \dots \ m_{2N}^{(k)}]^T$ where $m_p^{(k)} = [\mathbf{x}^{(k)}]^H \mathbf{M}_p \mathbf{x}^{(k)}$. In (4.11), the matrix \mathbf{A} is defined as $\mathbf{A} = [\mathbf{a}_1 \ | \ \mathbf{a}_2 \ | \ \dots \ | \ \mathbf{a}_{2N}]$ using \mathbf{a}_p which, in turn, was defined following (4.1). Calculation of $m_p^{(k)}$ for all p values using $m_p^{(k)} = [\mathbf{x}^{(k)}]^H \mathbf{M}_p \mathbf{x}^{(k)}$ is not computationally efficient. Therefore, we can modify this expression as $m_p^{(k)} = [\mathbf{x}^{(k)}]^H (\mathbf{A}_p \odot \mathbf{\Pi}) \mathbf{x}^{(k)} = [\mathbf{x}^{(k)} \odot \mathbf{a}_p^*]^H \mathbf{\Pi} [\mathbf{x}^{(k)} \odot \mathbf{a}_p^*]$, where \mathbf{a}_p^* corresponds to complex conjugation of all the elements of the vector \mathbf{a}_p . Let $\mathbf{M}^{(k)}$ be a $2N \times 2N$ matrix defined as

$$\mathbf{M}^{(k)} \triangleq [\mathbf{x}^{(k)} \odot \mathbf{A}^*]^H \mathbf{\Pi} [\mathbf{x}^{(k)} \odot \mathbf{A}^*] \tag{4.12}$$

where \mathbf{A}^* corresponds to complex conjugation of all the elements of the matrix \mathbf{A} . Then, diagonal elements of $\mathbf{M}^{(k)}$ correspond to the elements of $\mathbf{m}^{(k)}$ given above.

Noting that the minimization problem in (4.11) is quadratic in \mathbf{x} , we can apply a second majorization by choosing the matrix \mathbf{K} in Lemma 1 as $\mathbf{K} = \lambda_{\max} \left(\mathbf{\Pi} \odot \left(\mathbf{A} \text{Diag} \{ \mathbf{m}^{(k)} \} \mathbf{A}^H \right) \right) \mathbf{I}$. Now, after ignoring the constant terms, we can rewrite the problem as follows;

$$\begin{aligned}
& \underset{\mathbf{x}}{\text{minimize}} && \text{Re} \left[\mathbf{x}^H \left(\mathbf{\Pi} \odot \left(\mathbf{A} \text{Diag} \{ \mathbf{m}^{(k)} \} \mathbf{A}^H \right) \right. \right. \\
& && \left. \left. - \lambda_{\max} (\mathbf{\Sigma}) \mathbf{x}^{(k)} [\mathbf{x}^{(k)}]^H \right) \right. \\
& && \left. - \lambda_{\max} \left(\mathbf{\Pi} \odot \left(\mathbf{A} \text{Diag} \{ \mathbf{m}^{(k)} \} \mathbf{A}^H \right) \right) \mathbf{I} \right] \mathbf{x}^{(k)} \\
& \text{subject to} && |x_n| = 1, n = 1, \dots, N.
\end{aligned} \tag{4.13}$$

The above minimization problem can simply be expressed as

$$\begin{aligned} & \underset{\mathbf{x}}{\text{minimize}} \quad \text{Re}[\mathbf{x}^H \mathbf{y}] \\ & \text{subject to} \quad |x_n| = 1, n = 1, \dots, N \end{aligned} \quad (4.14)$$

where

$$\begin{aligned} \mathbf{y} = & \left(\mathbf{\Pi} \odot \left(\mathbf{A} \text{Diag} \{ \mathbf{m}^{(k)} \} \mathbf{A}^H \right) - \lambda_{\max}(\mathbf{\Sigma}_2) \mathbf{x}^{(k)} \left[\mathbf{x}^{(k)} \right]^H \right. \\ & \left. - \lambda_{\max} \left(\mathbf{\Pi} \odot \left(\mathbf{A} \text{Diag} \{ \mathbf{m}^{(k)} \} \mathbf{A}^H \right) \right) \mathbf{I} \right) \mathbf{x}^{(k)}. \end{aligned} \quad (4.15)$$

Thus, finally, the closed form solution is found as (He et al., 2010; Zhao et al., 2016)

$$x_n = e^{-j \arg(y_n)}, n = 1, \dots, N. \quad (4.16)$$

Since we obtained this solution by minimizing the WISL metric in the frequency domain using the MM method, we call the above derived algorithm FWISL (frequency domain WISL). The pseudocode of the developed algorithm is summarized in Algorithm 1 below.

Algorithm 1: FWISL Algorithm

- 1: Set sequence length N and weights $\{w_k \geq 0\}_{k=1}^{N-1}$.
Set $k = 0$ and initialize $\mathbf{x}^{(0)}$.
 - 2: **while** stopping criteria \geq Tol
 - 3: $\mathbf{M}^{(k)} = \left(\mathbf{x}^{(k)} \odot \mathbf{A}^* \right)^H \mathbf{\Pi} \left(\mathbf{x}^{(k)} \odot \mathbf{A} \right)$
 - 4: $\mathbf{m}^{(k)} = [m_1^{(k)} \quad m_2^{(k)} \quad \dots \quad m_{2N}^{(k)}]^T$
 - 5: $\mathbf{y} = \left\{ \mathbf{\Pi} \odot \left(\mathbf{A} \text{Diag} \{ \mathbf{m}^{(k)} \} \mathbf{A}^H \right) - \lambda_{\max}(\mathbf{\Sigma}_2) \mathbf{x}^{(k)} \left[\mathbf{x}^{(k)} \right]^H \right.$
 $\left. - \lambda_{\max} \left(\mathbf{\Pi} \odot \left(\mathbf{A} \text{Diag} \{ \mathbf{m}^{(k)} \} \mathbf{A}^H \right) \right) \mathbf{I} \right\} \mathbf{x}^{(k)}$
 - 6: $x_n = e^{-j \arg(y_n)}, n = 1, \dots, N$.
 - 7: $k = k + 1$
 - 8: **end while**
-

4.2 Simplifying Majorization for Efficient Computation

Algorithm 1 above requires calculation of the maximum eigenvalue of the matrix $\mathbf{\Pi} \odot (\mathbf{A} \text{Diag} \{ \mathbf{m}^{(k)} \} \mathbf{A}^H)$ which is computationally demanding. Therefore, alternative majorization functions could be looked for to decrease computational cost. For this purpose, a different matrix for \mathbf{K} in Lemma 1 is sought. This alternative matrix can be found using a property (Song et al., 2016b) for Hermitian Toeplitz matrices. Since the matrix $\mathbf{\Pi} \odot (\mathbf{A} \text{Diag} \{ \mathbf{m}^{(k)} \} \mathbf{A}^H)$ is Hermitian Toeplitz (see Appendix 3), we can invoke Lemma 2 (see Section 2.2.2) (Song et al., 2016b) in finding a different matrix for \mathbf{K} to allow fast computation.

Thus, we let \mathbf{K} in Lemma 1 be equal to $\lambda_u \mathbf{I}$ instead of $\lambda_{\max} (\mathbf{\Pi} \odot (\mathbf{A} \text{Diag} \{ \mathbf{m}^{(k)} \} \mathbf{A}^H)) \mathbf{I}$. λ_u is calculated as in (2.82) in Lemma 2 (see Section 2.2.2). In our proposed algorithm, we use this alternative matrix to reduce computational cost.

4.3 Numerical Examples for FWISL

In our numerical examples, we design unimodular sequences under different scenarios. The weights, $\{ \gamma_k \}_{k=1}^{N-1}$, of the correlation lags are selected as

$$\gamma_k = \begin{cases} 1, & k \in \{1, \dots, 20\} \cup \{51, \dots, 70\} \\ 0, & \text{otherwise.} \end{cases} \quad (4.17)$$

To obtain a narrow autocorrelation mainlobe, correlation weights are chosen as $\gamma_k = 1$ for small k values ($k \in \{1, \dots, 20\}$) which are the lags near the origin. As opposed to WeCAN introduced in (Stoica et al., 2009), for our proposed algorithm FWISL-accelerated (FWISL-acc) (see Appendix 2 for the acceleration scheme), there are not any restrictions on the value of γ_0 to make the matrix $\mathbf{\Pi}$ in (2.34) positive semidefinite. On the other hand, we have observed in our numerical experiments that the values in the interval $0 < \gamma_0 \leq 1$ work sufficiently well towards providing a smaller number of iterations for our minimization algorithm. Accordingly, we assigned

$\gamma_0 = \frac{1}{|\lambda_{\min}(\tilde{\mathbf{\Pi}})|}$ to make sure that γ_0 stays within the interval, $(0,1]$. We run the

algorithm until the stopping criterion is reached. As in (Stoica et al., 2009), the stopping criterion is determined as $\|\mathbf{x}^{(k+1)} - \mathbf{x}^{(k)}\| \leq \text{Tol}$.

Performance of the proposed algorithm, FWISL-acc, is compared against CAP (Stoica et al., 2009), WeCAN (Stoica et al., 2009), WeCAN+CAP (Stoica et al., 2009), MWISL-acc (Song et al., 2016b), and WPISL-SQUAREM (Zhao et al., 2016) algorithms in terms of number of iterations, CPU time, MMF, and correlation level which is defined in (2.22). WPISL-SQUAREM (Zhao et al., 2016) and MWISL-acc (Song et al., 2016b) algorithms (which are both time domain MM methods), CAP, WeCAN, and WeCAN+CAP algorithms (Stoica et al., 2009), and our proposed frequency domain MM-based algorithm, FWISL-acc, in Algorithm 6 (see Appendix 2), are implemented for the tolerance value of $\text{Tol} = 10^{-13}$.

In the first experiment, all the algorithms are initialized with Golomb sequence of length $N = 100$. The WISL metric versus the number of iterations for FWISL-acc, WPISL-SQUAREM, and MWISL-acc algorithms are shown in Figure 4.1. We can observe from Figure 4.1 that our proposed algorithm converges in a smaller number of iterations and attains a lower WISL value.

Figure 4.2 displays WISL values of the algorithms versus CPU time (in sec.). As can be seen, FWISL-acc terminates in less CPU time by reaching the tolerance value of $\text{Tol} = 10^{-13}$. Especially for WISL values below 10^{-18} , FWISL-acc requires less CPU time, although for larger WISL values, WPISL-SQUAREM and MWISL-acc algorithms spend less time. We would like to note that we did not include the CAP and WeCAN algorithms in Figure 4.1 and Figure 4.2 because their performance curves stayed much farther away (in a negative sense) from those of the other algorithms obscuring their readability.

Correlation level displays the relative strengths of autocorrelation sidelobes, r_k , with respect to the zero-lag coefficient, r_0 . Correlation level curves of the sequences designed by CAP, WeCAN, MWISL-acc, and FWISL-acc algorithms are plotted

together in Figure 4.3. Since the correlation level curve of WPISL-SQUAREM is very close to that of MWISL-acc, it is not included in Figure 4.3. It can be noticed that FWISL-acc is able to suppress autocorrelation sidelobes more at required lags.

In Table 4.1, we list the required number of iterations and CPU time of all the simulated algorithms for $\text{Tol} = 10^{-13}$ along with the achieved MMF values. The average correlation levels in the suppressed autocorrelation lags, $k \in \{1, \dots, 20\} \cup \{51, \dots, 70\}$, are also given in Table 4.1.

As a second experiment, CAP, WeCAN, MWISL-acc, WPISL-SQUAREM, and FWISL-acc algorithms are initialized with Golomb sequence for $N = 100, 140, 160,$ and 200 . Figure 4.4 displays the number of iterations versus sequence length and Figure 4.5 shows number of iterations and CPU time versus sequence length for $N = 100, 140, 160,$ and 200 . In Figure 4.4 and Figure 4.5, WeCAN+CAP algorithm is initialized by the sequence obtained by the CAP algorithm as proposed in (Stoica et al., 2009). Figures show that FWISL-acc outperforms CAP, WeCAN, and WeCAN+CAP algorithms and also converges in a smaller number of iterations and terminates in less CPU time than other MM-based algorithms. As can be seen, the WeCAN+CAP algorithm performs better than the WeCAN algorithm in terms of CPU time, MMF, iteration number and is able to suppress autocorrelation sidelobes more at given lags. This shows the importance of the initial sequence on performance. However, our proposed algorithm FWISL-acc still outperforms WeCAN+CAP. We also initialized MM-based algorithms, MWISL-acc, WPISL-SQUAREM, and FWISL-acc, with the sequence obtained by the CAP algorithm for lengths $N = 100, 140, 160,$ and 200 in order to perform a fair comparison with the WeCAN+CAP algorithm. We named those concatenated algorithms as MWISL-acc+CAP, WPISL-SQUAREM+CAP, and FWISL-acc+CAP, respectively.

Comparison of the algorithms in terms of MMF versus sequence length is shown in Figure 4.6. When the algorithms are initialized by the sequence obtained by the CAP algorithm, they achieve better performance. Figure 4.7 displays the average level of the suppressed autocorrelation sidelobes at given lags versus sequence length. It can be seen that the FWISL-acc algorithm is able to suppress autocorrelation lags more at

the required lags. In Table 4.2, we list the required number of iterations, CPU time, and the achieved MMF values of the simulated algorithms for the case of initialization with the sequence obtained by CAP. The average correlation levels in the suppressed autocorrelation lags are also given in Table 4.2.

As a last experiment, we employ the MM-based algorithms when the sequence length N is varied from $N=100$ to $N=1000$. Figure 4.8 displays number of iterations versus sequence length. As shown in Figure 4.8, our proposed algorithm converges in a smaller number of iterations. In Figure 4.9, CPU time versus sequence length is shown. It can be seen that FWISL-acc terminates in less CPU time by reaching the tolerance value. Figure 4.8 and Figure 4.9 indicate that FWISL-acc algorithm can be employed for designing long sequences as well. Performance of simulated algorithms in terms of MMF is compared in Figure 4.10 which displays that the sequence designed by the FWISL-acc algorithm has higher MMF even for long sequences. Finally, as can be seen in Figure 4.11, the FWISL-acc algorithm is able to suppress autocorrelation sidelobes more at the required lags.

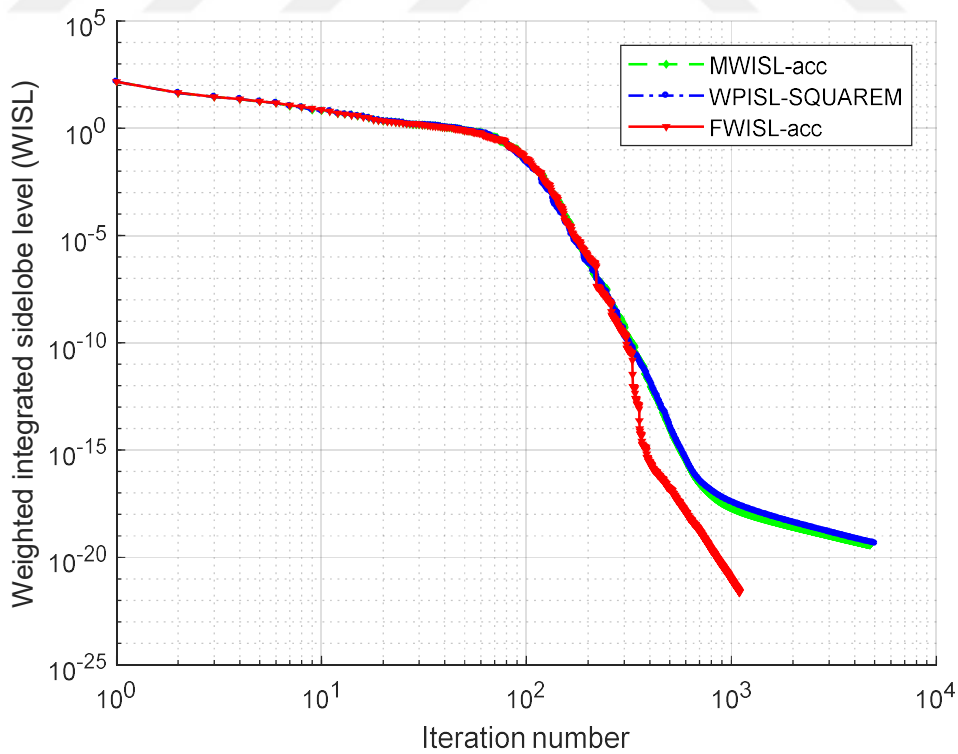


Figure 4.1 WISL versus the number of iterations

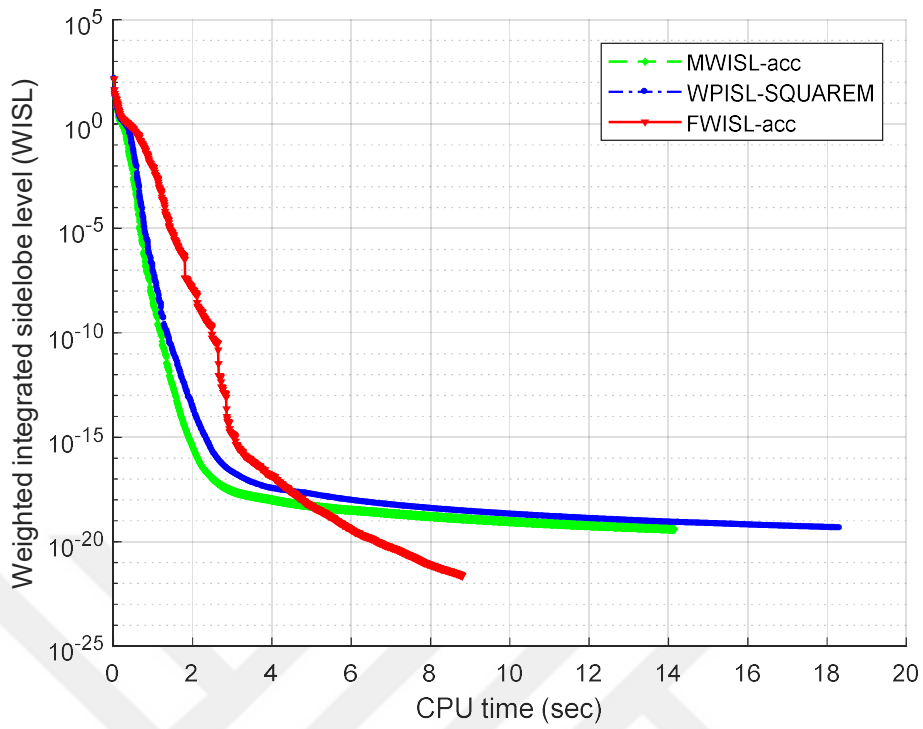


Figure 4.2 WISL versus CPU time

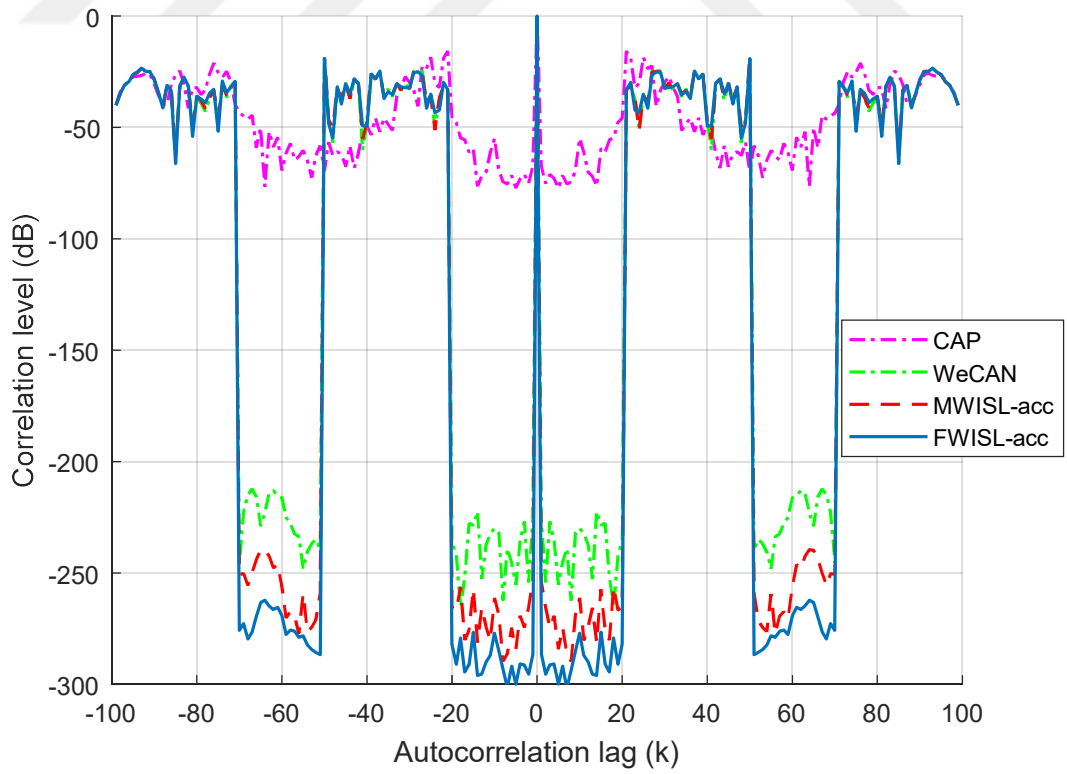


Figure 4.3 Correlation levels of the sequences designed by WeCAN, MWISL-acc, and FWISL-acc

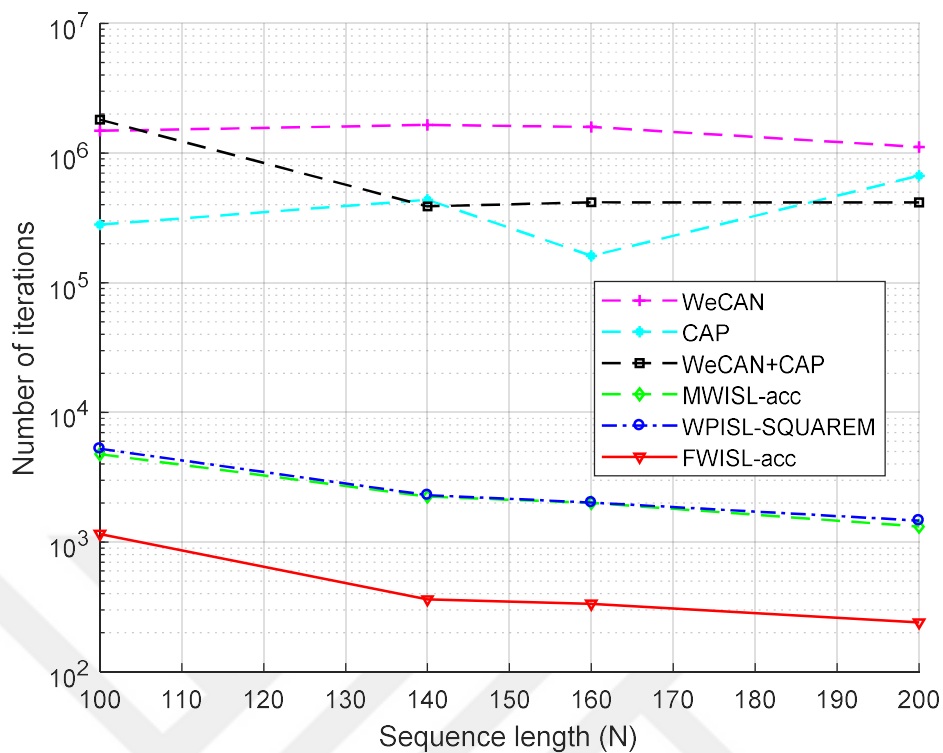


Figure 4.4 Number of iterations versus sequence length N

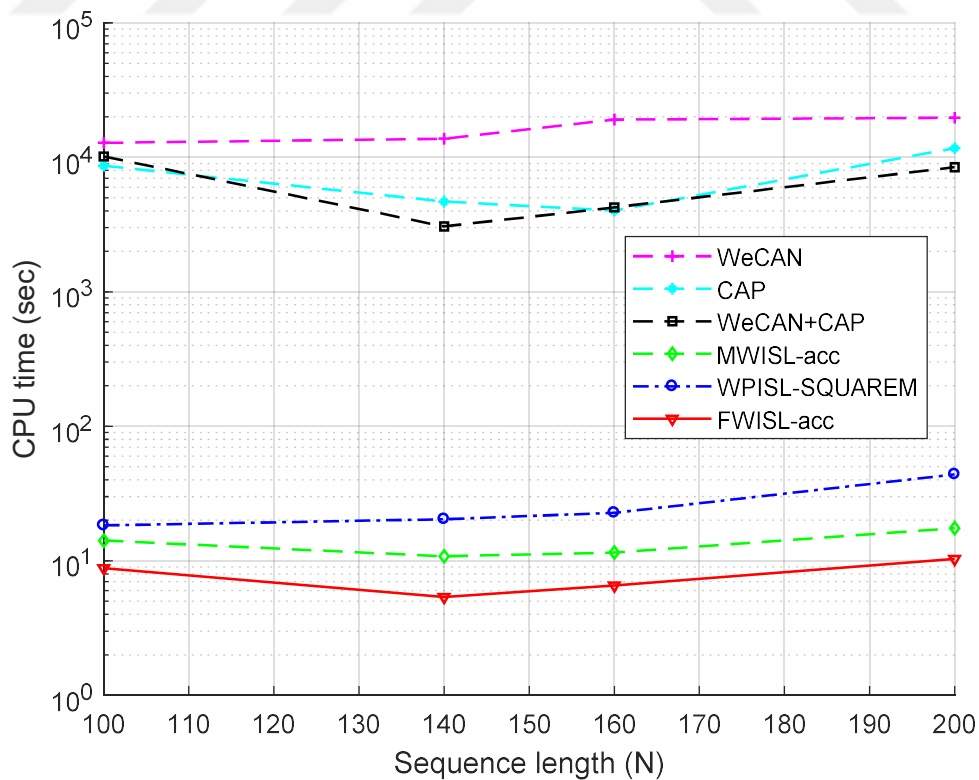


Figure 4.5 CPU time versus sequence length N

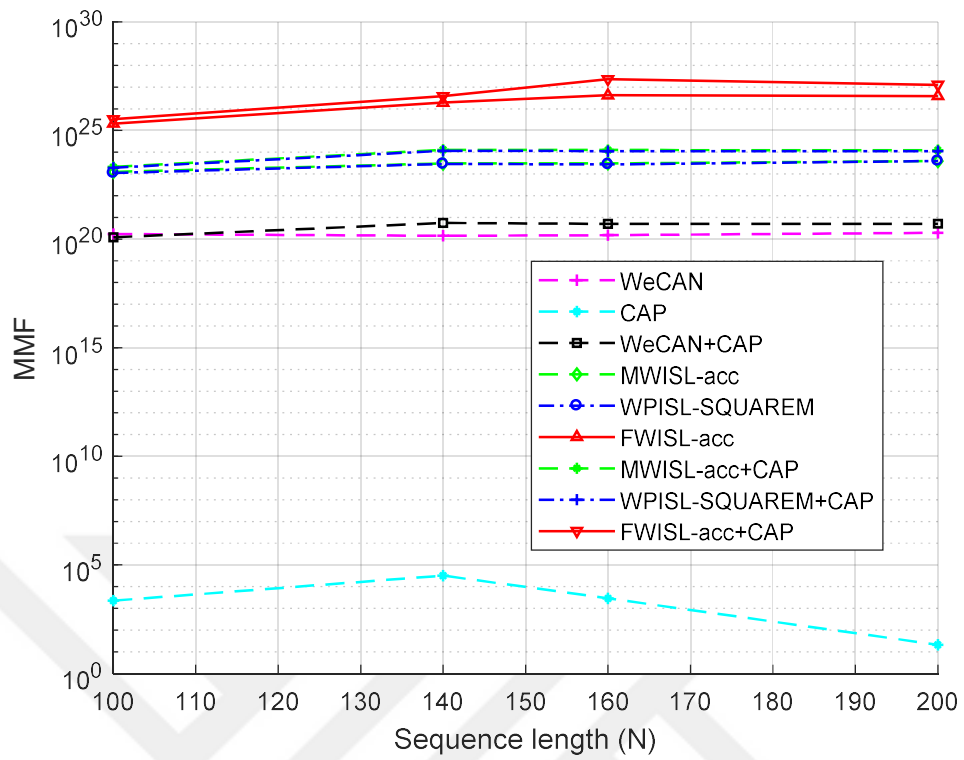


Figure 4.6 MMF versus sequence length N

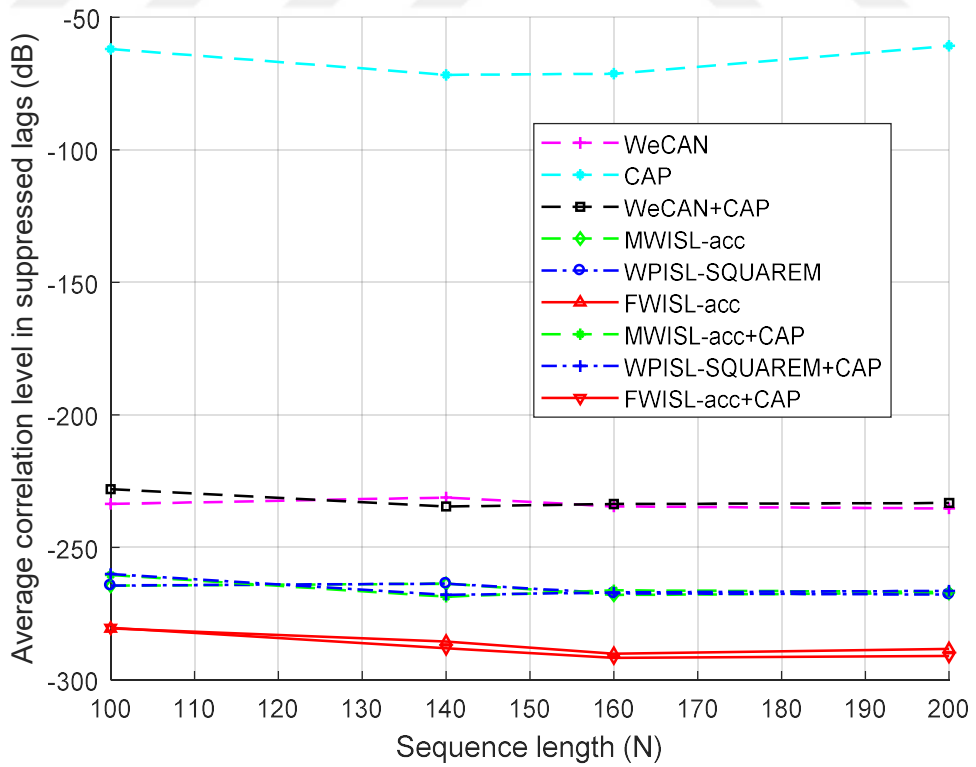


Figure 4.7 Average correlation level in suppressed lags (dB) versus sequence length N

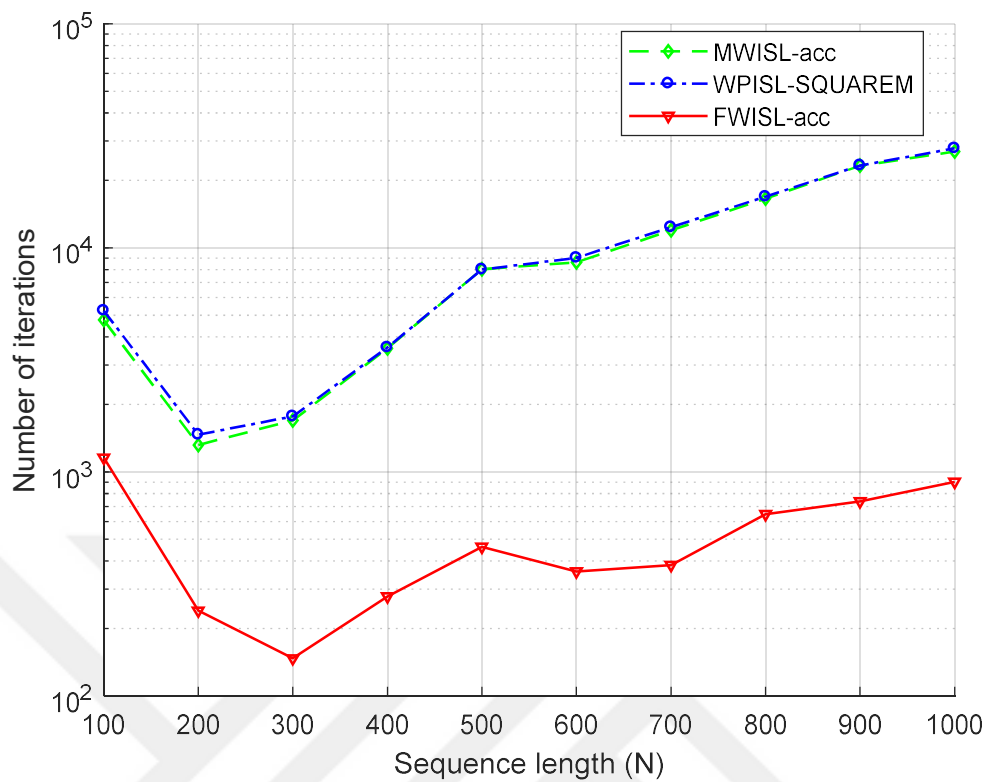


Figure 4.8 Number of iterations versus sequence length N

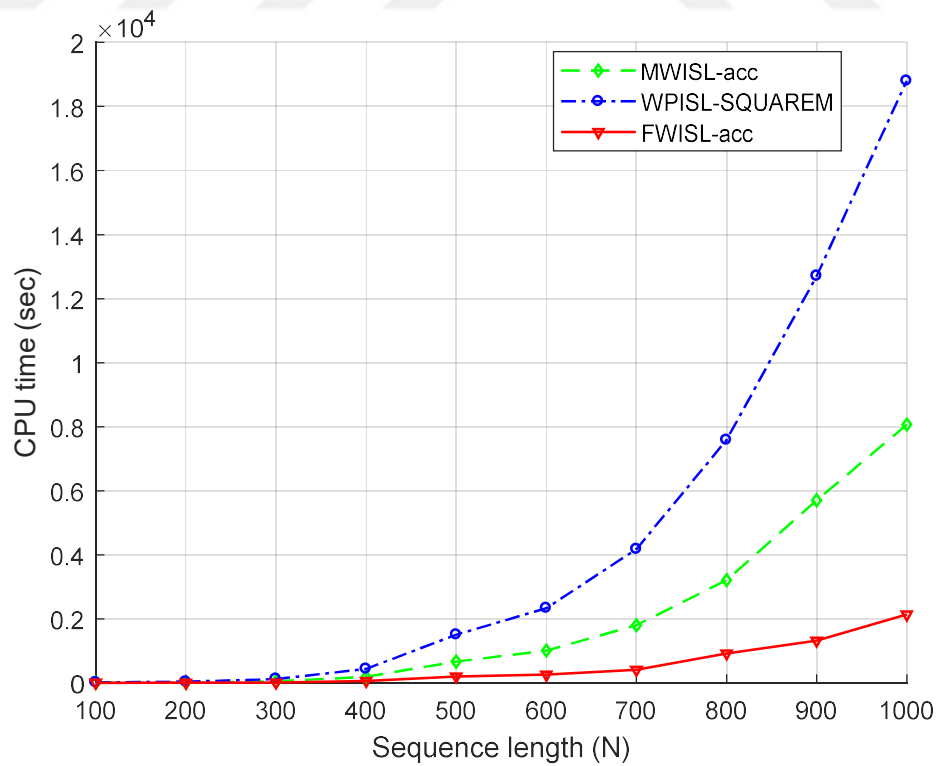


Figure 4.9 CPU time versus sequence length N

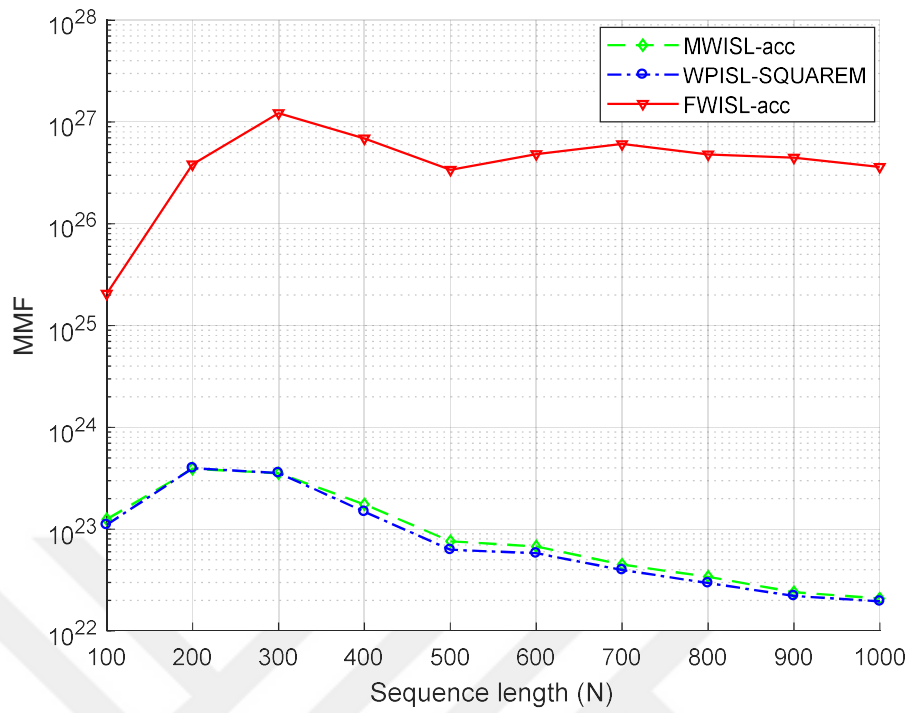


Figure 4.10 MMF versus sequence length N

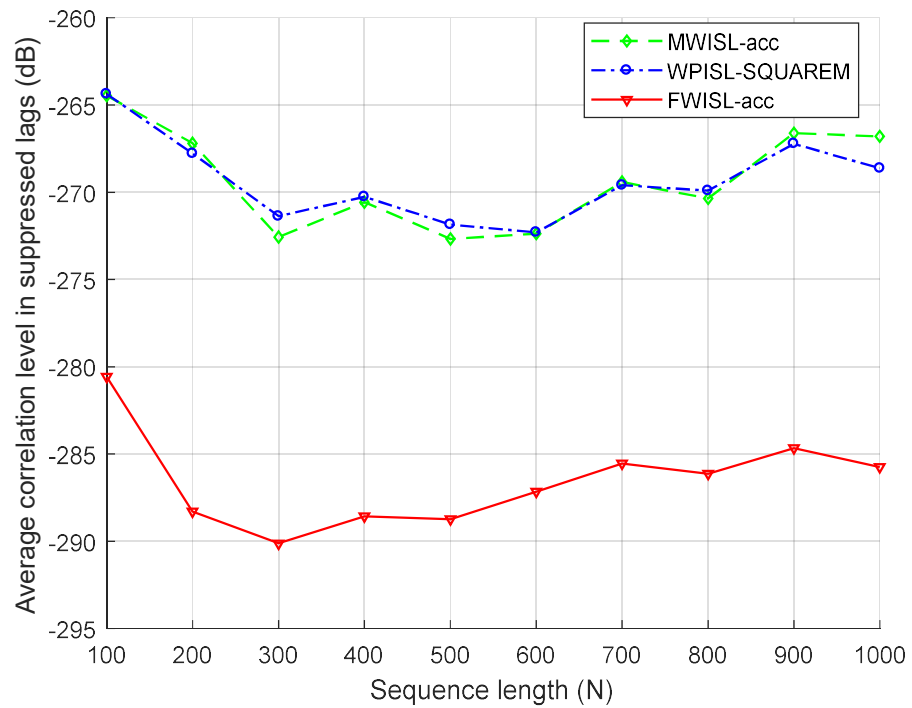


Figure 4.11 Average correlation level in suppressed lags (dB) versus sequence length N

Table 4.1 Required number of iterations, CPU time, MMF, and average correlation levels in suppressed lags ($N = 100$, Tol = 10^{-13} , initialization by Golomb sequence)

	MWISL- acc (Song et al., 2016b)	WPISL- SQUAREM (Zhao et al., 2016)	FWISL-acc	CAP (Stoica et al., 2009)	WeCAN (Stoica et al., 2009)	WeCAN+CAP (Stoica et al., 2009)
Number of iterations	4763 14.1508	5243 18.3309	1156 8.8006	280566 8.6588×10^4	1483502 1.2815×10^4	1808166 1.0150×10^4
CPU time (sec.)						
MMF	1.2508×10^{23}	1.1027×10^{23}	2.0544×10^{25}	2260.0754	1.7185×10^{20}	1.2063×10^{20}
Average correlation level in suppressed lags (dB)	-264.4584	-264.3665	-282.1925	-61.9229	-233.6052	-228.0404

Table 4.2 Required number of iterations, CPU time, MMF, and average correlation levels in suppressed lags ($N = 100$, $Tol = 10^{-13}$, initialization by the sequence designed by CAP)

	MWISL-acc (Song et al., 2016b)	WPISL- SQUAREM (Zhao et al., 2016)	FWISL-acc	WeCAN+CAP (Stoica et al., 2009)
Number of iterations	3261	3317	759	1808166
CPU time (sec.)	8.4462	18.9859	6.2371	1.0150×10^4
MMF	2.0930×10^{23}	1.9319×10^{23}	3.2794×10^{25}	1.2063×10^{20}
Average correlation level in suppressed lags (dB)	-260.3808	-260.0628	-280.3609	-228,0404

CHAPTER FIVE
DESIGNING SEQUENCES SATISFYING SIMULTANEOUS TEMPORAL
ISL AND SPECTRAL STOPBAND CONSTRAINTS

5.1 Sequence Design with ISL and Stopband Constraints

The SCAN algorithm was proposed to design sequences minimizing the ISL metric and satisfying some stopband constraints (He et al., 2010). SCAN minimizes a quadratic “approximation” of ISL instead of the exact ISL metric which is quartic with respect to the designed sequence. In this chapter, we minimize the exact quartic ISL metric itself for designing sequences having some additional stopband constraints.

In (He et al., 2010), the underlying optimization problem is given as follows

$$\begin{aligned} & \underset{\mathbf{x}}{\text{minimize}} && J(\mathbf{x}) = \lambda \text{SC} + (1 - \lambda) \text{ISL} \\ & \text{subject to} && |x_n| = 1, \quad n = 1, \dots, N \end{aligned} \tag{5.1}$$

where SC represents the stopband constraint and $\lambda \in [0, 1]$ is used to weight the metric of ISL and the stopband constraint. In order to solve the optimization problem in (5.1), a cyclic algorithm called SCAN was proposed in (He et al., 2010) (see Section 2.1.2).

In this chapter, we use the MM method to solve the problem in (5.1). We call our newly proposed algorithms for designing unimodular sequences with minimum ISL and having stopband constraints as SMISLN (stopband MISL-new) and SWPISL (stopband WPISL). These algorithms are extension of the MISL (Song et al., 2015a, 2015b) and WPISL (Zhao et al., 2016) algorithms, respectively.

5.2 Stopband MISL-New (SMISLN)

To design a unimodular waveform satisfying simultaneous temporal ISL and spectral stopband constraints we employ the MM method. In order to suppress the stopband frequencies, the quantity in (2.25) is minimized.

We first express the metric of ISL in the frequency domain and a modified version of the MISL method proposed in (Song et al., 2015a) is developed to minimize the autocorrelation sidelobes of the waveform. The optimization problem to minimize the metric of ISL in the frequency domain is given as (Song et al., 2015a, 2015b; Stoica et al., 2009)

$$\begin{aligned} \underset{\mathbf{x}}{\text{minimize}} \quad & \frac{1}{4N} \sum_{p=1}^{2N} \left[\left| \sum_{n=1}^N x_n e^{-j\omega_p n} \right|^2 - N \right]^2 \\ \text{subject to} \quad & |x_n| = 1, \quad n = 1, \dots, N \end{aligned} \quad (5.2)$$

where ω_p and $\bar{\mathbf{x}}$ are given in (2.10) and (2.16) (see Section 2.1.1), respectively. Let

us define $\mathbf{a}_p = \frac{1}{\sqrt{2N}} [1 \ e^{j\omega_p} \ \dots \ e^{j\omega_p(2N-1)}]^T$, $p = 1, \dots, 2N$. Then, (5.2) can be written

as

$$\begin{aligned} \underset{\mathbf{x}}{\text{minimize}} \quad & \frac{1}{4N} \sum_{p=1}^{2N} [2N \mathbf{a}_p^H \bar{\mathbf{x}} \bar{\mathbf{x}}^H \mathbf{a}_p - N]^2 \\ \text{subject to} \quad & |x_n| = 1, \quad n = 1, \dots, N. \end{aligned} \quad (5.3)$$

After expanding the square in the objective function, we obtain

$$\begin{aligned} \underset{\mathbf{x}}{\text{minimize}} \quad & \frac{1}{4N} \sum_{p=1}^{2N} \left[(2N \mathbf{a}_p^H \bar{\mathbf{x}} \bar{\mathbf{x}}^H \mathbf{a}_p)^2 - 4N^2 \mathbf{a}_p^H \bar{\mathbf{x}} \bar{\mathbf{x}}^H \mathbf{a}_p + N^2 \right] \\ \text{subject to} \quad & |x_n| = 1, \quad n = 1, \dots, N. \end{aligned} \quad (5.4)$$

Due to Parseval's relation, $\sum_{p=1}^{2N} |\mathbf{a}_p^H \bar{\mathbf{x}}|^2 = \|\bar{\mathbf{x}}\|^2 = N$, the second term in the above

objective function is constant. Therefore, the following minimization problem can be solved to suppress the autocorrelation sidelobes of the waveform

$$\begin{aligned} \underset{\mathbf{x}}{\text{minimize}} \quad & N \sum_{p=1}^{2N} (\mathbf{a}_p^H \bar{\mathbf{x}} \bar{\mathbf{x}}^H \mathbf{a}_p)^2 \\ \text{subject to} \quad & |x_n| = 1, \quad n = 1, \dots, N. \end{aligned} \quad (5.5)$$

Combining the stopband and correlation constraints in (2.25) and (5.5) as in (5.1) leads to the following problem (Biskin & Akay, 2018b)

$$\begin{aligned} & \underset{\mathbf{x}}{\text{minimize}} && \lambda \|\mathbf{S}^H \hat{\mathbf{x}}\|^2 + (1-\lambda)N \sum_{p=1}^{2N} \left(\mathbf{a}_p^H \bar{\mathbf{x}} \bar{\mathbf{x}}^H \mathbf{a}_p \right)^2 \\ & \text{subject to} && |x_n| = 1, \quad n = 1, \dots, N. \end{aligned} \quad (5.6)$$

We suggest to use the MM method to perform the minimization in (5.6). For this purpose, we apply Lemma 1 in Section 2.1.1 to our minimization problem term by term.

First, let us define the function $h_1(\mathbf{x}) = \lambda \|\mathbf{S}^H \hat{\mathbf{x}}\|^2 + (1-\lambda)N \sum_{p=1}^{2N} \left(\mathbf{a}_p^H \bar{\mathbf{x}} \bar{\mathbf{x}}^H \mathbf{a}_p \right)^2$. The first majorization step is performed by applying Lemma 1 to the first term, $\|\mathbf{S}^H \hat{\mathbf{x}}\|^2 = \hat{\mathbf{x}}^H \mathbf{S} \mathbf{S}^H \hat{\mathbf{x}}$, with $\mathbf{K} = \lambda_{\max}(\mathbf{\Sigma}_3) \mathbf{I}$ where $\mathbf{\Sigma}_3 = \mathbf{S} \mathbf{S}^H$ and $\lambda_{\max}(\mathbf{\Sigma}_3)$ is the maximum eigenvalue of $\mathbf{\Sigma}_3$. The term, $\hat{\mathbf{x}}^H \mathbf{\Sigma}_3 \hat{\mathbf{x}}$, is majorized at $\hat{\mathbf{x}}^{(k)}$ by $u_1(\hat{\mathbf{x}}, \hat{\mathbf{x}}^{(k)})$ given below

$$\begin{aligned} u_1(\hat{\mathbf{x}}, \hat{\mathbf{x}}^{(k)}) &= \lambda_{\max}(\mathbf{\Sigma}_3) \hat{\mathbf{x}}^H \hat{\mathbf{x}} + 2 \operatorname{Re} \left[\hat{\mathbf{x}}^H (\mathbf{\Sigma}_3 - \lambda_{\max}(\mathbf{\Sigma}_3) \mathbf{I}) \hat{\mathbf{x}}^{(k)} \right] \\ &\quad + \left(\hat{\mathbf{x}}^{(k)} \right)^H (\lambda_{\max}(\mathbf{\Sigma}_3) \mathbf{I} - \mathbf{\Sigma}_3) \hat{\mathbf{x}}^{(k)}. \end{aligned} \quad (5.7)$$

In (5.7), $\hat{\mathbf{x}}^{(k)}$ denotes the sequence obtained at the k^{th} iteration of the algorithm. The first and last terms in (5.7) are constant. Thus, the function $h_1(\mathbf{x})$ is majorized as

$$\begin{aligned} h_1(\mathbf{x}) &\leq 2\lambda \operatorname{Re} \left[\hat{\mathbf{x}}^H (\mathbf{\Sigma}_3 - \lambda_{\max}(\mathbf{\Sigma}_3) \mathbf{I}) \hat{\mathbf{x}}^{(k)} \right] \\ &\quad + (1-\lambda)N \sum_{p=1}^{2N} \left(\mathbf{a}_p^H \bar{\mathbf{x}} \bar{\mathbf{x}}^H \mathbf{a}_p \right)^2 + \text{constant}. \end{aligned} \quad (5.8)$$

Now, we apply Lemma 1 to the second term, $\sum_{p=1}^{2N} \left(\mathbf{a}_p^H \bar{\mathbf{x}} \bar{\mathbf{x}}^H \mathbf{a}_p \right)^2$, of $h_1(\mathbf{x})$. First, we

rewrite $\sum_{p=1}^{2N} \left(\mathbf{a}_p^H \bar{\mathbf{x}} \bar{\mathbf{x}}^H \mathbf{a}_p \right)^2$ in an alternative form. Defining $\mathbf{A}_p = \mathbf{a}_p \mathbf{a}_p^H$ and $\bar{\mathbf{X}} = \bar{\mathbf{x}} \bar{\mathbf{x}}^H$,

we can write

$$\sum_{p=1}^{2N} (\mathbf{a}_p^H \bar{\mathbf{x}} \bar{\mathbf{x}}^H \mathbf{a}_p)^2 = \sum_{p=1}^{2N} \text{Tr}(\bar{\mathbf{X}} \mathbf{A}_p)^2 \quad (5.9)$$

where $\text{Tr}(\cdot)$ denotes trace of a matrix. Since $\text{Tr}(\bar{\mathbf{X}} \mathbf{A}_p) = [\text{vec}(\bar{\mathbf{X}})]^H \text{vec}(\mathbf{A}_p)$ (Song et al., 2015a), we can express (5.9) as

$$\sum_{p=1}^{2N} (\mathbf{a}_p^H \bar{\mathbf{x}} \bar{\mathbf{x}}^H \mathbf{a}_p)^2 = [\text{vec}(\bar{\mathbf{X}})]^H \boldsymbol{\Sigma}_4 \text{vec}(\bar{\mathbf{X}}) \quad (5.10)$$

where $\text{vec}(\bar{\mathbf{X}})$ forms a column vector by stacking all the columns of the matrix $\bar{\mathbf{X}}$ and $\boldsymbol{\Sigma}_4 = \sum_{p=1}^{2N} \text{vec}(\mathbf{A}_p) [\text{vec}(\mathbf{A}_p)]^H$. If we apply Lemma 1 to (5.10) with $\mathbf{K} = \lambda_{\max}(\boldsymbol{\Sigma}_4)$, then, $[\text{vec}(\bar{\mathbf{X}})]^H \boldsymbol{\Sigma}_4 \text{vec}(\bar{\mathbf{X}})$ is majorized at $\mathbf{X}^{(k)}$ by $u_2(\bar{\mathbf{X}}, \bar{\mathbf{X}}^{(k)})$ given below

$$\begin{aligned} u_2(\bar{\mathbf{X}}, \bar{\mathbf{X}}^{(k)}) &= \lambda_{\max}(\boldsymbol{\Sigma}_4) [\text{vec}(\bar{\mathbf{X}})]^H \text{vec}(\bar{\mathbf{X}}) \\ &\quad + 2 \text{Re} \left\{ [\text{vec}(\bar{\mathbf{X}})]^H (\boldsymbol{\Sigma}_4 - \lambda_{\max}(\boldsymbol{\Sigma}_4) \mathbf{I}) \text{vec}(\bar{\mathbf{X}}^{(k)}) \right\} \\ &\quad + [\text{vec}(\bar{\mathbf{X}}^{(k)})]^H (\lambda_{\max}(\boldsymbol{\Sigma}_4) \mathbf{I} - \boldsymbol{\Sigma}_4) \text{vec}(\bar{\mathbf{X}}^{(k)}). \end{aligned} \quad (5.11)$$

Since $[\text{vec}(\bar{\mathbf{X}})]^H \text{vec}(\bar{\mathbf{X}}) = N^2$, the first term is a constant. The last term depends only on $\bar{\mathbf{X}}^{(k)}$, but not on the unknown sequence samples in $\bar{\mathbf{X}}$. Hence, the last term is also constant. Then, $h_1(\mathbf{x})$ in (5.8) is majorized as

$$\begin{aligned} h_1(\mathbf{x}) &\leq 2\lambda \text{Re} \left[\hat{\mathbf{x}}^H (\boldsymbol{\Sigma}_3 - \lambda_{\max}(\boldsymbol{\Sigma}_3) \mathbf{I}) \hat{\mathbf{x}}^{(k)} \right] \\ &\quad + 2(1-\lambda)N \text{Re} \left\{ [\text{vec}(\bar{\mathbf{X}})]^H (\boldsymbol{\Sigma}_4 - \lambda_{\max}(\boldsymbol{\Sigma}_4) \mathbf{I}) \text{vec}(\bar{\mathbf{X}}^{(k)}) \right\} \\ &\quad + \text{constant}. \end{aligned} \quad (5.12)$$

We can also express (5.12) as

$$\begin{aligned}
h_1(\mathbf{x}) &\leq 2\lambda \operatorname{Re} \left[\hat{\mathbf{x}}^H (\boldsymbol{\Sigma}_3 - \lambda_{\max}(\boldsymbol{\Sigma}_3) \mathbf{I}) \hat{\mathbf{x}}^{(k)} \right] \\
&\quad + 2(1-\lambda)N \left[\sum_{p=1}^{2N} \operatorname{Tr}(\bar{\mathbf{X}}^{(k)} \mathbf{A}_p) \operatorname{Tr}(\mathbf{A}_p \bar{\mathbf{X}}) - \lambda_{\max}(\boldsymbol{\Sigma}_4) \operatorname{Tr}(\bar{\mathbf{X}}^{(k)} \bar{\mathbf{X}}) \right] + \text{constant}. \tag{5.13}
\end{aligned}$$

The expression in (5.13) can be rewritten as follows

$$\begin{aligned}
h_1(\mathbf{x}) &\leq 2\lambda \operatorname{Re} \left[\hat{\mathbf{x}}^H (\boldsymbol{\Sigma}_3 - \lambda_{\max}(\boldsymbol{\Sigma}_3) \mathbf{I}) \hat{\mathbf{x}}^{(k)} \right] \\
&\quad + 2(1-\lambda)N \left[\sum_{p=1}^{2N} \left| \mathbf{a}_p^H \bar{\mathbf{x}}^{(k)} \right|^2 \left| \mathbf{a}_p^H \bar{\mathbf{x}} \right|^2 - \left| \bar{\mathbf{x}}^H \bar{\mathbf{x}}^{(k)} \right|^2 \right] + \text{constant}. \tag{5.14}
\end{aligned}$$

The inequality in (5.14) can be expressed more compactly as

$$\begin{aligned}
h_1(\mathbf{x}) &\leq 2\lambda \operatorname{Re} \left[\hat{\mathbf{x}}^H (\boldsymbol{\Sigma}_3 - \lambda_{\max}(\boldsymbol{\Sigma}_3) \mathbf{I}) \hat{\mathbf{x}}^{(k)} \right] \\
&\quad + 2(1-\lambda)N \bar{\mathbf{x}}^H \left(\mathbf{F}_{2N} \operatorname{Diag}(\mathbf{m}^{(k)}) \mathbf{F}_{2N}^H - \lambda_{\max}(\boldsymbol{\Sigma}_4) \bar{\mathbf{x}}^{(k)} (\bar{\mathbf{x}}^{(k)})^H \right) \bar{\mathbf{x}} \\
&\quad + \text{constant} \tag{5.15}
\end{aligned}$$

where \mathbf{F}_{2N}^H is $2N \times 2N$ unitary DFT matrix. \mathbf{F}_{2N} and the vector, $\mathbf{m}^{(k)}$, are defined, respectively, as $\mathbf{F}_{2N} = [\mathbf{a}_1 \mid \mathbf{a}_2 \mid \dots \mid \mathbf{a}_{2N}]$ and $\mathbf{m}^{(k)} = [m_1^{(k)} \ m_2^{(k)} \ \dots \ m_{2N}^{(k)}]^T$ with $m_p^{(k)} = \mathbf{a}_p^H \bar{\mathbf{x}}^{(k)} (\bar{\mathbf{x}}^{(k)})^H \mathbf{a}_p$. We apply the second majorization on the second term, $\bar{\mathbf{x}}^H \left(\mathbf{F}_{2N} \operatorname{Diag}(\mathbf{m}^{(k)}) \mathbf{F}_{2N}^H - \lambda_{\max}(\boldsymbol{\Sigma}_4) \bar{\mathbf{x}}^{(k)} (\bar{\mathbf{x}}^{(k)})^H \right) \bar{\mathbf{x}}$, in (5.15) with $\mathbf{K} = m_{\max}^{(k)} \mathbf{F}_{2N} \mathbf{F}_{2N}^H$ (Song et al., 2015a), where $m_{\max}^{(k)} = \max_p \{m_p^{(k)} : p = 1, \dots, 2N\}$. If we define $\boldsymbol{\Sigma}_5 = \mathbf{F}_{2N} \operatorname{Diag}(\mathbf{m}^{(k)}) \mathbf{F}_{2N}^H - \lambda_{\max}(\boldsymbol{\Sigma}_4) \bar{\mathbf{x}}^{(k)} (\bar{\mathbf{x}}^{(k)})^H$, then, $\bar{\mathbf{x}}^H \boldsymbol{\Sigma}_5 \bar{\mathbf{x}}$ is majorized as

$$\begin{aligned}
\bar{\mathbf{x}}^H \boldsymbol{\Sigma}_5 \bar{\mathbf{x}} &\leq u_3(\bar{\mathbf{x}}, \bar{\mathbf{x}}^{(k)}) \\
&= m_{\max}^{(k)} \bar{\mathbf{x}}^H \mathbf{F}_{2N} \mathbf{F}_{2N}^H \bar{\mathbf{x}} + 2 \operatorname{Re} \left[\bar{\mathbf{x}}^H (\boldsymbol{\Sigma}_5 - m_{\max}^{(k)} \mathbf{I}) \bar{\mathbf{x}}^{(k)} \right] \\
&\quad + \left(\bar{\mathbf{x}}^{(k)} \right)^H (m_{\max}^{(k)} \mathbf{I} - \boldsymbol{\Sigma}_5) \bar{\mathbf{x}}^{(k)}. \tag{5.16}
\end{aligned}$$

Since $\mathbf{F}_{2N} \mathbf{F}_{2N}^H = \mathbf{I}$, the first and last terms are constants. Ignoring them, we can see that (5.15) is majorized as

$$\begin{aligned}
h_1(\mathbf{x}) \leq & 2\lambda \operatorname{Re} \left[\hat{\mathbf{x}}^H (\boldsymbol{\Sigma}_3 - \lambda_{\max}(\boldsymbol{\Sigma}_3) \mathbf{I}) \hat{\mathbf{x}}^{(k)} \right] \\
& + 4N(1-\lambda) \operatorname{Re} \left[\bar{\mathbf{x}}^H (\boldsymbol{\Sigma}_5 - m_{\max}^{(k)} \mathbf{I}) \bar{\mathbf{x}}^{(k)} \right] + \text{constant}.
\end{aligned} \tag{5.17}$$

After omitting the constant terms within the majorizing function in (5.17), we can finally express the optimization problem in (5.6) as follows

$$\begin{aligned}
& \underset{\mathbf{x}}{\text{minimize}} && 2\lambda \operatorname{Re} \left[\hat{\mathbf{x}}^H (\boldsymbol{\Sigma}_3 - \lambda_{\max}(\boldsymbol{\Sigma}_3) \mathbf{I}) \hat{\mathbf{x}}^{(k)} \right] \\
& && + 4N(1-\lambda) \operatorname{Re} \left[\bar{\mathbf{x}}^H (\boldsymbol{\Sigma}_5 - m_{\max}^{(k)} \mathbf{I}) \bar{\mathbf{x}}^{(k)} \right] \\
& \text{subject to} && |x_n| = 1, \quad n = 1, \dots, N
\end{aligned} \tag{5.18}$$

which can also be rewritten as

$$\begin{aligned}
& \underset{\mathbf{x}}{\text{minimize}} && \operatorname{Re} \left[\lambda \hat{\mathbf{x}}^H (\boldsymbol{\Sigma}_3 - \lambda_{\max}(\boldsymbol{\Sigma}_3) \mathbf{I}) \hat{\mathbf{x}}^{(k)} + 2(1-\lambda) N \left(\bar{\mathbf{x}}^H (\boldsymbol{\Sigma}_5 - m_{\max}^{(k)} \mathbf{I}) \bar{\mathbf{x}}^{(k)} \right) \right] \\
& \text{subject to} && |x_n| = 1, \quad n = 1, \dots, N.
\end{aligned} \tag{5.19}$$

The above minimization problem can simply be expressed as

$$\begin{aligned}
& \underset{\mathbf{x}}{\text{minimize}} && \operatorname{Re} \left[\hat{\mathbf{x}}^H (\lambda \mathbf{y}_1) + \bar{\mathbf{x}}^H ((1-\lambda) \mathbf{y}_2) \right] \\
& \text{subject to} && |x_n| = 1, \quad n = 1, \dots, N
\end{aligned} \tag{5.20}$$

where

$$\begin{aligned}
\mathbf{y}_1 &= (\boldsymbol{\Sigma}_3 - \lambda_{\max}(\boldsymbol{\Sigma}_3) \mathbf{I}) \hat{\mathbf{x}}^{(k)} \\
\mathbf{y}_2 &= 2N (\boldsymbol{\Sigma}_5 - m_{\max}^{(k)} \mathbf{I}) \bar{\mathbf{x}}^{(k)}.
\end{aligned} \tag{5.21}$$

Letting the first N elements of \mathbf{y}_1 and \mathbf{y}_2 be denoted as $(\mathbf{y}_1)_{N \times 1}$ and $(\mathbf{y}_2)_{N \times 1}$, respectively, the closed form solution can be given as (Biskin & Akay, 2018b)

$$x_n = e^{-j \arg(\lambda y_{1n} + (1-\lambda) y_{2n})}, \quad n = 1, \dots, N \tag{5.22}$$

where y_{1_n} denotes the n^{th} element of the vector \mathbf{y}_1 . The sequence in (5.22) was obtained by simultaneously enforcing the ISL minimization and stopband constraints via the MM method. As an advantage, the above developed algorithm can minimize the stopband power in the frequency domain over an arbitrary number of frequency bins, similar to (He et al., 2010). We call this algorithm SMISLN (stopband MISL-new). Its pseudocode is given in Algorithm 2 below.

Algorithm 2: SMISLN Algorithm

- 1: Set sequence length N , set $k = 0$, and initialize $\mathbf{x}^{(0)}$
 - 2: **while** stopping criteria \geq Tol
 - 3: $m_p^{(k)} = \bar{\mathbf{a}}_p^H \bar{\mathbf{x}}^{(k)} (\bar{\mathbf{x}}^{(k)})^H \bar{\mathbf{a}}_p$, $p = 1, \dots, 2N$
 - 4: $\mathbf{m}^{(k)} = [m_1^{(k)} \quad m_2^{(k)} \quad \dots \quad m_{2N}^{(k)}]^T$
 - 5: $m_{\max}^{(k)} = \max_p \{m_p^{(k)} : p = 1, \dots, 2N\}$
 - 6: $\mathbf{y}_1 = (\boldsymbol{\Sigma}_3 - \lambda_{\max}(\boldsymbol{\Sigma}_3) \mathbf{I}) \hat{\mathbf{x}}^{(k)}$
 - 7: $\mathbf{y}_2 = 2N (\boldsymbol{\Sigma}_5 - m_{\max}^{(k)} \mathbf{I}) \bar{\mathbf{x}}^{(k)}$
 - 8: $x_n = e^{-j \arg(\lambda_1 y_{1_n} + (1-\lambda) y_{2_n})}$, $n = 1, \dots, N$
 - 9: $k = k + 1$
 - 10: **end while**
-

5.3 Stopband WPISL (SWPISL)

In (Zhao et al., 2016), a unified metric named “weighted peak or the integrated sidelobe level (WPISL)” was proposed as follows

$$\text{WPISL} = \sum_{k=1}^{N-1} w_k |r_k|^p \quad (5.23)$$

where $2 \leq p < +\infty$ and $\{w_k\}_{k=1}^{N-1}$ are nonnegative weights. This metric specializes into ISL, weighted ISL (WISL), or peak sidelobe level (PSL) depending on the values of p and $\{w_k\}_{k=1}^{N-1}$.

In this chapter, we are interested in designing sequences satisfying simultaneous temporal ISL and spectral stopband constraints. If we let $p = 2$ and $\{w_k\}_{k=1}^{N-1} = 1$, then (5.23) reduces to the ISL metric in (2.3) and becomes $\sum_{k=1}^{N-1} |r_k|^2$. Therefore, the optimization problem to be solved for designing sequences satisfying both temporal correlation and spectral stopband constraints is given as

$$\begin{aligned} & \underset{\mathbf{x}}{\text{minimize}} && \lambda \text{SC} + (1 - \lambda) \text{ISL} \\ & \text{subject to} && |x_n| = 1, \quad n = 1, \dots, N. \end{aligned} \quad (5.24)$$

By substituting the stopband and correlation constraints in (2.25) and (2.3), respectively, the optimization problem in (5.24) can be expressed as

$$\begin{aligned} & \underset{\mathbf{x}}{\text{minimize}} && \lambda N \|\mathbf{S}^H \hat{\mathbf{x}}\|^2 + (1 - \lambda) \sum_{k=1}^{N-1} |r_k|^2 \\ & \text{subject to} && |x_n| = 1, \quad n = 1, \dots, N \end{aligned} \quad (5.25)$$

where the sequence length N is included in the first part of the objective function to obtain the exact signal energy in the frequency domain. We propose to use the MM method to perform the minimization in (5.25). For this purpose, majorization for the objective function is performed by applying the MM method term by term. We start by defining the function $h_2(\mathbf{x}) = \lambda N \|\mathbf{S}^H \hat{\mathbf{x}}\|^2 + (1 - \lambda) \sum_{k=1}^{N-1} |r_k|^2$. The autocorrelation function in the second term can be written as $r_k = \mathbf{x}^H \mathbf{U}_k \mathbf{x}$ where \mathbf{U}_k is a Toeplitz matrix with only the k^{th} diagonal elements as 1 and the others 0. For $p = 2$ and $\{w_k\}_{k=1}^{N-1} = 1$, we utilize the following definitions given in (Zhao et al., 2016)

$$\mathbf{E}_3 \triangleq \sum_{\substack{k=-(N-1) \\ k \neq 0}}^{N-1} \text{vec}(\mathbf{U}_{-k}) [\text{vec}(\mathbf{U}_{-k})]^H, \quad (5.26)$$

$$\mathbf{R}_3 \triangleq \sum_{\substack{k=-(N-1) \\ k \neq 0}}^{N-1} \frac{1}{2} r_{-k}(\mathbf{x}^{(k)}) \mathbf{U}_k. \quad (5.27)$$

The second term of the objective function in (5.25) is majorized by the following function (Zhao et al., 2016)

$$u_3(\mathbf{x}, \mathbf{x}^{(l)}) = \frac{1}{2} \lambda_{\max}(\mathbf{E}_3) \|\mathbf{x}\|^4 + \lambda_R \|\mathbf{x}\|^2 - 2\lambda_R \operatorname{Re}[\mathbf{y}_3^H \mathbf{x}] + \text{constant} \quad (5.28)$$

where $\lambda_R \geq \lambda_{\max}(\mathbf{R}_3)$ and

$$\mathbf{y}_3 = \left(1 + \frac{\lambda_{\max}(\mathbf{E}_3)}{\lambda_R} \|\mathbf{x}^{(l)}\|^2\right) \mathbf{x}^{(l)} - \frac{1}{\lambda_R} \mathbf{R}_3 \mathbf{x}^{(l)}. \quad (5.29)$$

Then, majorization is applied on the first term of the objective function in (5.25) for which the majorizing function is given in (5.7). Thus, the function $h_2(\mathbf{x})$ is majorized as

$$\begin{aligned} h_2(\mathbf{x}) &\leq 2\lambda N \operatorname{Re}[\hat{\mathbf{x}}^H (\boldsymbol{\Sigma}_3 - \lambda_{\max}(\boldsymbol{\Sigma}_3) \mathbf{I}) \hat{\mathbf{x}}^{(l)}] \\ &\quad + (1 - \lambda) u_3(\mathbf{x}, \mathbf{x}^{(l)}) + \text{constant}. \end{aligned} \quad (5.30)$$

The first and second terms of $u_3(\mathbf{x}, \mathbf{x}^{(l)})$ in (5.28) are constants. Therefore, the expression in (5.30) can be rewritten as follows

$$\begin{aligned} h_2(\mathbf{x}) &\leq 2\lambda N \operatorname{Re}[\hat{\mathbf{x}}^H (\boldsymbol{\Sigma}_3 - \lambda_{\max}(\boldsymbol{\Sigma}_3) \mathbf{I}) \hat{\mathbf{x}}^{(l)}] \\ &\quad - 2(1 - \lambda) \lambda_R \operatorname{Re}[\mathbf{y}_3^H \mathbf{x}] + \text{constant}. \end{aligned} \quad (5.31)$$

Using the expression in (5.31), the optimization problem in (5.25) can be recast in terms of majorizing functions as

$$\begin{aligned} \underset{\mathbf{x}}{\text{minimize}} \quad & 2\lambda N \operatorname{Re}[\hat{\mathbf{x}}^H (\boldsymbol{\Sigma}_3 - \lambda_{\max}(\boldsymbol{\Sigma}_3) \mathbf{I}) \hat{\mathbf{x}}^{(l)}] \\ & - 2(1 - \lambda) \lambda_R \operatorname{Re}[\mathbf{y}_3^H \mathbf{x}] \\ \text{subject to} \quad & |x_n| = 1, \quad n = 1, \dots, N. \end{aligned} \quad (5.32)$$

Both terms in the objective function in (5.32) can be included within the $\operatorname{Re}(\cdot)$ operation. After omitting constants terms, (5.32) can also be expressed as

$$\begin{aligned}
& \underset{\mathbf{x}}{\text{minimize}} && \text{Re} \left[N \lambda \hat{\mathbf{x}}^H (\boldsymbol{\Sigma}_3 - \lambda_{\max}(\boldsymbol{\Sigma}_3) \mathbf{I}) \hat{\mathbf{x}}^{(l)} - (1-\lambda) \lambda_R \mathbf{y}_3^H \mathbf{x} \right] \\
& \text{subject to} && |x_n| = 1, \quad n = 1, \dots, N.
\end{aligned} \tag{5.33}$$

Then, we have

$$\begin{aligned}
& \underset{\mathbf{x}}{\text{minimize}} && \text{Re} \left[\hat{\mathbf{x}}^H (\lambda \mathbf{y}_1) - (1-\lambda) \mathbf{y}_3'^H \mathbf{x} \right] \\
& \text{subject to} && |x_n| = 1, \quad n = 1, \dots, N
\end{aligned} \tag{5.34}$$

where

$$\begin{aligned}
\mathbf{y}_1 &= N (\boldsymbol{\Sigma}_3 - \lambda_{\max}(\boldsymbol{\Sigma}_3) \mathbf{I}) \hat{\mathbf{x}}^{(l)} \\
\mathbf{y}_3' &= \lambda_R \mathbf{y}_3.
\end{aligned} \tag{5.35}$$

Letting the first N elements of \mathbf{y}_1 and \mathbf{y}_3' be denoted as $(\mathbf{y}_1)_{N \times 1}$ and $(\mathbf{y}_3')_{N \times 1}$, respectively, the closed form solution can be given as

$$x_n = e^{-j \arg(\lambda y_{1n} - (1-\lambda) y_{3n}')} , \quad n = 1, \dots, N \tag{5.36}$$

where y_{1n} denotes the n^{th} element of the vector \mathbf{y}_1 . This algorithm minimizes the stopband power in the frequency domain employing an arbitrary number of frequency bins and reduces the ISL metric as well. We call this algorithm SWPISL (stopband WPISL). Its pseudocode is given in Algorithm 3 below.

Algorithm 3: SWPISL Algorithm

- 1: Set sequence length N and weights, set $l = 0$, and initialize $\mathbf{x}^{(0)}$
 - 2: **while** stopping criteria \geq Tol
 - 3: $\mathbf{f} = \mathbf{F}_{2N}^H \begin{bmatrix} \mathbf{x}^{(l)} \\ \mathbf{0}_{N \times 1} \end{bmatrix}$
 - 4: $\mathbf{r} = \frac{1}{2N} \mathbf{F}_{2N} |\mathbf{f}|^2$
 - 5: $\mathbf{c} = \mathbf{r} \odot [0, w_1, w_2, \dots, 0, w_N, w_{N-1}, w_1]^T$ (see Appendix 4)
 - 6: $\mathbf{R}_3 = \frac{1}{2N} \mathbf{F}_{2N} \text{Diag}(\mathbf{F}_{2N}^H \mathbf{c}) \mathbf{F}_{2N}^H$ (see Appendix 4)
 - 7: $\mathbf{y}_1 = N(\boldsymbol{\Sigma}_3 - \lambda_{\max}(\boldsymbol{\Sigma}_3) \mathbf{I}) \hat{\mathbf{x}}^{(l)}$
 - 8: $\mathbf{y}_3 = \lambda_R \left(1 + \frac{\lambda_{\max}(\mathbf{E}_3)}{\lambda_R} \|\mathbf{x}^{(l)}\|^2 \right) \mathbf{x}^{(l)} - \mathbf{R}_3 \mathbf{x}^{(l)}$
 - 9: $x_n = e^{-j \arg(\lambda y_n - (1-\lambda) y_n')}$, $n = 1, \dots, N$
 - 10: $l = l + 1$
 - 11: **end while**
-

5.4 Numerical Examples for Designing Sequences with ISL and Stopband Constraints

We design a unimodular sequence of length $N = 100$ having two stopbands given as $\Omega = [0.2, 0.3) \cup [0.7, 0.8)$ Hz in terms of normalized frequency. In our simulations, relative weight parameter, λ , is assigned as $\lambda = 0.8$. The number of employed DFT bins is selected as $\tilde{N} = 1000$. The algorithms are initialized by Golomb sequence (Zhang & Golomb, 1993). We run the algorithms until reaching the stopping point which is determined by the inequality, $\|\mathbf{x}^{(k+1)} - \mathbf{x}^{(k)}\|^2 \leq \text{Tol}$, similar to the stopping

criterion utilized in (He et al., 2010; Stoica et al., 2009). All MM-based algorithms are accelerated by employing an appropriate acceleration scheme (see Appendix 2).

Performance of the proposed algorithms are compared against the SCAN (He et al., 2010) algorithm in terms of number of iterations, computation time, the ISL value, and the level of suppression in spectral stopbands. The SCAN algorithm proposed in (He et al., 2010) and the MM-based algorithms, SMISLN-acc (accelerated SMISLN) and SWPISL-acc (accelerated SWPISL) proposed in this thesis, are run for the tolerance value of $Tol = 10^{-3}$.

Figure 5.1, Figure 5.2, and Figure 5.3 show the normalized power spectra and correlation levels of the sequences designed by SCAN, SMISLN-acc (accelerated SMISLN), and SWPISL-acc (accelerated SWPISL), respectively. The power spectra are normalized to make the average value of the spectra in passbands equal to 1 dB (He et al., 2010). In Figure 5.4, the normalized power spectra of sequences designed by the three algorithms are plotted together. We can see that the algorithms proposed in this thesis provide better suppression in spectral stopbands than SCAN.

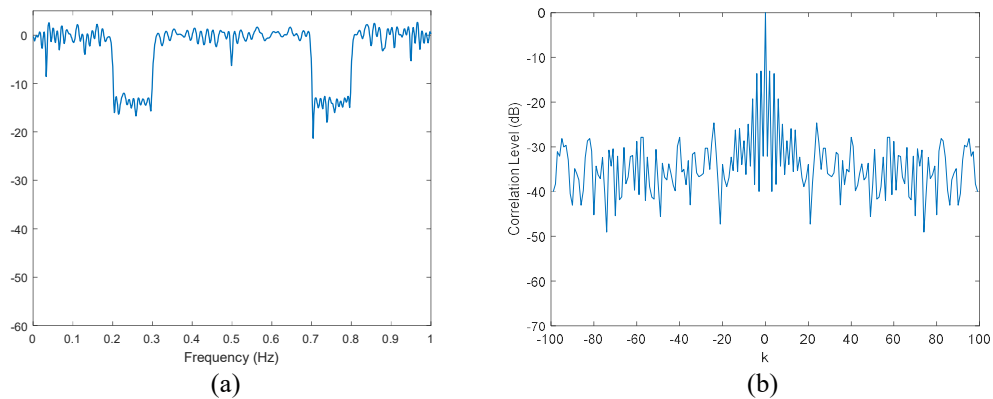
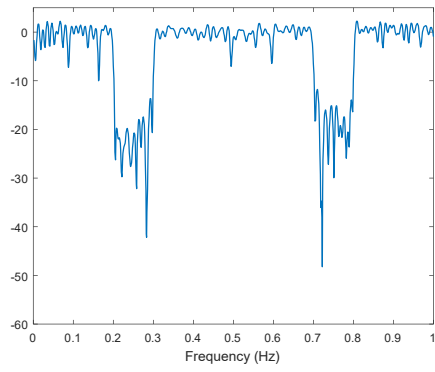
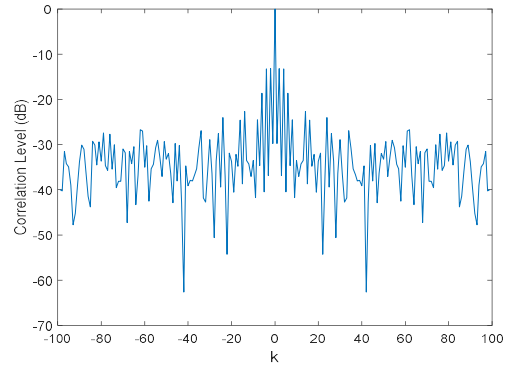


Figure 5.1 (a) Normalized power spectrum, (b) correlation level of the sequence designed by SCAN

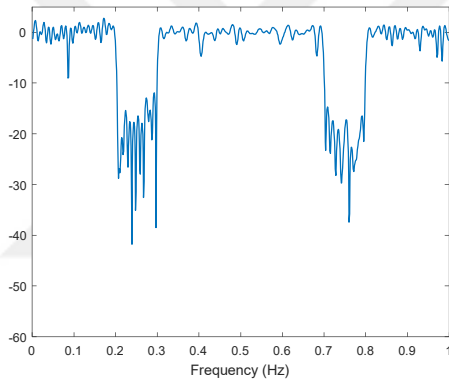


(a)

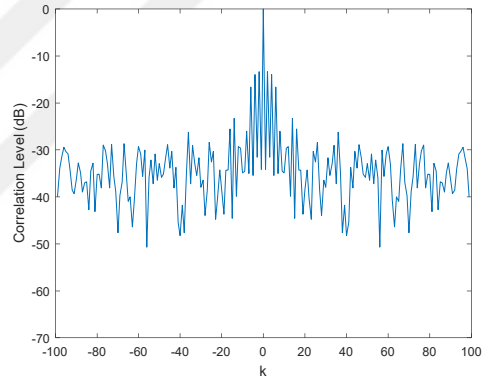


(b)

Figure 5.2 (a) Normalized power spectrum, (b) correlation level of the sequence designed by SMISLN-acc



(a)



(b)

Figure 5.3 (a) Normalized power spectrum, (b) correlation level of the sequence designed by SWPISL-acc

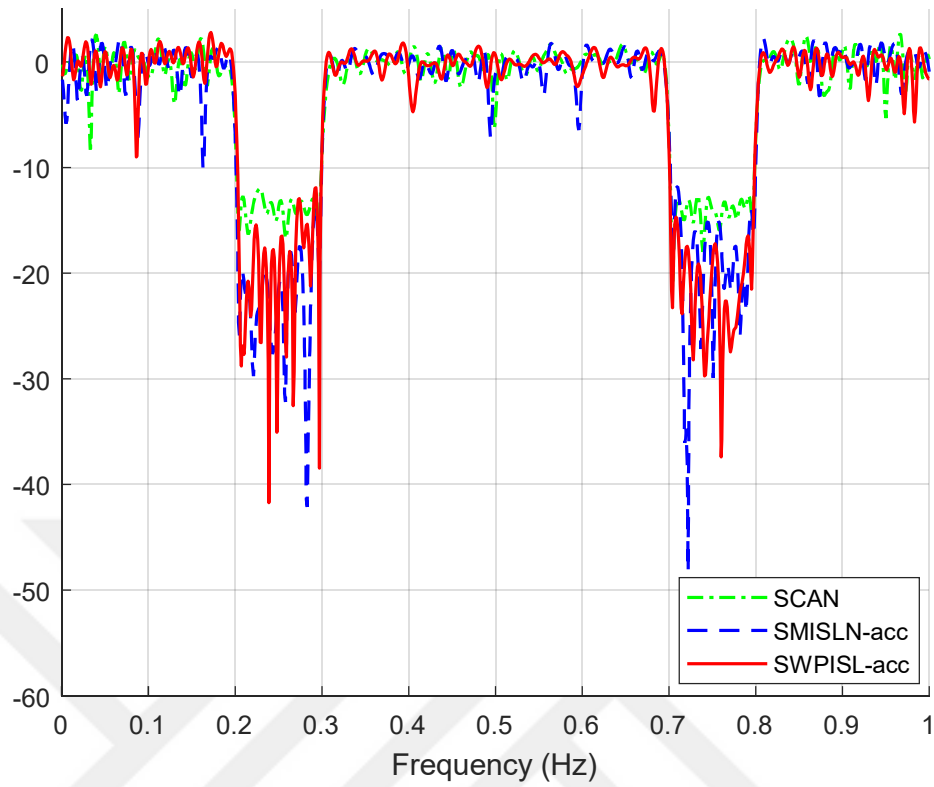


Figure 5.4 Normalized power spectra of sequences designed by SCAN, SMISLN-acc, and SWPISL-acc

Evolution of the objective function versus iteration number and CPU time (sec.) are presented in Figure 5.5 (a) and (b), respectively. Figure 5.5 indicates that the algorithms proposed in this study converge to a stationary point in a smaller number of iterations and CPU time (sec.) than SCAN.

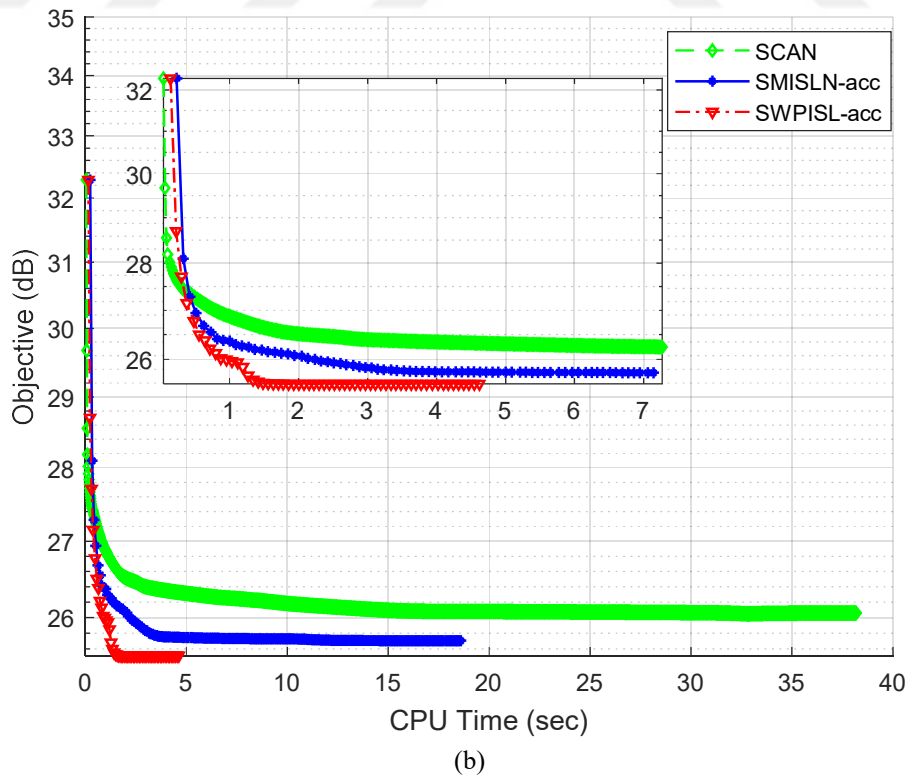
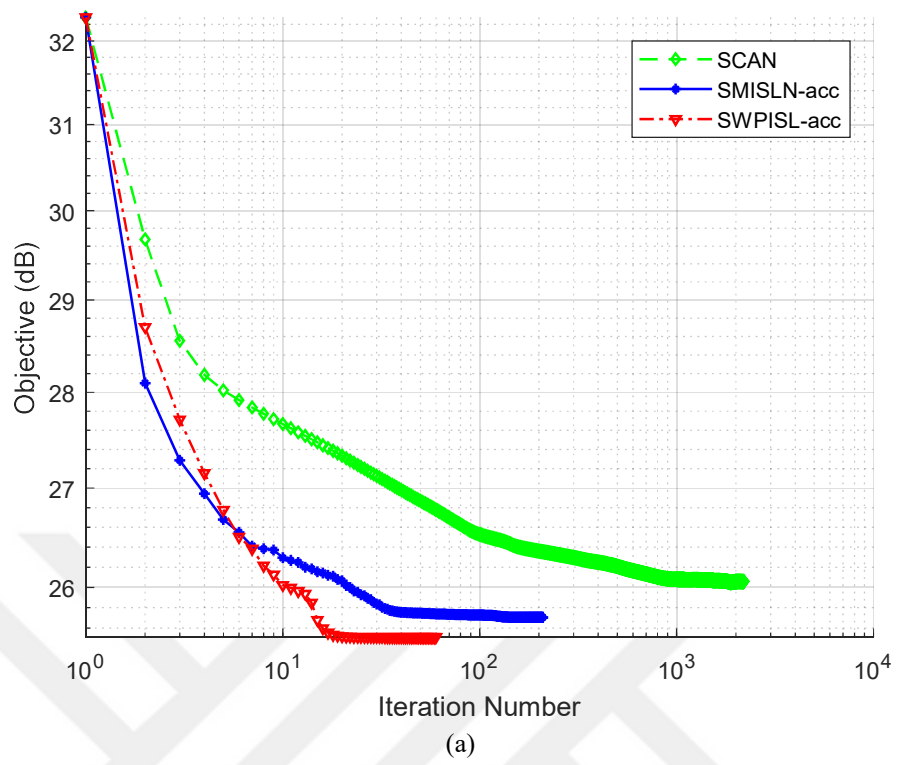


Figure 5.5 Objective function (dB) versus (a) iteration number and (b) CPU time (sec)

Numerical results belonging to SCAN, SMISLN-acc, and SWPISL-acc. are presented in Table 5.1 where the stopband power and normalized average stopband power (NASP) are defined as follows

$$\text{Stopband Power} = \|\mathbf{S}^H \hat{\mathbf{x}}\|^2 \quad (5.37)$$

$$\text{NASP} = \frac{1}{N_s} \sum_{k \in \Omega} \left(10 \log_{10} |\hat{\mathbf{x}}_f(k)|^2 \right) \text{ for } \hat{\mathbf{x}}_f = \mathbf{F}_{\tilde{N}} \hat{\mathbf{x}} \quad (5.38)$$

where N_s denotes the total number of frequency bins in stopbands as indicated after (2.23). In Table 5.1, both NASP and stopband power are expressed in dB. As can be seen from Table 5.1, the algorithms proposed in this thesis converge faster than SCAN in terms of CPU time and the number of iterations and achieve lower power values in stopband frequencies.

Table 5.1 Numerical results

	SCAN		SMISLN-acc		SWPISL-acc	
Number of Iterations	2193		209		60	
Stopband Power	106.3978		38.6290		45.7964	
MF	3.1410		2.9317		3.1314	
CPU Time (sec.)	38.1869		18.5920		4.6206	
Stopband Frequencies (Hz.)	0.2-0.3	0.7-0.8	0.2-0.3	0.7-0.8	0.2-0.3	0.7-0.8
NASP (dB)	-13.7339	-14.0198	-22.2054	-19.6748	-19.7315	-21.2712

CHAPTER SIX
DESIGNING SEQUENCES SATISFYING SIMULTANEOUS TEMPORAL
WISL AND SPECTRAL STOPBAND CONSTRAINTS

In this chapter, we propose new algorithms for designing sequences having minimum WISL values and satisfying additional stopband constraints. In (He et al., 2010), WeSCAN algorithm was proposed. This algorithm minimizes a quadratic “approximation” of WISL instead of the exact WISL metric which is quartic in the sequence, x_n . Therefore, we are interested in designing sequences by minimizing the exact WISL metric together with a stopband constraint.

6.1 Sequence Design with WISL and Stopband Constraints

In (He et al., 2010), the optimization problem is given as

$$\begin{aligned} & \underset{\mathbf{x}}{\text{minimize}} && J(\mathbf{x}) = (1 - \lambda)\text{WISL} + \lambda\text{SC} \\ & \text{subject to} && |x_n| = 1, \quad n = 1, \dots, N. \end{aligned} \tag{6.1}$$

In order to solve the above optimization problem, (He et al., 2010) proposed to use a cyclic algorithm named WeSCAN (Weighted SCAN). WeSCAN (see Section 2.1.4) is an extension of the WeCAN algorithm proposed in (Stoica et al., 2009).

In this chapter, we propose to use the MM method to solve the problem in (6.1). The two algorithms that we propose for designing unimodular sequences having minimum WISL value and satisfying a stopband constraint are named SMWISL (stopband MWISL) and SWPISL (stopband WPISL). These algorithms are extensions of the MWISL (Song et al., 2016b) and WPISL (Zhao et al., 2016) algorithms, respectively.

6.2 Stopband MWISL (SMWISL)

Autocorrelation function can be expressed alternatively as (Song et al., 2016b)

$$r_k = \text{Tr}(\mathbf{U}_k \mathbf{x} \mathbf{x}^H), \quad k = 0, \dots, N-1 \tag{6.2}$$

where $\text{Tr}(\cdot)$ represents trace of a matrix. Then, the metric of WISL can alternatively be written as

$$\text{WISL} = \frac{1}{2} \sum_{k=-(N-1)}^{N-1} w_k |\text{Tr}(\mathbf{U}_k \mathbf{X})|^2. \quad (6.3)$$

Using the above WISL expression, we propose an algorithm for designing sequences having minimum WISL values and satisfying some stopband constraints. As pointed out in the previous chapters, to suppress the frequency stopbands, the criterion in (2.25) is minimized. When the stopband and correlation constraints given in (2.25) and (2.70), respectively, are combined, the following optimization problem can be written

$$\begin{aligned} & \underset{\mathbf{x}}{\text{minimize}} \quad \lambda N \|\mathbf{S}^H \hat{\mathbf{x}}\|^2 + (1-\lambda) \frac{1}{2} \sum_{k=-(N-1)}^{N-1} w_k |\text{Tr}(\mathbf{U}_k \mathbf{X})|^2 \\ & \text{subject to} \quad |x_n| = 1, \quad n = 1, \dots, N. \end{aligned} \quad (6.4)$$

We use the MM method to solve the above minimization problem by applying Lemma 1 and Lemma 3 to (6.4) term by term. First of all, after applying the majorization steps on the second term of (6.4), the objective function can be rewritten as follows

$$\begin{aligned} & \lambda N \|\mathbf{S}^H \hat{\mathbf{x}}\|^2 + 2(1-\lambda) \text{Re} \left(\mathbf{x}^H \left(\mathbf{R}_1 - \lambda_{\max}(\mathbf{E}_1) \mathbf{x}^{(l)} \left(\mathbf{x}^{(l)} \right)^H - \lambda_u \mathbf{I} \right) \mathbf{x}^{(l)} \right) \\ & + \text{constant}. \end{aligned} \quad (6.5)$$

The other majorization step is accomplished by applying Lemma 1 in Section 2.2.1 on the first term. Then, the expression given in (6.5) is majorized by the majorizing function in (5.7) given below

$$u_1(\hat{\mathbf{x}}, \hat{\mathbf{x}}^{(k)}) + 2(1-\lambda) \text{Re} \left(\mathbf{x}^H \left(\mathbf{R}_1 - \lambda_{\max}(\mathbf{E}_1) \mathbf{x}^{(l)} \left(\mathbf{x}^{(l)} \right)^H - \lambda_u \mathbf{I} \right) \mathbf{x}^{(l)} \right) + \text{constant}. \quad (6.6)$$

After removing the constant terms, the optimization problem in (6.4) can be recast in terms of majorizing functions as follows

$$\begin{aligned}
& \underset{\mathbf{x}}{\text{minimize}} && 2\lambda N \operatorname{Re}\left(\hat{\mathbf{x}}^H (\boldsymbol{\Sigma}_3 - \lambda_{\max}(\boldsymbol{\Sigma}_3)\mathbf{I})\hat{\mathbf{x}}^{(k)}\right) \\
& && + 2(1-\lambda) \operatorname{Re}\left(\mathbf{x}^H \left(\mathbf{R}_1 - \lambda_{\max}(\mathbf{E}_1)\mathbf{x}^{(l)}(\mathbf{x}^{(l)})^H - \lambda_u \mathbf{I}\right)\mathbf{x}^{(l)}\right) \\
& \text{subject to} && |x_n| = 1, \quad n = 1, \dots, N.
\end{aligned} \tag{6.7}$$

It can also be expressed as

$$\begin{aligned}
& \underset{\mathbf{x}}{\text{minimize}} && \operatorname{Re}\left(\lambda N \hat{\mathbf{x}}^H (\boldsymbol{\Sigma}_3 - \lambda_{\max}(\boldsymbol{\Sigma}_3)\mathbf{I})\hat{\mathbf{x}}^{(k)}\right) \\
& && + (1-\lambda) \mathbf{x}^H \left(\mathbf{R}_1 - \lambda_{\max}(\mathbf{E}_1)\mathbf{x}^{(l)}(\mathbf{x}^{(l)})^H - \lambda_u \mathbf{I}\right)\mathbf{x}^{(l)} \\
& \text{subject to} && |x_n| = 1, \quad n = 1, \dots, N.
\end{aligned} \tag{6.8}$$

Then, we have

$$\begin{aligned}
& \underset{\mathbf{x}}{\text{minimize}} && \operatorname{Re}\left(\hat{\mathbf{x}}^H (\lambda \mathbf{y}_1) + \mathbf{x}^H ((1-\lambda)\mathbf{y}_4)\right) \\
& \text{subject to} && |x_n| = 1, \quad n = 1, \dots, N
\end{aligned} \tag{6.9}$$

where

$$\begin{aligned}
\mathbf{y}_1 &= N (\boldsymbol{\Sigma}_3 - \lambda_{\max}(\boldsymbol{\Sigma}_3)\mathbf{I})\hat{\mathbf{x}}^{(k)} \\
\mathbf{y}_4 &= \left(\mathbf{R}_1 - \lambda_{\max}(\mathbf{E}_1)\mathbf{x}^{(l)}(\mathbf{x}^{(l)})^H - \lambda_u \mathbf{I}\right)\mathbf{x}^{(l)}.
\end{aligned} \tag{6.10}$$

Let the first N elements of \mathbf{y}_1 and \mathbf{y}_4 be denoted as $(\mathbf{y}_1)_{N \times 1}$ and $(\mathbf{y}_4)_{N \times 1}$, respectively.

Then, the closed-form solution is given by

$$x_n = e^{-j \arg(\lambda y_{1n} + (1-\lambda)y_{4n})}, \quad n = 1, \dots, N \tag{6.11}$$

where y_{1n} denotes the n^{th} element of the vector \mathbf{y}_1 . This algorithm minimizes the stopband power in the frequency domain employing an arbitrary number of frequency bins and reduces the WISL metric as well. We call this algorithm SMWISL (stopband MWISL). Its pseudocode is given in Algorithm 4 below.

Algorithm 4: SMWISL Algorithm

- 1: Set sequence length N , and weights, set $k = 0$, and initialize $\mathbf{x}^{(0)}$
 - 2: **while** stopping criteria \geq Tol
 - 3: $\mathbf{f} = \mathbf{F} \begin{bmatrix} \mathbf{x}^{(k)} \\ \mathbf{0}_{N \times 1} \end{bmatrix}$,
 - 4: $\mathbf{r} = \frac{1}{2N} \mathbf{F}^H |\mathbf{f}|^2$
 - 5: $\mathbf{c} = \mathbf{r} \odot [0, w_1, w_2, \dots, 0, w_N, w_{N-1}, w_1]^T$
 - 6: $\mathbf{R} = \frac{1}{2N} \mathbf{F}^H \text{Diag}(\mathbf{F}\mathbf{c})\mathbf{F}$
 - 7: $\mathbf{y}_1 = -N(\boldsymbol{\Sigma}_3 - \lambda_{\max}(\boldsymbol{\Sigma}_3)\mathbf{I})\hat{\mathbf{x}}^{(k)}$
 - 8: $\mathbf{y}_4 = -\left(\mathbf{R}_1 - \lambda_{\max}(\mathbf{E}_1)\mathbf{x}^{(l)}(\mathbf{x}^{(l)})^H - \lambda_u\mathbf{I}\right)\mathbf{x}^{(l)}$
 - 9: $x_n = e^{j\arg(\lambda N y_n + (1-\lambda)y_4^n)}$, $n = 1, \dots, N$
 - 10: $k = k + 1$
 - 11: **end while**
-

6.3 Stopband WPISL (SWPISL)

In order to modify the stopband WPISL algorithm in Section 5.3 for the minimization of WISL metric, one can simply set $p=2$ and choose $\{w_k\}_{k=1}^{N-1}$ as nonnegative weights. Derivations between (5.25) and (5.36) would be the same, notwithstanding the values of $p=2$ and $\{w_k\}_{k=1}^{N-1}$. Hence, the pseudocode in Algorithm 2 also applies here.

6.4 Stopband FWISL (SFWISL)

First, we express the WISL metric alternatively in the frequency domain as follows

$$\begin{aligned}
\text{WISL} &= \frac{\gamma_0^2}{4N} \sum_{p=1}^{2N} [\tilde{\mathbf{x}}_p^H \mathbf{\Pi} \tilde{\mathbf{x}}_p - N]^2 \\
&= \frac{\gamma_0^2}{4N} \sum_{p=1}^{2N} [\mathbf{x}^H (\mathbf{A}_p \odot \mathbf{\Pi}) \mathbf{x} - N]^2
\end{aligned} \tag{6.12}$$

where $\mathbf{A}_p = \mathbf{a}_p \mathbf{a}_p^H$ and $\mathbf{a}_p = [e^{j\omega_p} \quad e^{j2\omega_p} \quad \dots \quad e^{jN\omega_p}]^T$. In (6.12), \odot represents the Hadamard product. Then, the spectral stopband and temporal correlation constrains in (2.25) and (6.12), respectively, are combined. Thus, we propose the following optimization problem

$$\begin{aligned}
&\underset{\mathbf{x}}{\text{minimize}} && \lambda N \|\mathbf{S}^H \hat{\mathbf{x}}\|^2 + (1-\lambda) \frac{\gamma_0^2}{4N} \sum_{p=1}^{2N} [\tilde{\mathbf{x}}_p^H \mathbf{\Pi} \tilde{\mathbf{x}}_p - N]^2 \\
&\text{subject to} && |x_n| = 1, \quad n = 1, \dots, N.
\end{aligned} \tag{6.13}$$

We use the MM method to solve the problem in (6.13) by applying Lemma 1 in Section 2.2.1 and Lemma 2 in Section 2.2.2 to our minimization problem term by term. First of all, as stated in Chapter Four, after employing the majorization steps on the second term of the objective function in (6.13), the objective function can be written as follows

$$\begin{aligned}
&\lambda N \|\mathbf{S}^H \hat{\mathbf{x}}\|^2 + (1-\lambda) \frac{\gamma_0^2}{4N} 4 \text{Re} \left[\mathbf{x}^H \left(\mathbf{\Pi} \odot (\mathbf{A} \text{Diag}(\mathbf{m}^{(k)}) \mathbf{A}^H) \right. \right. \\
&\quad \left. \left. - \lambda_{\max}(\mathbf{\Sigma}) \mathbf{x}^{(k)} (\mathbf{x}^{(k)})^H - \lambda_{\max} \left(\mathbf{\Pi} \odot (\mathbf{A} \text{Diag}(\mathbf{m}^{(k)}) \mathbf{A}^H) \right) \right) \mathbf{x}^{(k)} \right] \\
&\quad + \text{constant}.
\end{aligned} \tag{6.14}$$

Secondly, by applying Lemma 1 on the first term as stated in the previous chapters, the expression in (6.14) is majorized by using the majorizing function in (5.7) as follows

$$\begin{aligned}
&2\lambda N \text{Re} \left(\hat{\mathbf{x}}^H (\mathbf{\Sigma}_3 - \lambda_{\max}(\mathbf{\Sigma}_3) \mathbf{I}) \hat{\mathbf{x}}^{(k)} \right) \\
&\quad + (1-\lambda) \frac{\gamma_0^2}{4N} 4 \text{Re} \left[\mathbf{x}^H \left(\mathbf{\Pi} \odot (\mathbf{A} \text{Diag}(\mathbf{m}^{(k)}) \mathbf{A}^H) \right. \right. \\
&\quad \left. \left. - \lambda_{\max}(\mathbf{\Sigma}) \mathbf{x}^{(k)} (\mathbf{x}^{(k)})^H - \lambda_{\max} \left(\mathbf{\Pi} \odot (\mathbf{A} \text{Diag}(\mathbf{m}^{(k)}) \mathbf{A}^H) \right) \right) \mathbf{x}^{(k)} \right] + \text{constant}.
\end{aligned} \tag{6.15}$$

After removing the constant terms, optimization problem in (6.13) can be proposed in terms of majorizing functions as follows

$$\begin{aligned}
& \underset{\mathbf{x}}{\text{minimize}} && 2\lambda N \text{Re}\left(\hat{\mathbf{x}}^H (\boldsymbol{\Sigma}_3 - \lambda_{\max}(\boldsymbol{\Sigma}_3) \mathbf{I}) \hat{\mathbf{x}}^{(k)}\right) \\
& && + (1-\lambda) \frac{\gamma_0^2}{4N} 4 \text{Re}\left[\mathbf{x}^H \left(\boldsymbol{\Pi} \odot (\mathbf{A} \text{Diag}(\mathbf{m}^{(k)}) \mathbf{A}^H) \right. \right. \\
& && \left. \left. - \lambda_{\max}(\boldsymbol{\Sigma}_2) \mathbf{x}^{(k)} (\mathbf{x}^{(k)})^H - \lambda_{\max} \left(\boldsymbol{\Pi} \odot (\mathbf{A} \text{Diag}(\mathbf{m}^{(k)}) \mathbf{A}^H)\right)\right) \mathbf{x}^{(k)}\right] \\
& \text{subject to} && |x_n| = 1, \quad n = 1, \dots, N.
\end{aligned} \tag{6.16}$$

The above problem can also be expressed as

$$\begin{aligned}
& \underset{\mathbf{x}}{\text{minimize}} && \text{Re}\left\{\lambda N \hat{\mathbf{x}}^H (\boldsymbol{\Sigma}_3 - \lambda_{\max}(\boldsymbol{\Sigma}_3) \mathbf{I}) \hat{\mathbf{x}}^{(k)} \right. \\
& && + (1-\lambda) \frac{\gamma_0^2}{2N} \left[\mathbf{x}^H \left(\boldsymbol{\Pi} \odot (\mathbf{A} \text{Diag}(\mathbf{m}^{(k)}) \mathbf{A}^H) \right. \right. \\
& && \left. \left. - \lambda_{\max}(\boldsymbol{\Sigma}_2) \mathbf{x}^{(k)} (\mathbf{x}^{(k)})^H \right. \right. \\
& && \left. \left. - \lambda_{\max} \left(\boldsymbol{\Pi} \odot (\mathbf{A} \text{Diag}(\mathbf{m}^{(k)}) \mathbf{A}^H)\right)\right) \mathbf{x}^{(k)}\right\} \\
& \text{subject to} && |x_n| = 1, \quad n = 1, \dots, N.
\end{aligned} \tag{6.17}$$

Then, we have

$$\begin{aligned}
& \underset{\mathbf{x}}{\text{minimize}} && \text{Re}\left(\hat{\mathbf{x}}^H (\lambda \mathbf{y}_1) + \mathbf{x}^H ((1-\lambda) \mathbf{y}_5)\right) \\
& \text{subject to} && |x_n| = 1, \quad n = 1, \dots, N
\end{aligned} \tag{6.18}$$

where

$$\begin{aligned}
\mathbf{y}_1 &= N (\boldsymbol{\Sigma}_3 - \lambda_{\max}(\boldsymbol{\Sigma}_3) \mathbf{I}) \hat{\mathbf{x}}^{(k)} \\
\mathbf{y}_5 &= \frac{\gamma_0^2}{2N} \left(\boldsymbol{\Pi} \odot (\mathbf{A} \text{Diag}(\mathbf{m}^{(k)}) \mathbf{A}^H) - \lambda_{\max}(\boldsymbol{\Sigma}_2) \mathbf{x}^{(k)} (\mathbf{x}^{(k)})^H \right. \\
& \quad \left. - \lambda_{\max} \left(\boldsymbol{\Pi} \odot (\mathbf{A} \text{Diag}(\mathbf{m}^{(k)}) \mathbf{A}^H)\right) \mathbf{I}\right) \mathbf{x}^{(k)}
\end{aligned} \tag{6.19}$$

Let the first N elements of \mathbf{y}_1 and \mathbf{y}_5 be $(\mathbf{y}_1)_{N \times 1}$ and $(\mathbf{y}_5)_{N \times 1}$, respectively. Then, the closed-form solution is given by

$$x_n = e^{-j \arg(\lambda y_n + (1-\lambda)y_{5n})}, \quad n=1, \dots, N. \quad (6.20)$$

This algorithm minimizes the stopband power in the frequency domain employing an arbitrary number of frequency bins and reduces the WISL metric as well. We call this algorithm SFWISL (stopband FWISL). Its pseudocode is given in Algorithm 5 below.

Algorithm 5: SFWISL Algorithm

- 1: Set sequence length N , weights $\{w_k \geq 0\}_{k=1}^{N-1}$, select γ_0 ,
 set $k = 0$, and initialize $\mathbf{x}^{(0)}$
 - 2: **while** stopping criteria \geq Tol
 - 3: $m_p = (\mathbf{x}^{(k)})^H \mathbf{M}_p \mathbf{x}^{(k)}$, $p=1, \dots, 2N$
 - 4: $\mathbf{m}^{(k)} = [m_1^{(k)} \quad m_2^{(k)} \quad \dots \quad m_{2N}^{(k)}]^T$
 - 5: $\mathbf{y}_1 = N(\boldsymbol{\Sigma}_3 - \lambda_{\max}(\boldsymbol{\Sigma}_3)\mathbf{I})\hat{\mathbf{x}}^{(k)}$
 - 5: $\mathbf{y}_5 = \frac{\gamma_0^2}{2N} \left(\boldsymbol{\Pi} \odot (\mathbf{A} \text{Diag}(\mathbf{m}^{(k)}) \mathbf{A}^H) \right.$
 $\left. - \lambda_{\max}(\boldsymbol{\Sigma}_2) \mathbf{x}^{(k)} (\mathbf{x}^{(k)})^H - m_{\max}^{(k)} \boldsymbol{\Pi} \odot (\mathbf{A} \mathbf{A}^H) \right) \mathbf{x}^{(k)}$
 - 6: $x_n = e^{j \arg(\lambda y_n + (1-\lambda)y_{5n})}$, $n=1, \dots, N$
 - 7: $k = k + 1$
 - 8: **end while**
-

6.5 Numerical Examples for Designing with WISL and Stopband Constraints

We provide a numerical example in which we design a unimodular sequence of length $N = 100$. The frequency stopband is given as $\Omega = [0.2, 0.3)$ Hz in terms of normalized frequency. The relative weight parameter, λ , is taken as $\lambda = 0.8$. The number of DFT bins is selected as $\tilde{N} = 1000$. The simulated algorithms are initialized with Golomb sequence (Zhang & Golomb, 1993). The tolerance value for the stopping

criterion is determined as $\text{Tol} = 10^{-4}$. The weights, $\{\gamma_k\}_{k=1}^{N-1}$, of the correlation lags are selected as

$$\gamma_k = \begin{cases} 1, & k \in \{1, \dots, 20\} \cup \{51, \dots, 70\} \\ 0, & \text{otherwise.} \end{cases} \quad (6.21)$$

Performance of the proposed algorithms are compared against the WeSCAN (He et al., 2010) algorithm in terms of number of iterations, computation time, the value of the WISL metric, and the level of suppression in spectral stopbands.

Figure 6.1, Figure 6.2, Figure 6.3, and Figure 6.4 show the normalized power spectra and correlation levels of the sequences designed by WeSCAN, SMWISL-acc (accelerated SMWISL), SWPISL-acc (accelerated SWPISL), and SFWISL-acc (accelerated SFWISL), respectively. The power spectra are normalized to make the average value of the spectra in passbands equal to 1 dB (He et al., 2010). In Figure 6.5, the normalized power spectra of the sequences designed by those four algorithms are plotted together. We can see that the algorithms proposed in this thesis provide better suppression in stopbands than SCAN.

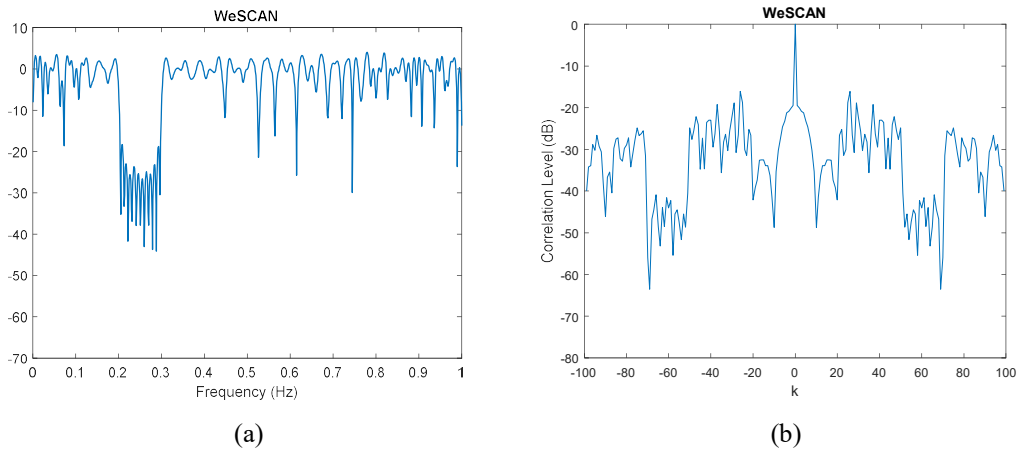
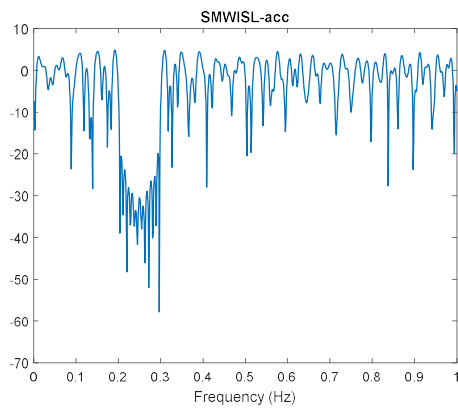
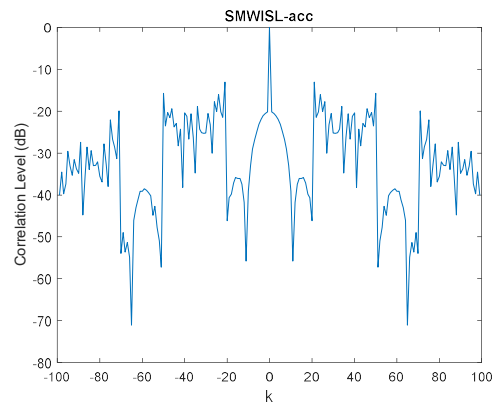


Figure 6.1 (a) Normalized power spectrum, (b) correlation level of the sequence designed by WeSCAN

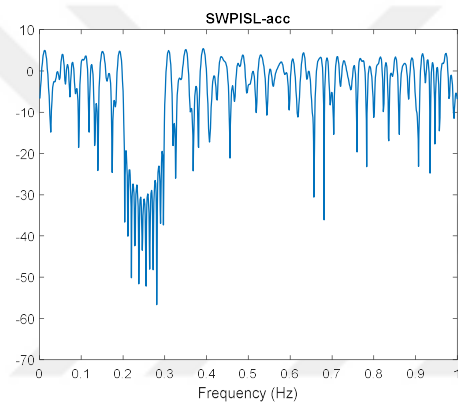


(a)

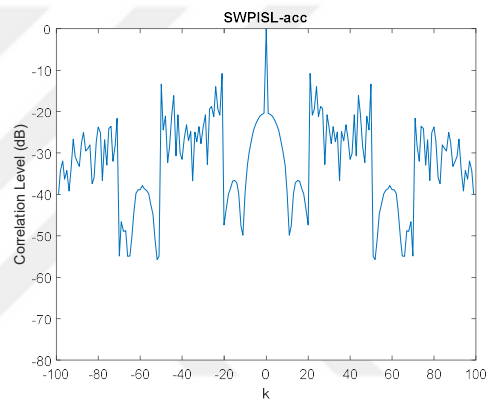


(b)

Figure 6.2 (a) Normalized power spectrum, (b) correlation level of the sequence designed by SMWISL-acc

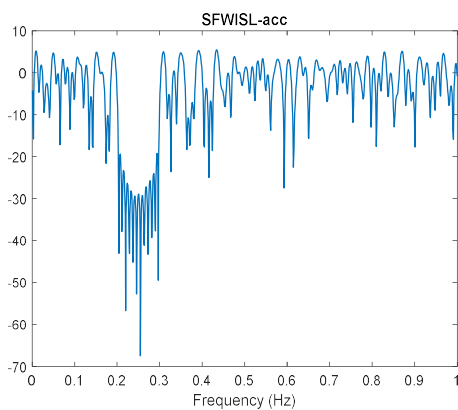


(a)

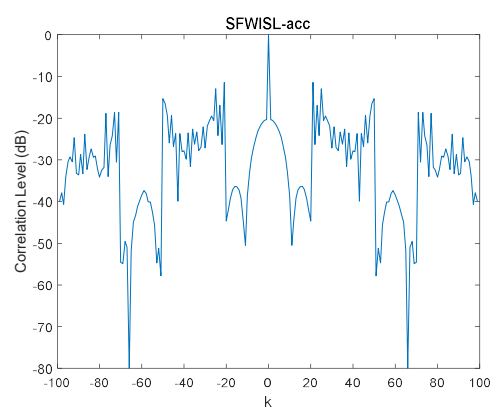


(b)

Figure 6.3 (a) Normalized power spectrum, (b) correlation level of the sequence designed by SWPISL-acc



(a)



(b)

Figure 6.4 (a) Normalized power spectrum, (b) correlation level of the sequence designed by SFWISL-acc

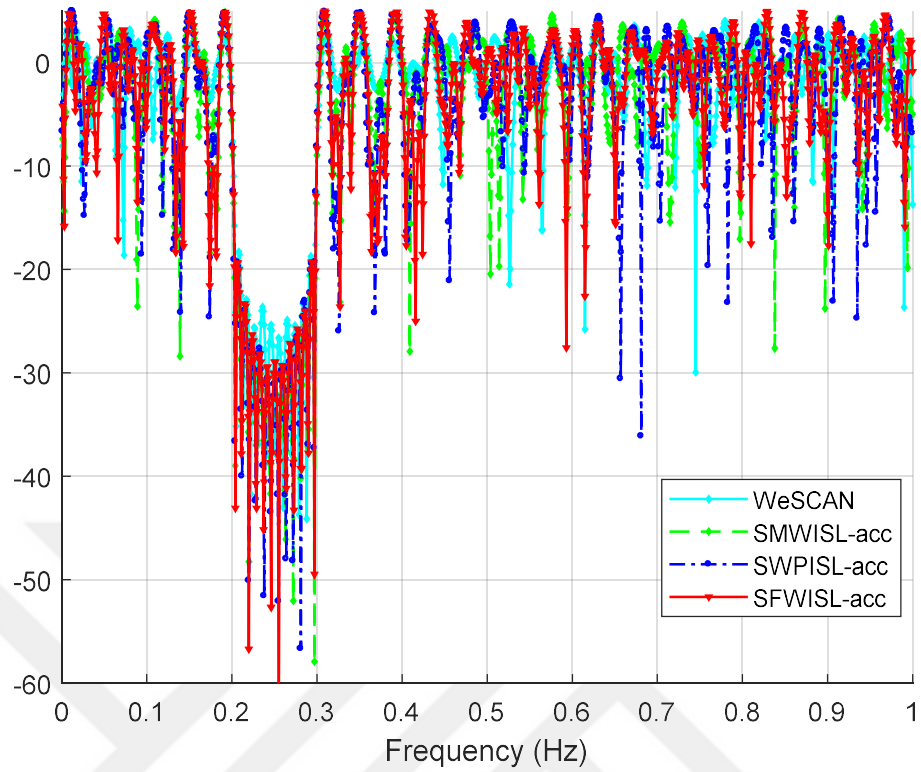


Figure 6.5 Normalized power spectra of sequences designed by WeSCAN, SMWISL-acc, SWPISL-acc, and SFWISL-acc

Evolution of the objective function versus iteration number and CPU time (sec.) is shown in Figure 6.6 (a) and (b), respectively. As can be seen from Figure 6.6, the proposed algorithms in this thesis, SMWISL-acc, SWPISL-acc, SFWISL-acc, converge to a stationary point in a smaller number of iterations and less CPU time (sec.) than WeSCAN and achieve lower power levels in stopband frequencies.

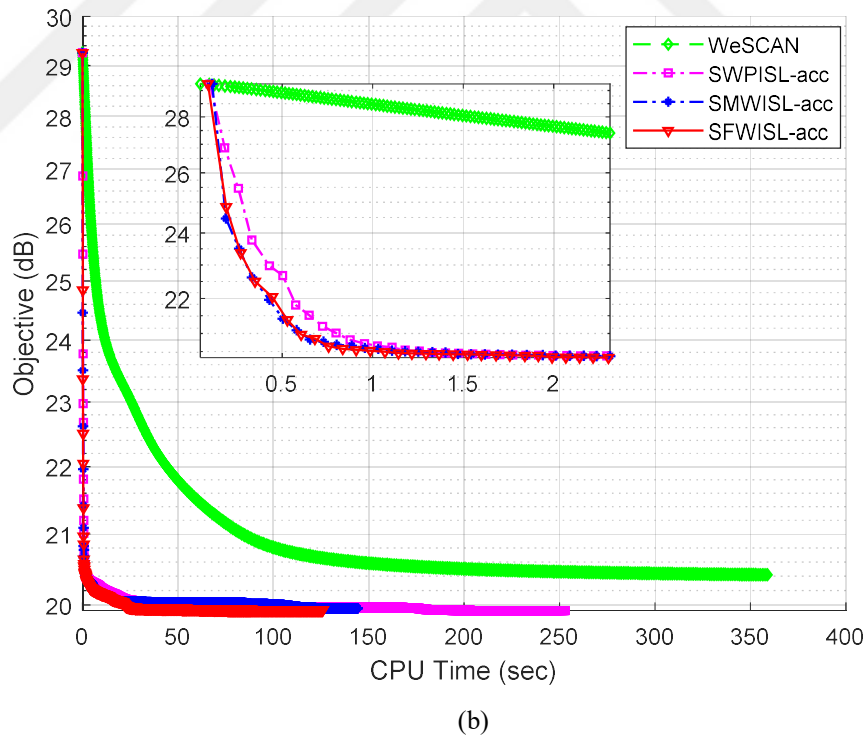
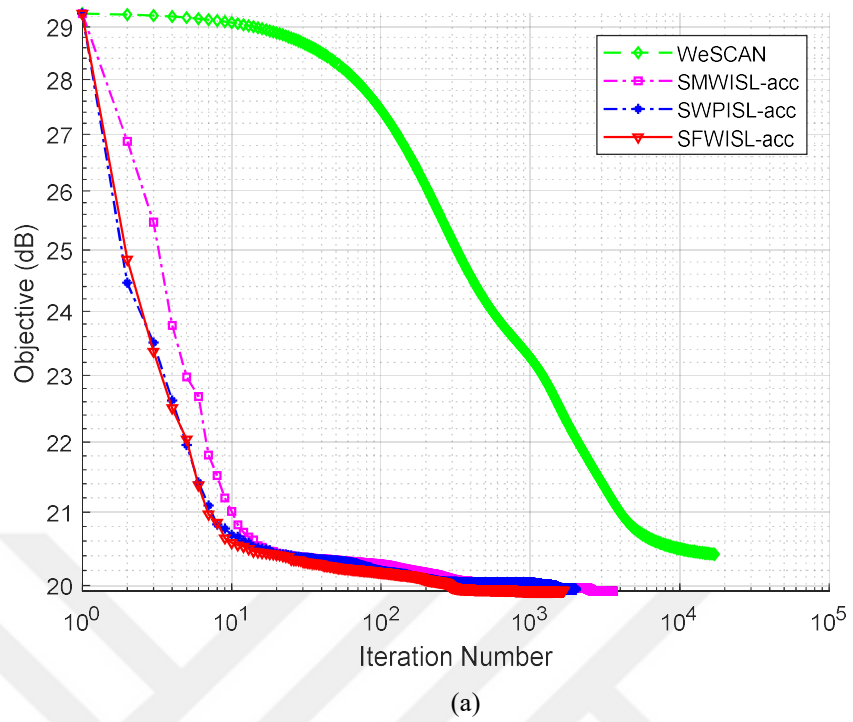


Figure 6.6 Objective function (dB) versus (a) iteration number and (b) CPU time (sec.)

Numerical results belonging to WeSCAN, SMWISLN-acc, SWPISL-acc, and SFWISL-acc are displayed in Table 6.1. In Table 6.1, both NASP and stopband power

are presented in dB. As can be seen from Table 6.1, the algorithms proposed in this thesis converge faster than WeSCAN in terms of CPU time and number of iterations and achieve lower power values in stopband frequencies.

Table 6.1 Numerical results

	WeSCAN	SMWISL-acc	SWPISL-acc	SFWISL-acc
Number of Iterations	17216	1963	3662	1669
Stopband Power	8.2512	5.5623	6.8357	6.5650
MMF	9.6570	10.5835	10.7801	10.7291
CPU Time (sec.)	408.8024	36.6301	62.1615	32.8279
Stopband Frequencies	0.2-0.3 Hz	0.2-0.3 Hz	0.2-0.3 Hz	0.2-0.3 Hz
NASP (dB)	-27.2538	-30.9146	-30.7757	-30.4878

CHAPTER SEVEN

CONCLUSIONS

In this thesis, we focus on developing algorithms to design transmit sequences satisfying temporal correlation and spectral stopband constraints. For this purpose, several algorithms are proposed for designing unimodular sequences for radar and communication systems. We believe that the proposed algorithms provide good alternatives to the ones already existing in the literature.

In Chapter Three, we have proposed to use GA in order to design unimodular constant modulus sequences attaining minimum ISL values. We compared performance of GA against that of the CAN and MISL algorithms in terms of MF. The already existing CAN algorithm was proposed for designing sequences with good correlation properties by minimizing an approximate quadratic ISL-related metric instead of the exact quartic ISL metric itself. Therefore, one of our aims in this thesis is to minimize the original quartic metric of ISL using GA and compare its performance against CAN. In (Song et al., 2015a), MISL was also proposed to minimize the original quartic metric of ISL. Although, the evaluation time required for termination of CAN and MISL are shorter than GA, GA performs slightly better than CAN and MISL in terms of resulting MF. The difference between those two algorithms on minimizing the ISL-related metric in (2.13) and the exact ISL metric in (2.12) become more evident when they are initialized by random sequences. In short, we can state that sequences designed by minimizing the exact metric of ISL using GA possess higher MFs than those designed by the CAN and MISL algorithm. However, execution time of CAN and MISL are shorter than GA. Since we employed GA as a benchmark method towards finding the global optimum solution of the design problem, one can infer from the results in Chapter 3 that the CAN and MISL algorithms converge near the global minimum. However, we must emphasize that the design parameters of GA were not optimized for the larger sequence lengths because of its long execution time. Hence, we cannot state confidently whether the CAN and MISL algorithms reach the optimum solution or not.

In Chapter Four, we have proposed an alternative algorithm shortly named as FWISL for designing unimodular sequences by minimizing the WISL metric in the frequency domain. We have applied the MM method in two stages and a closed-form expression has been obtained. A computationally efficient version of FWISL (FWISL-acc) is also proposed by employing an acceleration scheme. Performance of the proposed algorithm is compared against CAP, WeCAN, WeCAN+CAP, MWISL-acc, and WPISL-SQUAREM algorithms. Our results indicate that the proposed algorithm, FWISL-acc, terminates in lower number of iterations and in less CPU time, and attains smaller WISL (or larger MMF) values than other algorithms. Performance of the algorithm can be further improved when it is initialized by the sequence designed by the CAP algorithm. Numerical results show that our proposed algorithm allows design of long sequences in lower number of iterations, less CPU time, and with larger MMF values.

In Chapter Five, we have proposed alternative algorithms for designing unimodular sequences satisfying simultaneous temporal correlation and spectral stopband constraints. These algorithms are split into two categories. In the first part, we developed new algorithms to design sequences with low ISL and having stopband constraints. We have modified the MISL and WPISL algorithms in order to use them with stopband constraints. Then, we have employed the MM method with both temporal and spectral constraints. By this way, SMISLN and SWPISL algorithms are proposed as alternative algorithms to SCAN. The results show that the new algorithms converge to stationary points faster than SCAN and achieve lower stopband powers.

In Chapter Six, we have developed new algorithms to design sequences with low WISL values and having stopband constraints. For this purpose, we have modified the MWISL and WPISL algorithms in order to use them with stopband constraints and named the new algorithms as SMWISL and SWPISL, respectively. The SMWISL and SWPISL algorithms are proposed as alternatives to WeSCAN. We also modified the FWISL algorithm and proposed the SFWISL algorithm. Simulation results show that performance of SFWISL is better than other algorithms in terms of iteration number, CPU time and stopband power.

We would like to stress that performances of the algorithms proposed in this thesis are evaluated numerically in terms of CPU time, number of iterations, MFs or MMFs of designed sequences, stopband power, and NASP. Although, a theoretical computational complexity analysis could also be carried out, it would require a thorough study of local rate of convergence analysis approach (Bertsekas, 1999). Therefore, it is left out as the topic of a future study.

As a final remark, in light of the obtained results, we believe that the developed algorithms in this thesis can be good alternatives to the ones already existing in the literature.



REFERENCES

- Barker, R. H. (1953). Group synchronizing of binary digital systems. In W. Jackson (Ed.), *Communication Theory* (273–287). Butterworths, London, U.K.
- Bertsekas, D. P. (1999). *Nonlinear Programming*. Belmont, MA: Athena scientific.
- Biskin, O. T., & Akay, O. (2018a). *A new frequency domain sequence design algorithm minimizing the weighted integrated sidelobe level*, IET Radar, Sonar & Navigation, submitted (under revision).
- Biskin, O. T., & Akay, O. (2018b). A new algorithm for designing sequences using stopband and correlation constraints. In *IEEE 26th Signal Processing and Communications Applications Conference (SIU)*, (1–4), Izmir, Türkiye.
- Bişkin, O. T., & Akay, O. (2017). Design of sequences with low autocorrelation sidelobes using genetic algorithms. In *2017 10th International Conference on Electrical and Electronics Engineering, ELECO 2017*, (3–7), Bursa, Türkiye.
- Borwein, P., & Ferguson, R. (2005). Polyphase sequences with low autocorrelation. *IEEE Transactions on Information Theory*, 51(4), 1564–1567.
- Capraro, C. T., Bradaric, I., Capraro, G. T., & Lue, T. K. (2008). Using genetic algorithms for radar waveform selection. In *2008 IEEE Radar Conference, RADAR 2008* (1–6), Rome, Italy.
- Chu, D. C. (1972). Polyphase codes with good periodic correlation properties. *IEEE Transactions on Information Theory*, 18(4), 531–532.
- Frank, R. L. (1963). Polyphase codes with good nonperiodic correlation properties. *IEEE Transactions on Information Theory*, 9(1), 43–45.
- Haykin, S. (2006). Cognitive radar: A way of the future. *IEEE Signal Processing Magazine*, 23(1), 30–40.
- He, H., Li, J., & Stoica, P. (2012). *Waveform design for active sensing systems: A computational approach*. *Waveform Design for Active Sensing Systems: A*

Computational Approach. Cambridge, UK: Cambridge University Press.

- He, H., Stoica, P., & Li, J. (2010). Waveform design with stopband and correlation constraints for cognitive radar. In *2nd International Workshop on Cognitive Information Processing, CIP2010* (344–349). Elba, Italy.
- Jian, L., Stoica, P., & Xiayu, Z. (2008). Signal synthesis and receiver design for MIMO radar imaging. *IEEE Transactions on Signal Processing*, *56*(8), 3959–3968.
- Kocabaş, Ş. E., & Atalar, A. (2003). Binary sequences with low aperiodic autocorrelation for synchronization purposes. *IEEE Communications Letters*, *7*(1), 36–38.
- Lellouch, G., Mishra, A., & Inggs, M. (2015). Convex optimization for optimal PMEPR and mismatched filter design in OFDM radar. In *2015 IEEE Radar Conference - Proceedings* (37–41). Johannesburg, South Africa.
- Lellouch, G., Mishra, A., & Inggs, M. (2016). Design of OFDM radar pulses using genetic algorithm based techniques. *IEEE Transactions on Aerospace and Electronic Systems*, *52*(4), 1953–1966.
- Levanon, N., & Mozeson, E. (2004). *Radar Signals*. Hoboken, New Jersey, USA: John Wiley & Sons, Inc.
- Lewis, B. L., & Kretschmer, F. F. (1981). A new class of polyphase pulse compression codes and techniques. *IEEE Transactions on Aerospace and Electronic Systems*, *AES-17*(3), 364–372.
- Lewis, B. L., & Kretschmer, F. F. (1982). Linear frequency modulation derived polyphase pulse compression codes. *IEEE Transactions on Aerospace and Electronic Systems*, *AES-18*(5), 637–641.
- Lindenfeld, M. J. (2004). Sparse frequency transmit and receive waveform design. *IEEE Transactions on Aerospace and Electronic Systems*, *40*(3), 851–861.
- Martone, A., Ranney, K., & Sherbondy, K. (2016). Genetic algorithm for adaptable

- radar bandwidth. In *2016 IEEE Radar Conference, RadarConf 2016* (1–6). Philadelphia, PA, USA.
- Petrolati, D., Angeletti, P., & Toso, G. (2012). New piecewise linear polyphase sequences based on a spectral domain synthesis. *IEEE Transactions on Information Theory*, 58(7), 4890–4898.
- Proakis, J. G., & Manolakis, D. G. (2006). *Digital Signal Processing*. Upper Saddle River, NJ: Pearson Prentice Hall.
- Rapajic, P. B., & Kennedy, R. A. (1998). Merit factor based comparison of new polyphase sequences. *IEEE Communications Letters*, 2(10), 269–270.
- Roberts, W., He, H., Li, J., & Stoica, P. (2010). Probing waveform synthesis and receiver filter design. *IEEE Signal Processing Magazine*, 27(4), 99–112.
- Rowe, W., Stoica, P., & Li, J. (2014). Spectrally constrained waveform design. *IEEE Signal Processing Magazine*, 31(3), 157–162.
- Skolnik, M. I. (2008). *Radar Handbook* (Third Edit). New York: The McGraw-Hill.
- Smith-Martinez, B., Agah, A., & Stiles, J. M. (2013). A Genetic Algorithm for Generating Radar Transmit Codes to Minimize the Target Profile Estimation Error. *Journal of Intelligent Systems*, 22(4), 503–525.
- Song, J., Babu, P., & Palomar, D. P. (2015a). Optimization methods for designing sequences with low autocorrelation sidelobes. *IEEE Transactions on Signal Processing*, 63(15), 3998–4009.
- Song, J., Babu, P., & Palomar, D. P. (2015b). Optimization methods for sequence design with low autocorrelation sidelobes. In *ICASSP, IEEE International Conference on Acoustics, Speech and Signal Processing - Proceedings* (3033–3037), Brisbane, QLD, Australia.
- Song, J., Babu, P., & Palomar, D. P. (2016a). Sequence design to minimize the peak sidelobe level. In *ICASSP, IEEE International Conference on Acoustics, Speech*

- and Signal Processing - Proceedings* (3896–3900). Shanghai, China.
- Song, J., Babu, P., & Palomar, D. P. (2016b). Sequence design to minimize the weighted integrated peak sidelobe level. *IEEE Transactions on Signal Processing*, 64(8), 2051–2064.
- Stoica, P., He, H., & Li, J. (2009). New algorithms for designing unimodular sequences with good correlation properties. *IEEE Transactions on Signal Processing*, 57(4), 1415–1425.
- Stoica, P., Li, J., & Xue, M. (2008). Transmit codes and receive filters for radar: A look at the design process. *IEEE Signal Processing Magazine*, 25(6), 94–109.
- Stoica, P., Li, J., & Zhu, X. (2008). Waveform synthesis for diversity-based transmit beampattern design. *IEEE Transactions on Signal Processing*, 56(6), 99–112.
- Stoica, P., Li, J., Zhu, X., & Guo, B. (2007). Waveform synthesis for diversity-based transmit beampattern design. In *IEEE/SP 14th Workshop on Statistical Signal Process.* (473–477).
- Stoica, P., & R. L. Moses. (2005). *Spectral Analysis of Signals*. Upper Saddle River, NJ: Prentice-Hall.
- Stoica, P., & Selen, Y. (2004). Cyclic Minimizers, Majorization Techniques, and the Expectation-Maximization Algorithm: A Refresher. *IEEE Signal Processing Magazine*, 21(1), 112–114.
- Sun, G., Wang, J., Zhang, Z., Tao, M., & Zhou, F. (2016). System parameter optimisation for moving target detection and imaging in multi-band synthetic aperture radar based on genetic algorithm. *IET Radar, Sonar & Navigation*, 10(1), 146–154.
- Sun, Y., Babu, P., & Palomar, D. P. (2017). Majorization-minimization algorithms in signal processing, communications, and machine learning. *IEEE Transactions on Signal Processing*, 65(3), 794–816.

- Varadhan, R., & Roland, C. (2008). Simple and globally convergent methods for accelerating the convergence of any EM algorithm. *Scandinavian Journal of Statistics*, 35(2), 335–353.
- Wang, S. (2008). Efficient heuristic method of search for binary sequences with good aperiodic autocorrelations. *Electronic Letters*, 44(12), 731–732.
- Weile, D. S., & Michielssen, E. (1997). Genetic algorithm optimization applied to electromagnetics: a review. *Antennas and Propagation, IEEE Transactions On*, 45(3), 343–353.
- Wu, L., Babu, P., & Palomar, D. P. (2017). Cognitive radar-based sequence design via SINR maximization. *IEEE Transactions on Signal Processing*, 65(3), 779–793.
- Zhang, N., & Golomb, S. W. (1993). Polyphase sequence with low autocorrelations. *IEEE Transactions on Information Theory*, 39(3), 1085–1089.
- Zhao, L., Song, J., Babu, P., & Palomar, D. (2016). A unified framework for low autocorrelation sequence design via majorization-minimization. *IEEE Transactions on Signal Processing*, 65(2), 438–453.

APPENDICES

APPENDIX 1: CAZAC Sequences

By sampling the chirp signal in (1.1) at time intervals $T_s = n/B$ for $n = 1, \dots, N, (N = BT)$ the following sequence can be obtained (neglecting the multiplicative term, $1/\sqrt{\tau}$)

$$x_n = s(nT_s) = e^{j\pi \frac{B}{T} \left(\frac{n}{B}\right)^2} = e^{j\pi \frac{n^2}{N}}, \quad n = 1, \dots, N. \quad (\text{A.1})$$

The sequence $\{x_n\}_{n=1}^N$ has perfect periodic autocorrelation for even values of N . Waveforms with perfect periodic autocorrelations are named as constant amplitude with zero autocorrelation (CAZAC) sequences. Periodic autocorrelation sidelobes of CAZAC sequences are zero (Roberts et al., 2010).

Golomb sequence is constructed for odd values of N and is defined as follows (Roberts et al., 2010)

$$x[n] = e^{j\pi \frac{n(n-1)}{N}}, \quad n = 1, \dots, N. \quad (\text{A.2})$$

Frank code is also a CAZAC sequence and is only defined for square lengths, $N = K^2$, as (Roberts et al., 2010)

$$x[(m-1)K + p] = e^{j2\pi \frac{(m-1)(p-1)}{K}}, \quad m, p = 1, \dots, K. \quad (\text{A.3})$$

Another CAZAC sequence, P4, is defined for any length N and is given as (Roberts et al., 2010)

$$c[n] = e^{j\frac{2\pi}{N}(n-1)\left(\frac{n-1-N}{2}\right)}, \quad n = 1, \dots, N. \quad (\text{A.4})$$

APPENDIX 2: Acceleration Scheme

By using an acceleration scheme, MM-based iterative methods are allowed to converge faster (Song et al., 2015a, 2015b, 2016b; Zhao et al., 2016). The acceleration scheme that can be used in our MM-based proposed methods is the so-called squared iterative method (SQUAREM) which is originally proposed in (Varadhan & Roland, 2008) to accelerate expectation-maximization (EM) algorithm and applied to MM methods in (Song et al., 2015a, 2015b, 2016b; Wu, Babu, & Palomar, 2017; Zhao et al., 2016). As an example, following a similar acceleration scheme, the accelerated version of FWISL in Algorithm 3 is given in Algorithm 6 below.

Let $\mathbf{P}_{\text{FWISL}}(\cdot)$ represent the nonlinear fixed-point iteration map of the FWISL algorithm as expressed below

$$\mathbf{x}^{(k+1)} = \mathbf{P}_{\text{FWISL}}(\mathbf{x}^{(k)}) \quad (\text{A.5})$$

corresponding to the mapping in (4.16). SQUAREM may violate the descent property (Song et al., 2015a, 2016b; Wu et al., 2017; Zhao et al., 2016) of the original MM algorithm. For this reason, a backtracking based strategy is adopted which halves the distance between δ and -1 in Algorithm 6 below until the descent property is satisfied. Therefore, $\text{WISL}(\mathbf{x}_3) \leq \text{WISL}(\mathbf{x}^{(k)})$ is guaranteed while $\delta \rightarrow -1$ because $\text{WISL}(\mathbf{x}_2) \leq \text{WISL}(\mathbf{x}^{(k)})$ due to the descent property of the original MM algorithm.

Algorithm 6: FWISL-acc Algorithm

- 1: Set sequence length N , weights $\{w_k \geq 0\}_{k=1}^{N-1}$, select γ_0 ,
set $k = 0$ and initialize $\mathbf{x}^{(0)}$
 - 2: **while** stopping criteria \geq Tol
 - 3: $\mathbf{x}_1 = \mathbf{F}_{\text{FWISL}}(\mathbf{x}^{(k)})$
 - 4: $\mathbf{x}_2 = \mathbf{F}_{\text{FWISL}}(\mathbf{x}_1)$
 - 5: $\mathbf{r} = \mathbf{x}_1 - \mathbf{x}^{(k)}$
 - 6: $\mathbf{v} = \mathbf{x}_2 - \mathbf{x}_1 - \mathbf{r}$
 - 7: $\alpha = -\|\mathbf{r}\| / \|\mathbf{v}\|$
 - 8: $\mathbf{x}_3 = e^{j\arg(\mathbf{x}^{(k)} - 2\alpha\mathbf{r} + \alpha^2\mathbf{v})}$
 - 9: **while** $\text{WISL}(\mathbf{x}_3) \geq \text{WISL}(\mathbf{x}^{(k)})$
 - 10: $\alpha \leftarrow (\alpha - 1) / 2$
 - 11: $\mathbf{x}_3 = e^{j\arg(\mathbf{x}^{(k)} - 2\alpha\mathbf{r} + \alpha^2\mathbf{v})}$
 - 12: **end while**
 - 13: $\mathbf{x}^{(k+1)} = \mathbf{x}_3$
 - 14: $k = k + 1$
 - 15: **end while**
-

APPENDIX 3: Proof of Hermitian Toeplitz Matrix

We prove that $\mathbf{\Pi} \odot \left(\mathbf{A} \text{Diag} \{ \mathbf{m}^{(k)} \} \mathbf{A}^H \right)$ is Hermitian Toeplitz. Let \mathbf{B} denote a $N \times N$ Hermitian Toeplitz matrix and $\mathbf{B}(m, n)$ be its $(m, n)^{\text{th}}$ element. Then, to be Hermitian Toeplitz the matrix \mathbf{B} must satisfy the following equalities:

- (i) $\mathbf{B}(m, n) = \mathbf{B}^*(n, m)$ (Hermitian condition),
- (ii) $\mathbf{B}(m, n) = \mathbf{B}(k, l)$ if $m - n = k - l$ (Toeplitz condition).

Firstly, $\mathbf{\Pi}$ is clearly Hermitian Toeplitz as can be seen from (2.34). Since the Hadamard product of two Hermitian Toeplitz matrices is also Hermitian Toeplitz, to complete the proof, it is sufficient to show that $\mathbf{A} \text{Diag} \{ \mathbf{m}^{(k)} \} \mathbf{A}^H$ is Hermitian Toeplitz. Then, we can proceed by writing the following equation

$$\mathbf{A} \text{Diag} \{ \mathbf{m}^{(k)} \} \mathbf{A}^H = \begin{bmatrix} \mathbf{a}_1 & | & \mathbf{a}_2 & | & \dots & | & \mathbf{a}_{2N} \end{bmatrix} \begin{bmatrix} m_1^{(k)} & & & & & & \\ & m_2^{(k)} & & & & & \\ & & \ddots & & & & \\ & & & \ddots & & & \\ & & & & m_{2N}^{(k)} & & \end{bmatrix} \begin{bmatrix} \mathbf{a}_1^H \\ \mathbf{a}_2^H \\ \vdots \\ \mathbf{a}_{2N}^H \end{bmatrix}. \quad (\text{A.6})$$

Performing the matrix product in (A.6), we obtain

$$\begin{aligned} \mathbf{A} \text{Diag} \{ \mathbf{m}^{(k)} \} \mathbf{A}^H &= m_1^{(k)} \mathbf{a}_1 \mathbf{a}_1^H + m_2^{(k)} \mathbf{a}_2 \mathbf{a}_2^H + \dots + m_{2N}^{(k)} \mathbf{a}_{2N} \mathbf{a}_{2N}^H \\ &= m_1^{(k)} \mathbf{A}_1 + m_2^{(k)} \mathbf{A}_2 + \dots + m_{2N}^{(k)} \mathbf{A}_{2N}. \end{aligned} \quad (\text{A.7})$$

In writing (A.7), we used the definition, $\mathbf{A}_p = \mathbf{a}_p \mathbf{a}_p^H$, which was given following (4.1) in terms of $\mathbf{a}_p = \begin{bmatrix} e^{j\omega_p} & e^{j2\omega_p} & \dots & e^{jN\omega_p} \end{bmatrix}^T$. Thus, the $(m, n)^{\text{th}}$ element of the matrix \mathbf{A}_p is given as $\mathbf{A}_p(m, n) = e^{-j(n-m)\omega_p}$. Then, the following equalities are satisfied:

- (i) $\mathbf{A}_p(m, n) = e^{-j(n-m)\omega_p} = \mathbf{A}_p^*(n, m)$,
- (ii) $\mathbf{A}_p(m, n) = e^{-j(n-m)\omega_p} = \mathbf{A}_p(k, l) = e^{-j(l-k)\omega_p}$ if $m - n = k - l$.

Therefore, it can be seen that the matrix \mathbf{A}_p for $p = 1, \dots, 2N$, and thus, the expression given in (A.7) is Hermitian Toeplitz. Thus, finally, $\mathbf{\Pi} \odot (\mathbf{A} \text{Diag} \{ \mathbf{m}^{(k)} \} \mathbf{A}^H)$ is Hermitian Toeplitz.



APPENDIX 4: Computation of the Matrix \mathbf{T}

Lemma 4 (Song et al., 2016b): Let \mathbf{T} be an $N \times N$ Hermitian Toeplitz matrix given as

$$\mathbf{T} = \begin{bmatrix} t_0 & t_1^* & \dots & t_{N-1}^* \\ t_1 & t_0 & \ddots & \vdots \\ \vdots & \ddots & \ddots & t_1^* \\ t_{N-1} & \dots & t_1 & t_1^* \end{bmatrix}. \quad (\text{A.8})$$

\mathbf{T} can be represented as $\mathbf{T} = \frac{1}{2N} \mathbf{A}_{:,1:N}^H \text{Diag}(\mathbf{Ac}) \mathbf{A}_{:,1:N}$ where $\mathbf{A}_{:,1:N}$ is the first N columns of $2N \times 2N$ FFT matrix and $\mathbf{c} = [t_0 \ t_1 \ \dots \ t_{N-1} \ 0 \ t_{N-1}^* \ \dots \ t_{N-1}^*]^T$. Notice that \mathbf{A} is not unitary.

Let the l^{th} element of the vector \mathbf{c} be c_l . Then, c_l can be given as follows (Zhao et al., 2016)

$$c_l = \begin{cases} 0 & l = 0, N \\ w_l \left((\mathbf{x}^{(k)})^H \mathbf{U}_l \mathbf{x}^{(k)} \right) & l = 1, \dots, N-1 \\ c_{2N-l}^* & l = N+1, \dots, 2N-1. \end{cases} \quad (\text{A.9})$$

Since the l^{th} lag of the autocorrelation function of the sequence at the k^{th} iteration is

$r_l(\mathbf{x}^{(k)}) = (\mathbf{x}^{(k)})^H \mathbf{U}_l \mathbf{x}^{(k)}$ and \mathbf{r} is given as follows

$$\mathbf{r} = [r_0(\mathbf{x}^{(k)}) \ r_1(\mathbf{x}^{(k)}) \ \dots \ r_{N-1}(\mathbf{x}^{(k)}) \ 0 \ r_{N-1}^*(\mathbf{x}^{(k)}) \ \dots \ r_1^*(\mathbf{x}^{(k)})]^T, \quad (\text{A.10})$$

then, the vector \mathbf{c} can be written as

$$\mathbf{c} = \mathbf{w} \odot \mathbf{r} \quad (\text{A.11})$$

where $\mathbf{w} = [0 \ w_1 \ \dots \ w_{N-1} \ 0 \ w_{N-1} \ \dots \ w_1]^T$ and \odot represents the Hadamard product.

Then, the vector \mathbf{c} in Algorithm 3 can be written as follows

$$\mathbf{c} = \mathbf{r} \odot [0 \ w_1 \ w_2 \ \dots \ 0 \ w_N \ w_{N-1} \ w_1]^T. \quad (\text{A.12})$$

Since the matrix \mathbf{R} is Hermitian Toeplitz, it can be written using Lemma 4 as follows

$$\mathbf{R} = \frac{1}{2N} \mathbf{A}_{:,1:N}^H \text{Diag}(\mathbf{Ac}) \mathbf{A}_{:,1:N}. \quad (\text{A.13})$$

